Bimetallic Polymerization of Lactide with Binaphthol-Derived *Bis*-heteroscorpionate Dizinc and Dimagnesium Complexes

Maxym Tansky, Robert J. Comito*

Department of Chemistry, The University of Houston, 4800 Calhoun Road, Houston, Texas 77004

Supporting Information

Contents

S1. General Information. All reactions with metal complexes were performed in an atmosphere of dry, oxygen-free dinitrogen using standard Schlenk techniques or in a nitrogen glovebox. The *rac*-lactide and ε-caprolactone were obtained from Millipore Sigma. *L*-lactide and *meso*-lactide were purchased from Natureworks, LLC. Lactides were recrystallized from toluene then sublimated twice before use. ε-Caprolactone was distilled from CaH_2 followed by three freeze-pump-thaw cycles before use. Other commercial reagents were purified prior to use following the guidelines of Perrin and Armarego.[1] All solvents were purified according to the method of Grubbs.[2] Organic solutions were concentrated under reduced pressure on a Büchi rotary evaporator. Chromatographic purification of products was accomplished using force-flow chromatography on Silicycle silica gel according to the method of Still.[3] Thin-layer chromatography (TLC) was performed on Silicycle 250 μm silica gel plates. Compounds were visualized by irradiation with UV light, treatment with a solution of potassium permanganate followed by heating, or exposure to iodine. Yields refer to pure compounds, unless otherwise indicated.

^{1}H-NMR spectra were recorded on a JEOL 400 MHz NMR spectrometer and are internally referenced relative to residual protio solvent signals ($CDCl_3$) at δ=7.26 ppm (^{1}H) and C_6D_6 at δ = 7.16 ppm (^{1}H) and to carbon signals ($CDCl_3$) at δ = 77.00 ppm (^{13}C) and C_6D_6 at δ = 128 ppm (^{13}C). Data for ^{1}H-NMR are reported as follows: chemical shift (ppm), multiplicity (s = singlet, d = doublet, t = triplet, q = quartet, h = heptet, m = multiplet, ap = apparent), integration, and coupling

---

[1]Perrin, D. D.; Armarego, W. L. F. *Purification of Laboratory Chemicals*. 3rd ed., Pergamon Press, Oxford, 1988.
[2]Pangborn, A. B.; Giardello, M. A.; Grubbs, R. H.; Rosen, R. K.; Timmers, F. J. *Organometallic*. **1996**, *15*, 1518.
[3]Still, W. C.; Kahn, M.; Mitra, A. J. *J. Org. Chem.* **1978**, *43*, 2923.

constant (Hz). ^{13}C spectra were recorded on a JEOL (101 MHz) and are referenced relative to $CDCl_3$ at δ 77.16 ppm or DMSO-d_6 at 39.52 ppm. Data for ^{13}C NMR are reported in terms of chemical shift and multiplicity where appropriate. Infrared (IR) spectra were recorded on a Bruker Platinum ATR spectrometer with monolithic diamond crystal plate and are reported in terms of wavenumber of absorption (cm^{-1}). Differential Scanning Calorimetry (DSC) was conducted on a TA-DSC 2500 operated between –90 °C and 250 °C at a rate of 10 °C /minute for heating and cooling cycle under nitrogen atmosphere. All thermal data reported were taken from the second heat curve. Gel Permeation Chromatography (GPC) analyses were performed using a Tosoh high performance GPC system HLC-8320 equipped with an auto injector, a dual differential refractive index (RI) detector, and three TSKgel HHR series columns connected in series (7.8×300 mm TSKgel G5000HHR, TSKgel G4000HHR, TSKgel G3000HHR). GPC analyses were carried out in HPLC grade tetrahydrofuran with a flow rate of 1.0 mL/min at 40 °C. Relative molecular weights (M_n and M_w) and molecular weight distributions ($Đ$) were calculated using conventional column calibration with polystyrene (PS) standards. High resolution mass spectra were obtained from the University of Illinois Urbana-Champaign School of Chemical Sciences Mass Spectrometry Laboratory on a Waters Synapt G2-Si with an ESI source, or a Bruker Daltonics UltrafleXtreme MALDI TOFTOF using a DCTB/NaTFA matrix.

S2. Preparation of Ligands

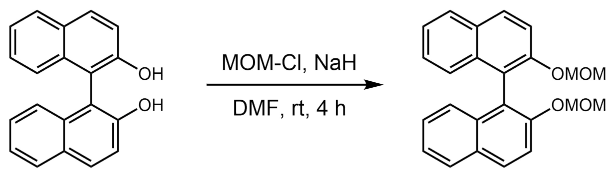

(±)-2,2'-bis(methoxymethoxy)-1,1'-binaphthalene. To a stirring suspension of sodium hydride (2.10 g, 87.5 mmol, 5 equivalents) and *N,N*-dimethylformamide (40 mL) in a round bottom flask was added (±)-2,2'-hydroxy-1,1'-binaphthalene (5.0 g, 18 mmol, 1 equivalent). After 10 minutes, methyl chloromethyl ether (4.0 mL, 52 mmol, 3 equiv) was added in one portion. The resulting suspension was then stirred at room temperature for another 4 hours and then the reaction mixture was partitioned between dichloromethane (200 mL) and saturated sodium bicarbonate (200 mL) solution. The organic phase was washed twice with sodium bicarbonate solution, dried over $MgSO_4$, filtered, and concentrated in vacuo. The residue was separated by silica gel column chromatography using 0-20% diethyl ether in hexanes to obtain the desired material as a white solid (6.20 g, 16.6 mmol, 95% yield). ^{1}H-NMR (400 MHz, $CDCl_3$) δ 7.96 (d, J = 8.9 Hz, 2H), 7.88 (d, J = 8.2 Hz, 2H), 7.59 (d, J = 8.9 Hz, 2H), 7.35 (t, J = 7.0 Hz, 2H), 7.23 (t, J = 7.4 Hz, 2H), 7.17 (d, J = 8.5 Hz, 2H), 5.09 (d, J = 6.9 Hz, 2H), 4.98 (d, J = 6.9 Hz, 2H), 3.15 (s, 6H). ^{13}C-NMR (101 MHz, $CDCl_3$) δ 152.7, 134.1, 123.0, 129.5, 128.0, 126.4, 125.7, 124.2, 121.4, 117.4, 95.3, 56.0. These NMR data are consistent with those reported for this compound.[4] *Note that the racemic product has much lower solubility than its enantioenriched counterpart, which meant that procedures for synthesis of enantioenriched BINOL derivatives had to be modified for use on the racemate*.

---

[4] Wu, T. R.; Shen, L.; Chong, M. J. Asymmetric Allylboration of Aldehydes and Ketones using 3,3'-disubstituted Binaphthol-modified Boronates. *Org. Lett.* **2004**, *6*, 2701.

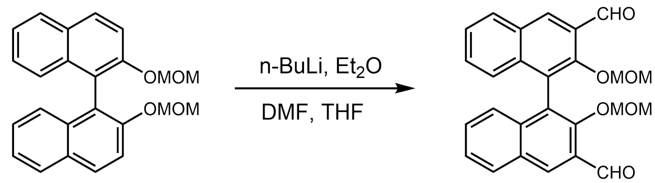

(±)-2,2'-bis(methoxymethoxy)-[1,1'-binaphthalene]-3,3'-dicarbaldehyde. To a room temperature solution of (±)-2,2'-bis(methoxymethoxy)-1,1'-binaphthalene (955 mg, 2.55 mmol, 1 equivalent) in anhydrous diethyl ether (43 mL) under nitrogen was added n-butyllithium (2.5 M in hexanes, 3.06 mL, 7.65 mmol, 3 equivalents) dropwise. The resulting suspension was stirred for 3 hours and then anhydrous tetrahydrofuran (28 mL) was added by syringe and stirred for another 30 minutes. After cooling the solution to 0 ºC using an ice bath, *N,N*-dimethylformamide (1.0 mL, 13 mmol, 5 equivalents) was injected rapidly. After stirring for 30 min at 0 ºC the solution was allowed to warm to room temperature and then quenched by the careful addition of saturated ammonium chloride solution (30 mL). The mixture was then extracted twice with diethyl ether, the combined organic layer washed once with brine, dried over Na_2SO_4, filtered, and concentrated in vacuo. The residue was separated by silica gel column chromatography using 20-50% ethyl acetate in hexanes to obtain the desired material as a light yellow solid (599 mg, 1.39 mmol, 55% yield). ^{1}H-NMR (400 MHz, $CDCl_3$) δ 10.53 (s, 2H), 8.60 (s, 2H), 8.06 (d, J = 8.0 Hz, 2H), 7.50 (t, J = 7.4 Hz, 2H), 7.41 (t, J = 7.5 Hz, 2H), 7.21 (d, J = 8.5 Hz, 2H), 4.72 (d, J = 6.4 Hz, 2H), 4.67 (d, J = 6.4 Hz, 2H), 2.85 (s, 6H). ^{13}C-NMR (101 MHz, $CDCl_3$) δ 190.8, 154.2, 136.8, 132.4, 130.4, 130.2, 129.8, 129.0, 126.4, 126.2, 126.0, 100.7, 57.1. These NMR data are consistent with those reported for this compound.[5]

[5] Li, X.; Li, Q.; Wang, Y.; Quan, Y.; Chen, D.; Cheng, Y. Strong Aggregation-Induced CPL Response Promoted by Chiral Emissive Nematic Liquid Crystals (N*-LCs). *Chem. Eur. J.* **2018**, *24*, 12607.

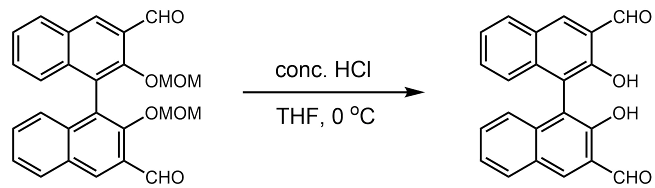

(±)-2,2'-bis(hydroxy)-[1,1'-binaphthalene]-3,3'-dicarbaldehyde (2). A stirring solution of (±)-2,2'-bis(methoxymethoxy)-[1,1'-binaphthalene]-3,3'-dicarbaldehyde (656 mg, 1.52 mmol, 1 equivalent) and tetrahydrofuran (11 mL) was treated with concentrated HCl (4.8 mL) at 0 ºC and then gradually allowed to warm to room temperature. The resulting suspension was stirred for 6 hours and then poured into ice water (40 mL), filtered, and the bright yellow solid washed with water until the washings were neutral by pH paper. Drying in vacuo gave the desired material as a bright yellow solid (520 mg, 1.51 mmol, 99% yield). ^{1}H-NMR (400 MHz, $CDCl_3$) δ 10.57 (s, 2H), 10.18 (s, 2H), 8.34 (s, 2H), 7.99 (d, J = 6.6 Hz, 2H), 7.38-7.43 (m, 4H), 7.19 (d, J = 8.7 Hz, 2H). ^{13}C-NMR (101 MHz, $CDCl_3$) δ 196.9, 153.7, 138.6, 137.5, 130.8, 130.1, 127.7, 124.9, 124.6, 122.2, 116.6. These NMR data are consistent with those reported for this compound.[5]

3-H, **3**-Me_2, **3**-iPr, and **3**-Ph were all prepared according to the previously reported method.[6]

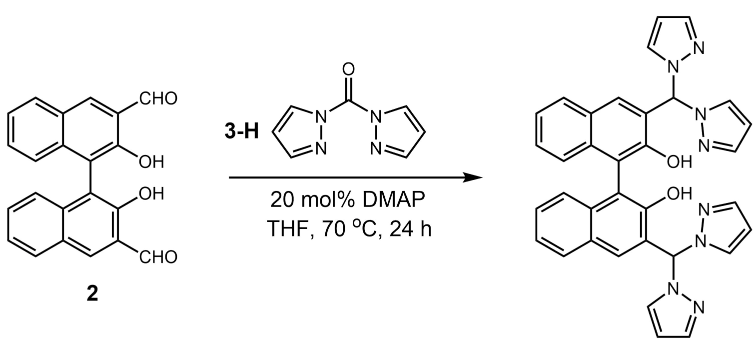

1-H.

A suspension of **2** (200 mg, 0.584 mmol, 1 equivalent), **3**-H (190 mg, 1.17 mmol, 2 equivalents), DMAP (14 mg, 12 mmol, 0.20 equivalent), and tetrahydrofuran (10 mL) was packed under nitrogen into a vial equipped with a stir bar. The vial was tightly sealed and heated to 70ºC with stirring for 24 hours. The reaction was next cooled to room temperature, and all volatiles removed in vacuo. Then the residue redissolved in dichloromethane (30 mL). The resulting solution was washed with water (2 x 20 mL) and brine (20 mL), and then dried over Na_2SO_4, filtered, and concentrated in vacuo. The resulting residue was separated on silica gel column chromatography using an eluent of 1:1 ethyl acetate : hexanes. The isolate was recrystallized by dissolving in boiling isopropanol and then cooling to room temperature, and then dried in vacuo to give the product as a colorless solid (172 mg, 0.297 mmol, 51% yield). ^{1}H-NMR (400 MHz, $CDCl_3$) δ 7.97 (s, 2H), 7.79 (d, J = 8.0 Hz, 2H), 7.64-7.66 (m, 6H), 7.59 (s, 2H), 7.55 (s, 2H), 7.27-7.35 (m, 4H), 7.09 (d, J = 8.2 Hz, 2H), 6.32 (s, 4H). ^{13}C-NMR (101 MHz, $CDCl_3$) δ 150.5, 140.9, 140.7, 134.4, 130.4, 130.1, 130.0, 129.0, 128.5, 128.1, 124.8, 124.5, 124.4, 114.8, 106.6, 106.5, 75.1. IR (Diamond ATR) 3140, 3122, 3057, 1624, 1599, 1514, 1436, 1384, 1362, 1292, 1209, 1191, 1176, 1142, 1090, 1052, 1014, 974, 918, 909, 891, 826, 803, 788, 743, 711, 653, 615, 568, 559, 541, 525, 467, 440 cm^{-1}. HRMS (based on formula $C_{34}H_{26}N_8O_2Na$) m/z: expected: 601.2076 amu ($[M+Na]^+$), found: 601.2064 amu, difference: -2.0 ppm. Elemental analysis (based on formula $C_{34}H_{26}N_8O_2$): C (69.89% found, 70.58% expected, -0.7% difference), H (4.58% found, 4.53% expected, 0.05% difference), N (18.89% found, 19.37% expected, -0.5% difference).

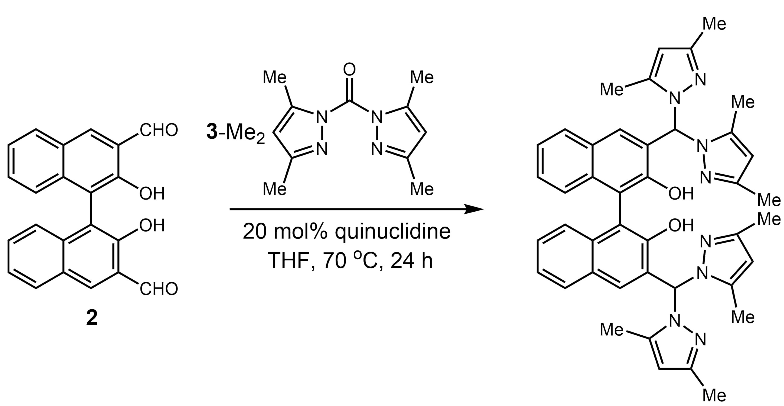

1-Me$_2$.

A solution of **2** (223 mg, 0.651 mmol, 1 equivalent), **3**-Me$_2$ (284 mg, 1.30 mmol, 2 equivalents), quinuclidine (15 mg, 0.13 mmol, 0.20 equivalent), and tetrahydrofuran (10 mL) was packed under nitrogen into a vial equipped with a stir bar. The vial was tightly sealed and heated to 70ºC with stirring for 24 hours. The reaction was next cooled to room temperature and all volatiles removed in vacuo. The resulting residue was separated on silica gel column chromatography using an eluent of 1:2 ethyl acetate : hexanes. Excess 3,5-dimethylpyrazole was removed by sublimation (110 °C, 0.1 Torr), leaving behind the product as a light yellow solid (289 mg, 0.418 mmol, 64% yield). ^{1}H-NMR (400 MHz, $CDCl_3$) δ 7.73-7.75 (m, 4H), 7.25-7.31 (m, 6H), 7.18 (d, J = 7.5 Hz, 2H), 5.91 (s, 2H), 5.86 (s, 2H), 2.24 (s, 6H), 2.15 (s, 6H), 2.06 (s, 6H), 2.05 (s, 6H). ^{13}C-NMR (101 MHz, $CDCl_3$) δ 151.6, 148.6, 147.8, 140.9, 140.1, 134.4, 128.9, 128.8, 128.2, 127.5, 125.8, 124.6, 123.8, 113.1, 107.0, 106.6, 70.5, 14.0, 13.4, 11.1, 10.1. IR (Diamond ATR) 3053, 2958, 2923, 2654, 1626, 1605, 1558, 1503, 1463, 1435, 1417, 1378, 1350, 1331, 1305, 1242, 1208, 1169, 1146, 1108, 1096, 1027, 974, 932, 908, 871, 853, 843, 820, 791, 777, 755, 731, 712, 661, 632, 607, 566, 549, 531, 488, 460, 440 cm^{-1}. HRMS (based on formula $C_{42}H_{42}N_8O_2Na$) m/z: expected: 713.3328 amu ($[M+Na]^+$), found: 713.3309 amu, difference: –2.7 ppm. Elemental analysis (based on formula $C_{42}H_{42}N_8O_2$): C (73.08% found, 73.02% expected, 0.1% difference), H (6.12% found, 6.13% expected, -0.01% difference), N (16.09% found, 16.22% expected, -0.1 % difference).

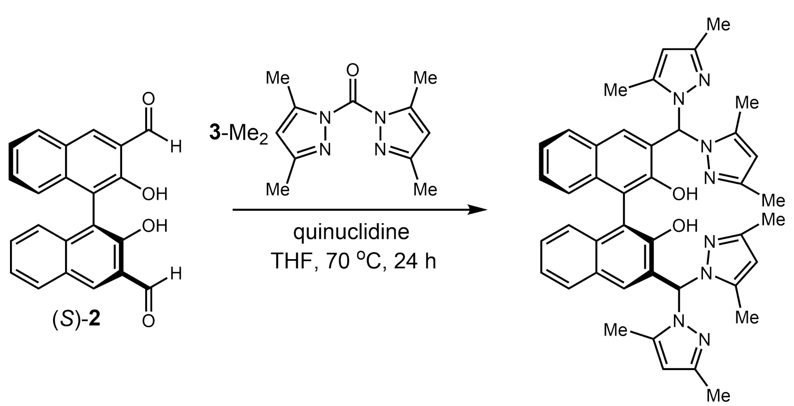

(*S*)-**1**-Me_2.

Prepared in an identical manner as **1**-Me_2 using (*S*)-**2** (342 mg, 1.00 mmol, 1 equivalent), **3**-Me_2 (436 mg, 2.00 mmol, 2 equivalent), quinuclidine (55 mg, 0.20 mmol, 0.20 equivalent) to obtain a light yellow solid (504 mg, 0.730 mmol, 73% yield). NMR Data matched that for racemic **1**-Me_2. This compound exhibits significantly higher solubility in organic solvents than the racemic **1**-

Me$_2$. HRMS (based on formula $C_{42}H_{42}N_8O_2Na$) m/z: expected: 713.3328 amu ($[M+Na]^+$), found: 713.3313 amu, difference: -2.1 ppm. $[\alpha]_D$ = –18.0 (0.0484, $CHCl_3$, 21 ºC).

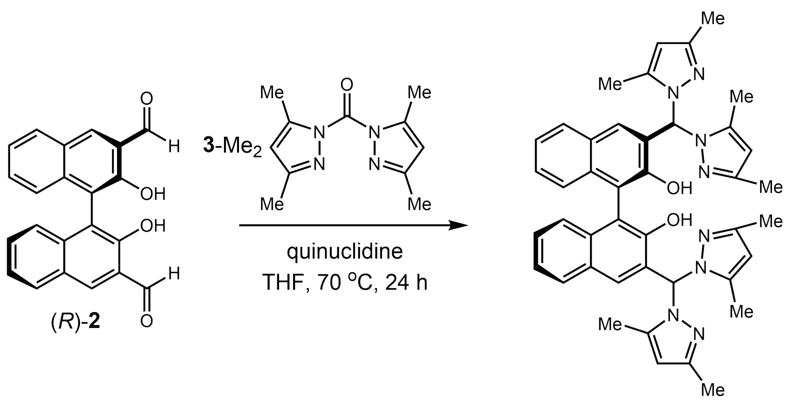

(*R*)-**1**-Me$_2$.

Prepared in an identical manner as **1**-Me$_2$ using (*R*)-**2** (252 mg, 0.736 mmol, 1 equivalent), **3**-Me$_2$ (321 mg, 1.47 mmol, 2 equivalents), quinuclidine (16 mg, 0.15 mmol, 0.20 equivalent). The crude product was isolated from column chromatography using an eluent of 1:2 ethyl acetate : hexanes and then recrystallized by dissolving in boiling toluene and hexanes and then cooling to room temperature, giving the title compound as a light yellow solid (215 mg, 0.310 mmol, 42% yield). NMR data matched that for racemic **1**-Me$_2$. This compound exhibits significantly higher solubility in organic solvents than the racemic **1**-Me$_2$. HRMS (based on formula $C_{42}H_{43}N_8O_2$) m/z: expected: 691.3509 amu ($[M+H]^+$), found: 691.3514 amu, difference: –0.7 ppm. $[\alpha]_D$ = +18.5 (0.0452, $CHCl_3$, 21 ºC).

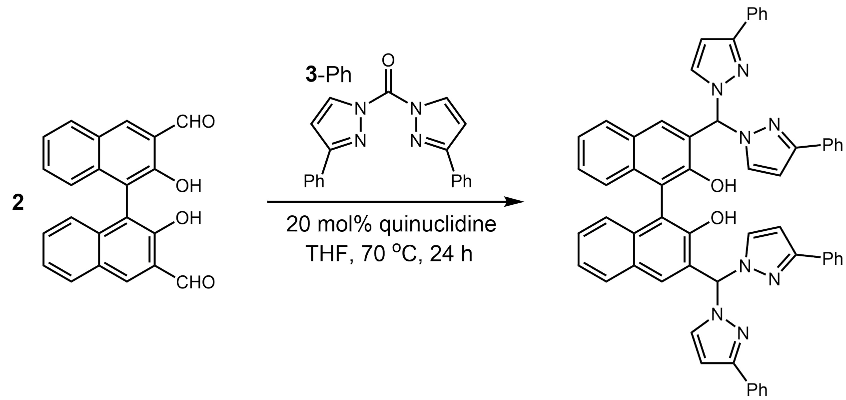

1-Ph.

In a sealed vial with a stir bar, a solution of **2** (100 mg, 0.292 mmol, 1 equivalent), **3**-Ph (184 mg, 0.584 mmol, 2 equivalents), quinuclidine (6.5 mg, 0.058 mmol, 0.20 equivalents), and tetrahydrofuran (4 mL) was heated to 70ºC and stirred for 24 hours under nitrogen. The reaction was cooled to room temperature and all volatiles removed in vacuo. The resulting residue was separated on silica gel column chromatography using an eluent of 1:8:8 ethyl acetate : hexanes : dichloromethane to obtain the desired material as a pale yellow solid (70 mg, 0.079 mmol, 27% yield). ^{1}H-NMR (400 MHz, $CDCl_3$) δ 8.55 (br, 2H), 7.97 (s, 2H), 7.70-7.75 (m, 14H), 7.66 (s, 2H), 7.25-7.34 (m, 14H), 7.18-7.22 (m, 4H), 6.63 (s, 2H), 6.59 (s, 2H). ^{13}C-NMR (101 MHz, $CDCl_3$) δ 152.7, 152. 7, 150.4, 134.4, 132.7, 132. 7, 131.6, 131.4, 130.8, 129.0, 128.7, 128.7, 128.6, 128.2, 128.1, 126.0, 126.0, 124.7, 124.6, 124.4, 116.0, 104.0, 104.0. IR (Diamond ATR) 3136, 3115, 3062, 3035, 2958, 2920, 2851, 1743, 1657, 1626, 1604, 1583, 1529, 1499, 1457, 1403, 1381, 1355, 13214, 1301, 1283, 1262, 1230, 1214, 1179, 1149, 1098, 1074, 1048, 1025, 948, 916, 896, 863, 829, 808, 747, 691, 609, 571, 509, 475, 434 cm^{-1}. HRMS (based on formula $C_{58}H_{43}N_8O_2$) m/z: expected: 883.3509 amu ($[M+H]^+$), found: 883.3501 amu, difference: –0.9 ppm.

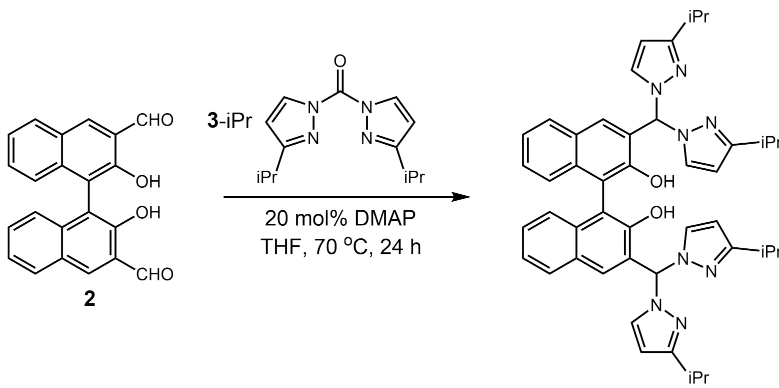

1-iPr.

In a sealed vial with a stir bar, **2** (150 mg, 0.438 mmol, 1 equivalent), **3**-iPr (216 mg, 0.876 mmol, 2.00 equivalents), DBU (13 mL, 0.088 mmol, 0.020 equivalents), and tetrahydrofuran was heated to 70 ºC for 24 hours under nitrogen. The reaction mixture was cooled to room temperature and all volatiles removed in vacuo. The resulting residue was separated on silica gel column chromatography using an eluent of 10% ethyl acetate in dichloromethane to obtain the desired material as a pale yellow solid, which was further purified by recrystallization from boiling hexanes/pentane (1:1) and cooling to –20 ºC giving colorless crystals. (40 mg, 0.054 mmol, 12% yield). ^{1}H-NMR (400 MHz, $CDCl_3$) δ 9.52 (br, 2H), 7.78 (d, J = 8.3 Hz, 2H), 7.73 (s, 2H), 7.67 (s, 2H), 7.59 (q, J = 2.3 Hz, 4H), 7.31 (t, J = 7.3 Hz, 2H), 7.25 (t, J = 7.3 Hz, 2H), 7.12 (d, J = 8.3 Hz, 2H), 6.10 (t, J = 2.0 Hz, 4H), 2.88-3.01 (m, 4H), 1.17-1.22 (m, 24H). ^{13}C-NMR (101 MHz, $CDCl_3$) δ 160.4, 160.4, 150.4, 134.8, 131.1, 130.6, 130.5, 128.7, 128.4, 127.8, 125.0, 124.8, 124.1, 117.6, 103.2, 77.5 (overlaps with solvent signal), 27.9, 27.9, 22.8, 22.8, 22.7. IR (Diamond ATR) 3122, 2963, 2929, 2871, 2629, 1627, 1602, 1565, 1523, 1473, 1457, 1440, 1403, 1380, 1353, 1288, 1258, 1239, 1195, 1149, 1111, 1098, 1069, 1048, 1021, 991, 945, 898, 826, 805, 749, 720, 692, 628, 603, 565, 526, 476, 461, 437, 423 cm^{-1}. HRMS (based on formula $C_{46}H_{51}N_8O_2$) m/z: expected: 747.4135 amu ($[M+H]^+$), found: 747.4119 amu, difference: –2.1

ppm. **2-*bis*(3,5-dimethylpyrazol-1-yl)methylphenol (4)** Prepared according to the previously reported method.[6]

[6] Tansky, M.; Gu, Z.; Comito, R. J. Metal-free, mild, and selective synthesis of *bis*(pyrazolyl)alkanes by nucleophile-catalyzed condensation. *J. Org. Chem.* **2021**, *86*, 1601-1611.

S3. Spectral Data for Ligands

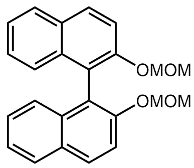

(±)-2,2'-bis(methoxymethoxy)-1,1'-binaphthalene

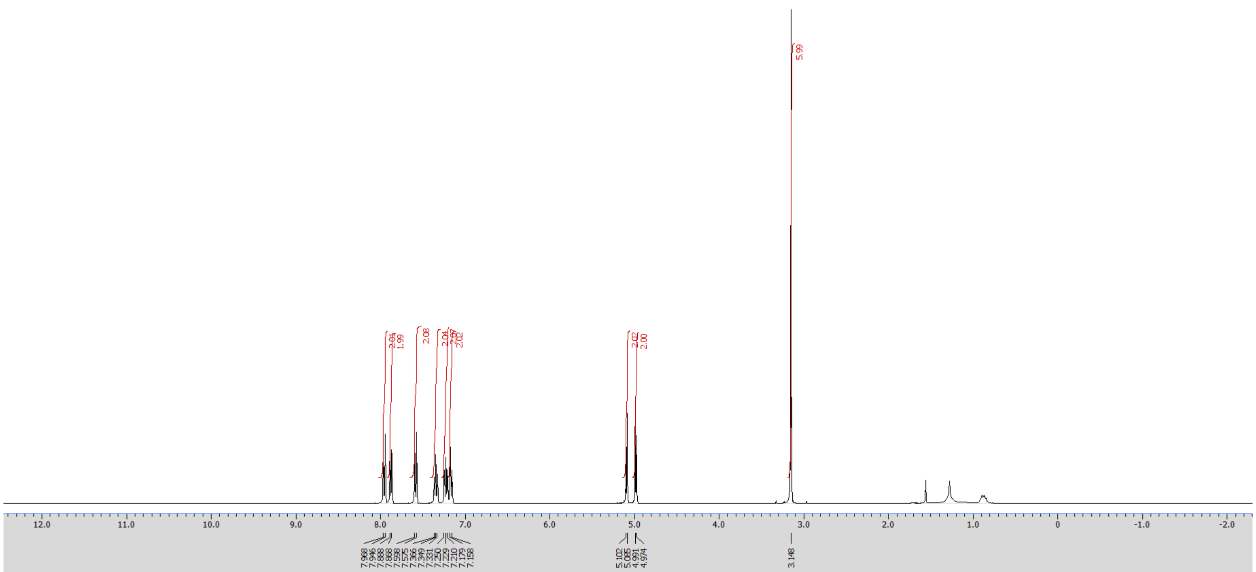

Figure S3.1. ^{1}H-NMR of **(±)-2,2'-bis(methoxymethoxy)-1,1'-binaphthalene**, $CDCl_3$, 400 MHz.

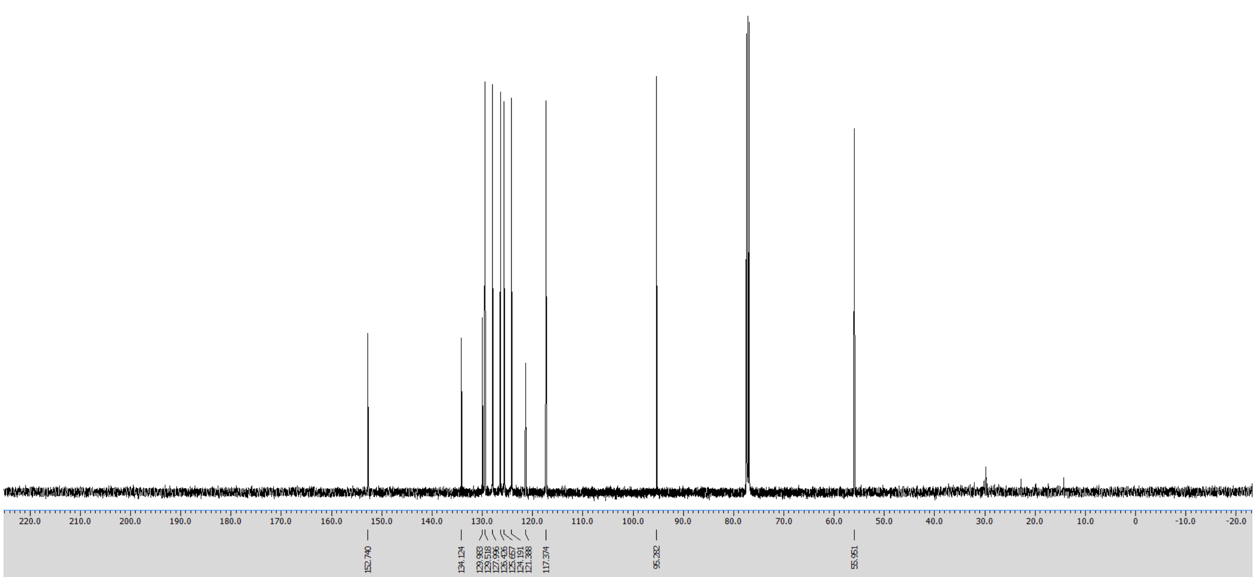

Figure S3.2. ^{13}C-NMR of (±)-**2,2'-bis(methoxymethoxy)-1,1'-binaphthalene**, $CDCl_3$, 100 MHz.

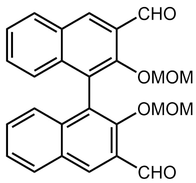

(±)-2,2'-bis(methoxymethoxy)-[1,1'-binaphthalene]-3,3'-dicarbaldehyde

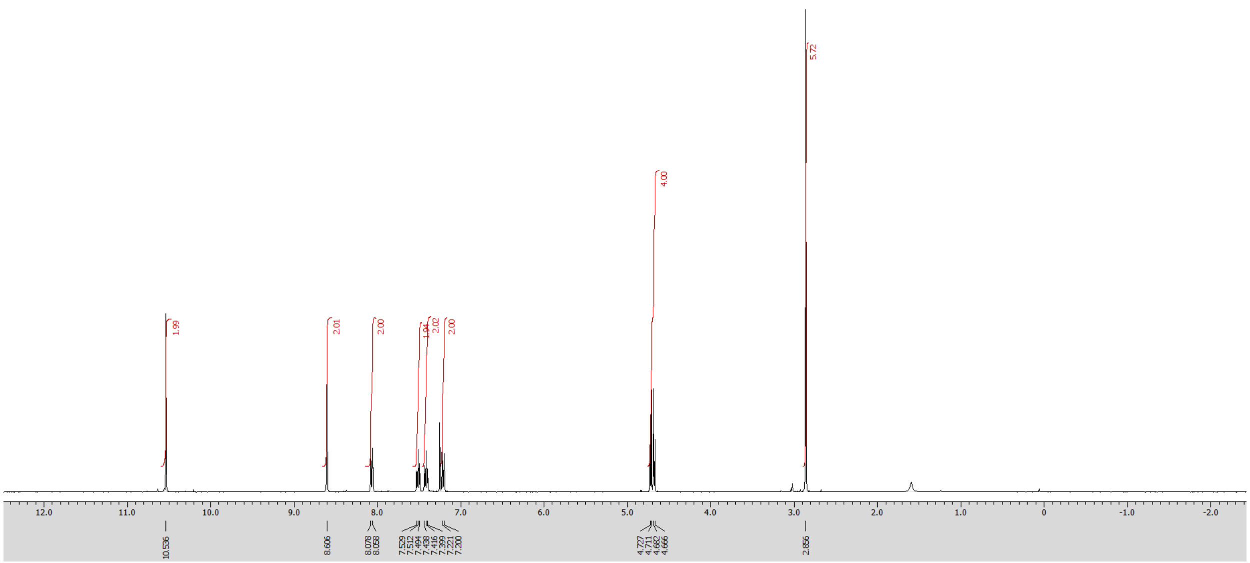

Figure S3.3. [1]H-NMR of **(±)-2,2'-bis(methoxymethoxy)-[1,1'-binaphthalene]-3,3'-dicarbaldehyde**, $CDCl_3$, 400 MHz.

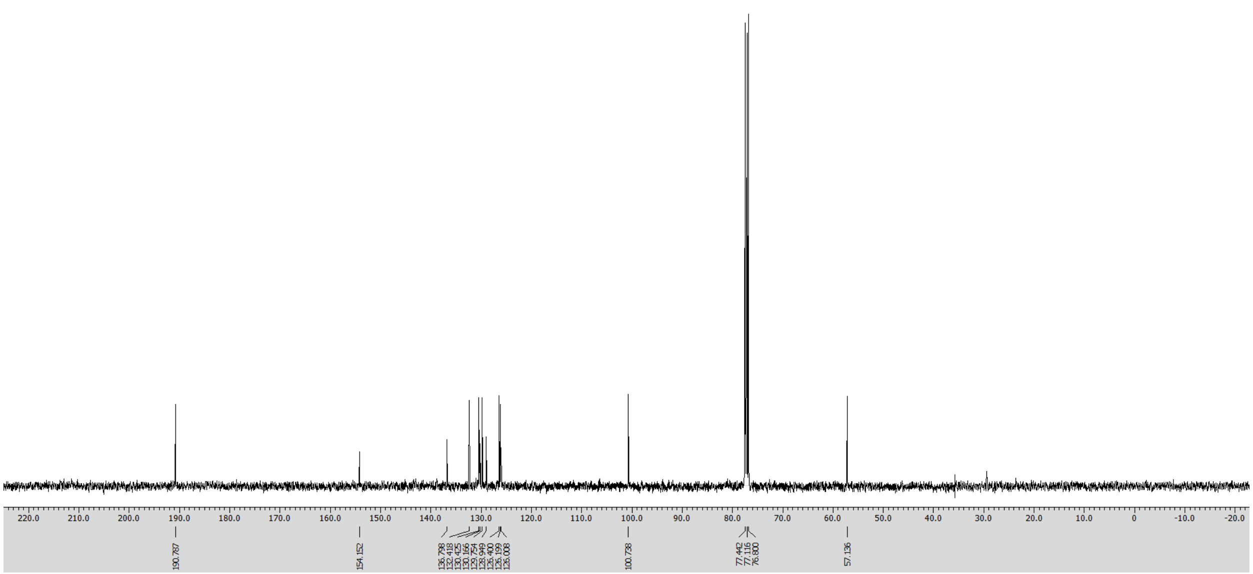

Figure S3.4. [13]C-NMR of **(±)-2,2'-bis(methoxymethoxy)-[1,1'-binaphthalene]-3,3'-dicarbaldehyde**, $CDCl_3$, 100 MHz.

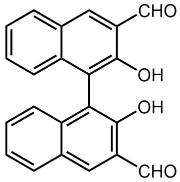

2

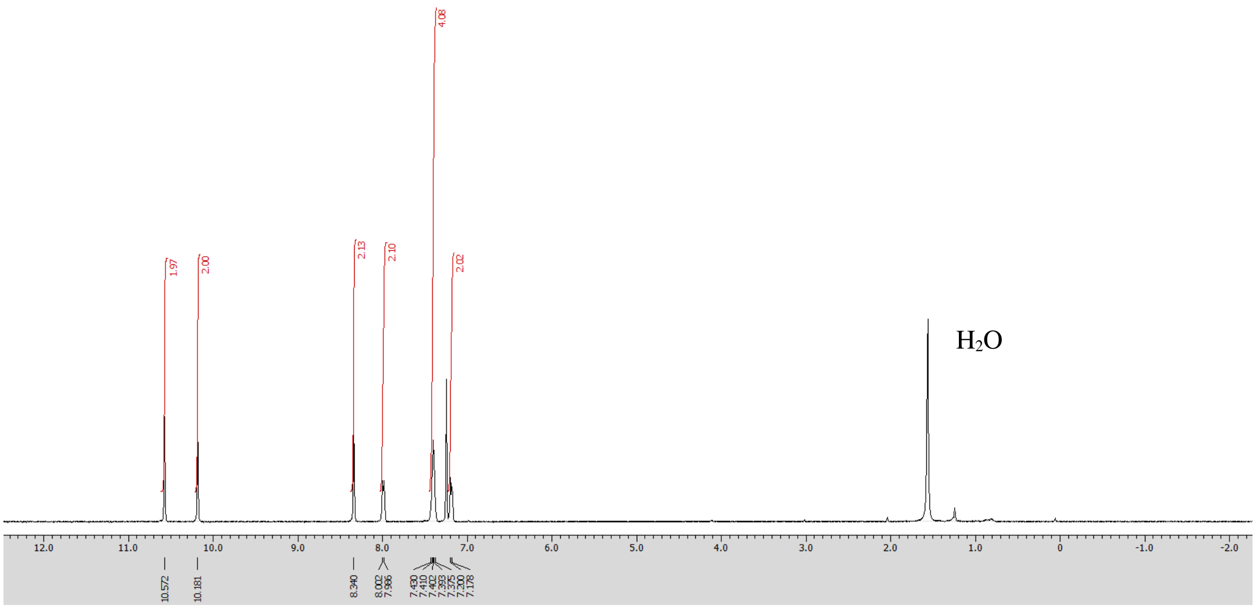

Figure S3.5. [1]H-NMR of **2**, $CDCl_3$, 400 MHz.

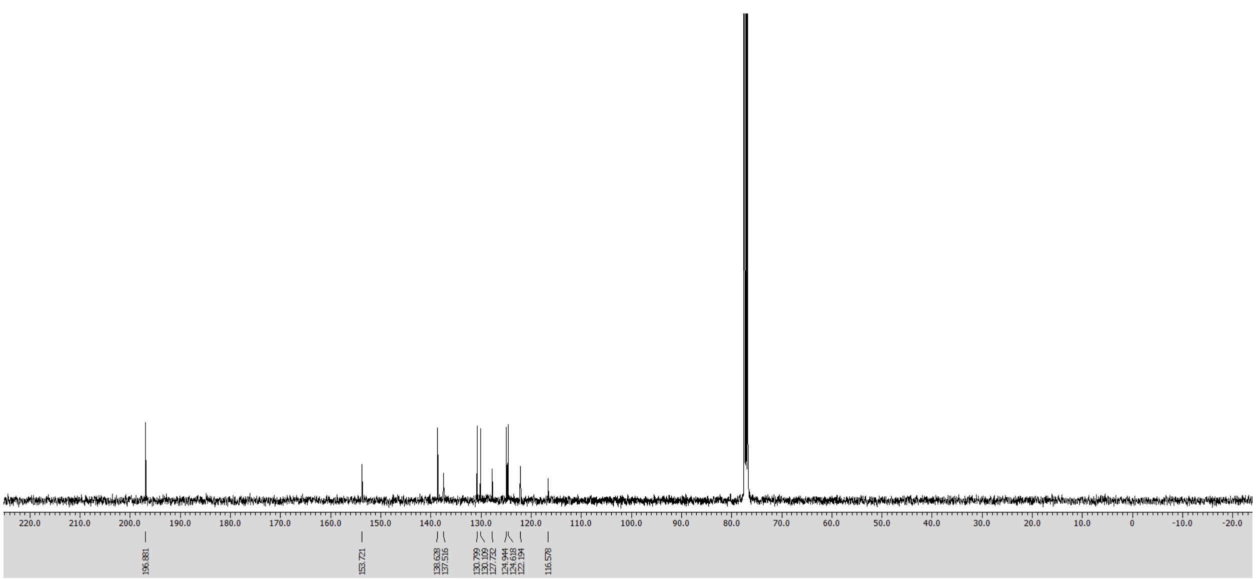

Figure S3.6. [13]C-NMR of **2**, $CDCl_3$, 100 MHz.

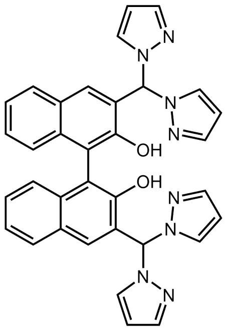

1-H.

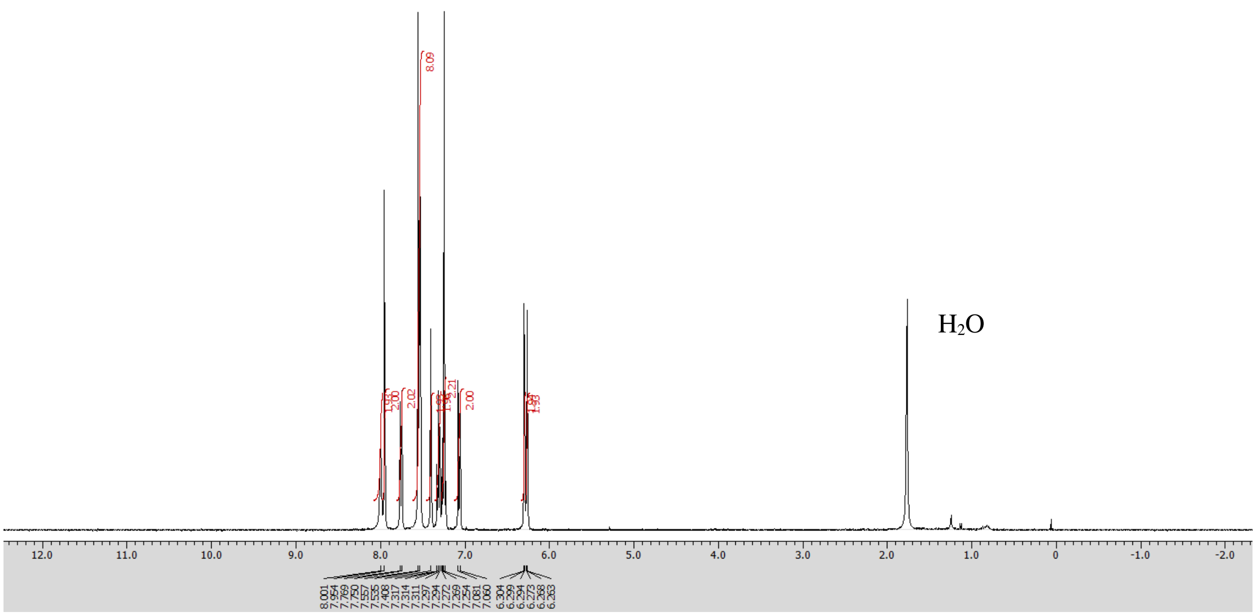

Figure S3.7. ^{1}H-NMR of **1**-H, $CDCl_3$, 400 MHz.

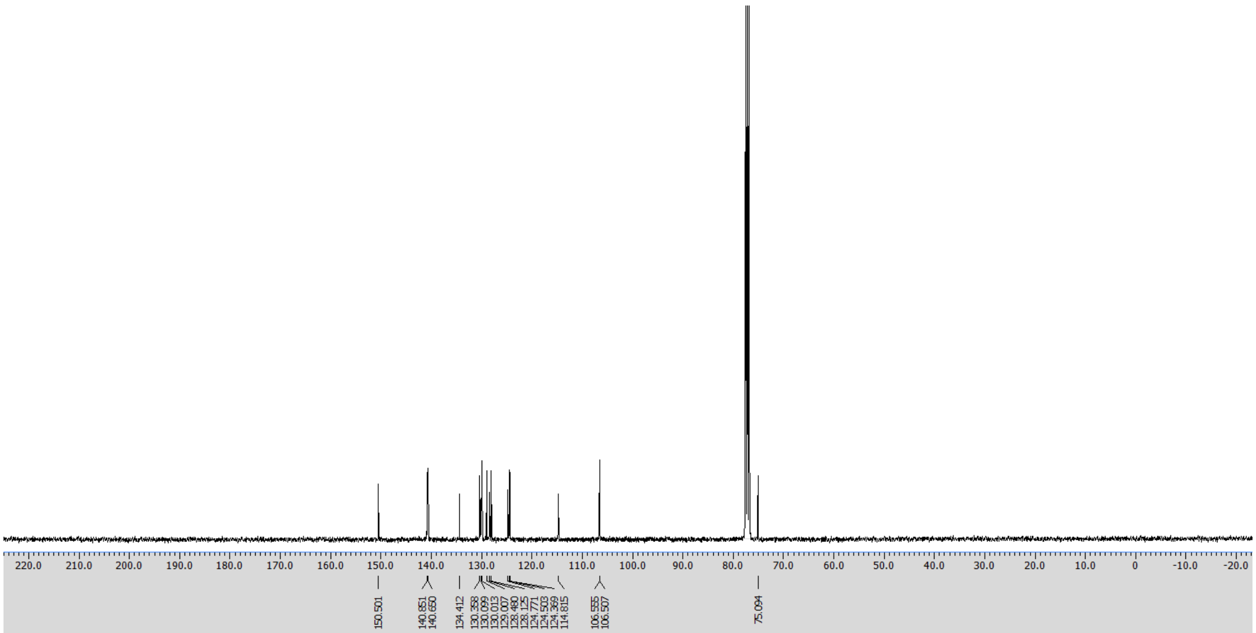

Figure S3.8. ^{13}C-NMR of **1**-H, $CDCl_3$, 100 MHz.

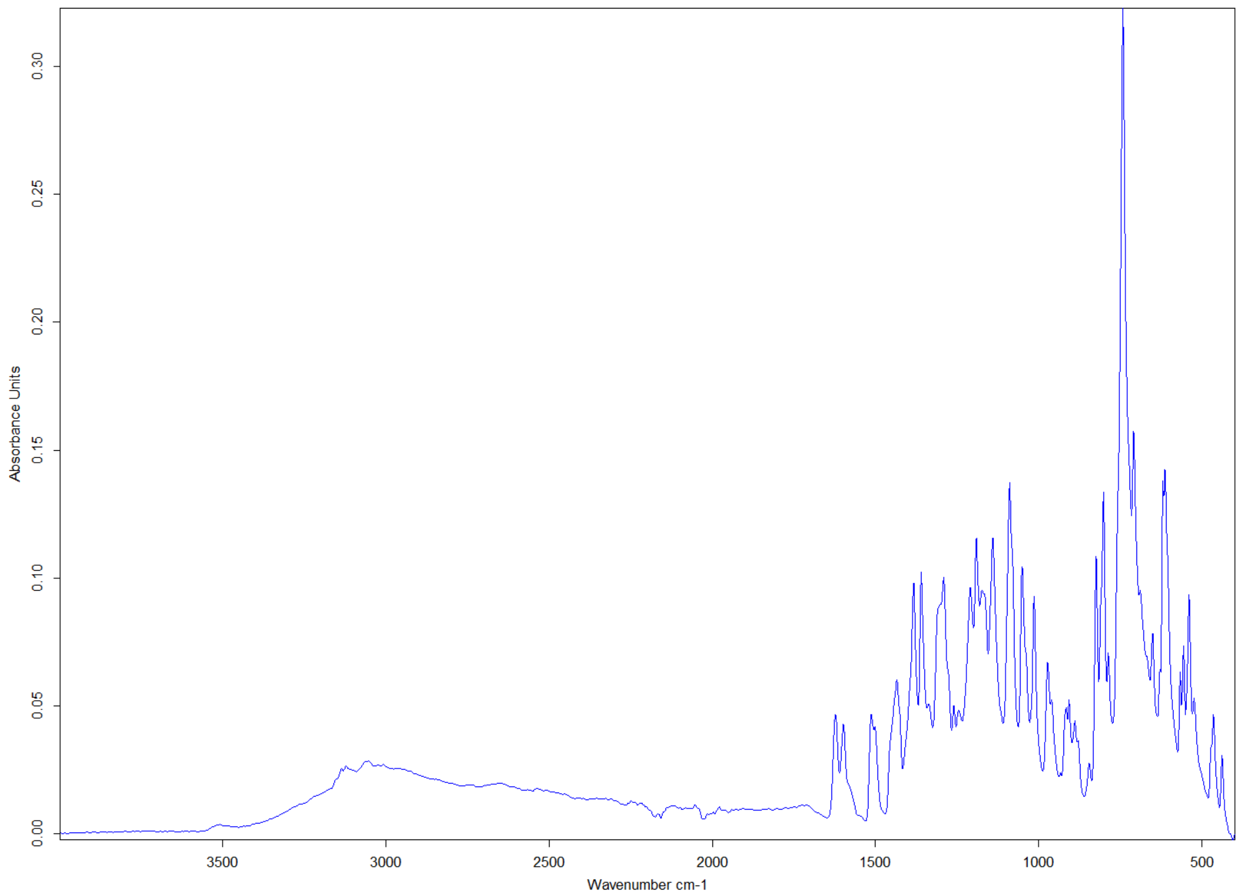

Figure S3.9. Infrared spectrum of **1**-H, diamond ATR.

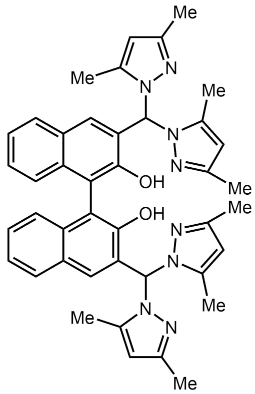

1-Me$_2$.

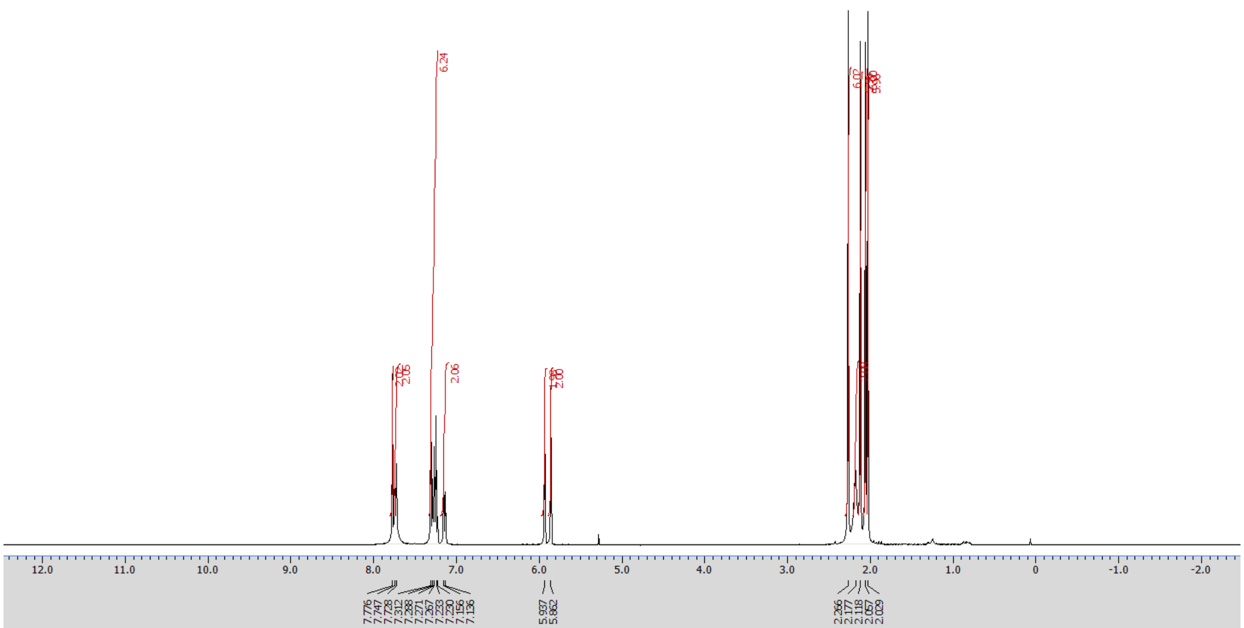

Figure S3.10. ^{1}H-NMR of **1**-Me$_2$, $CDCl_3$, 400 MHz.

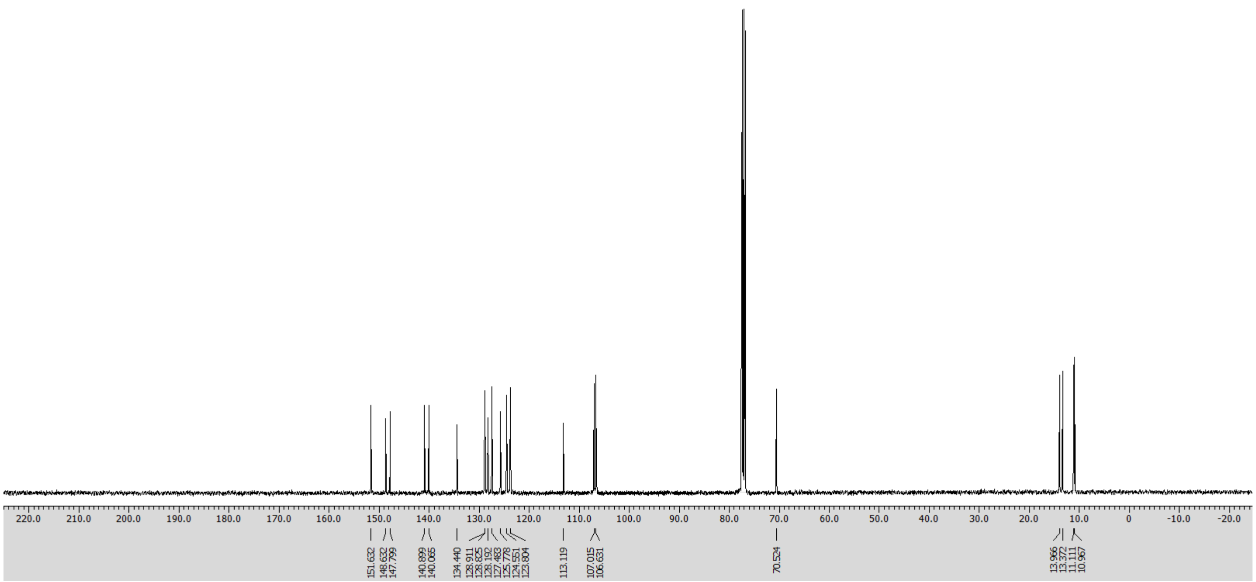

Figure S3.11. ^{13}C-NMR of **1**-Me_2, $CDCl_3$, 100 MHz.

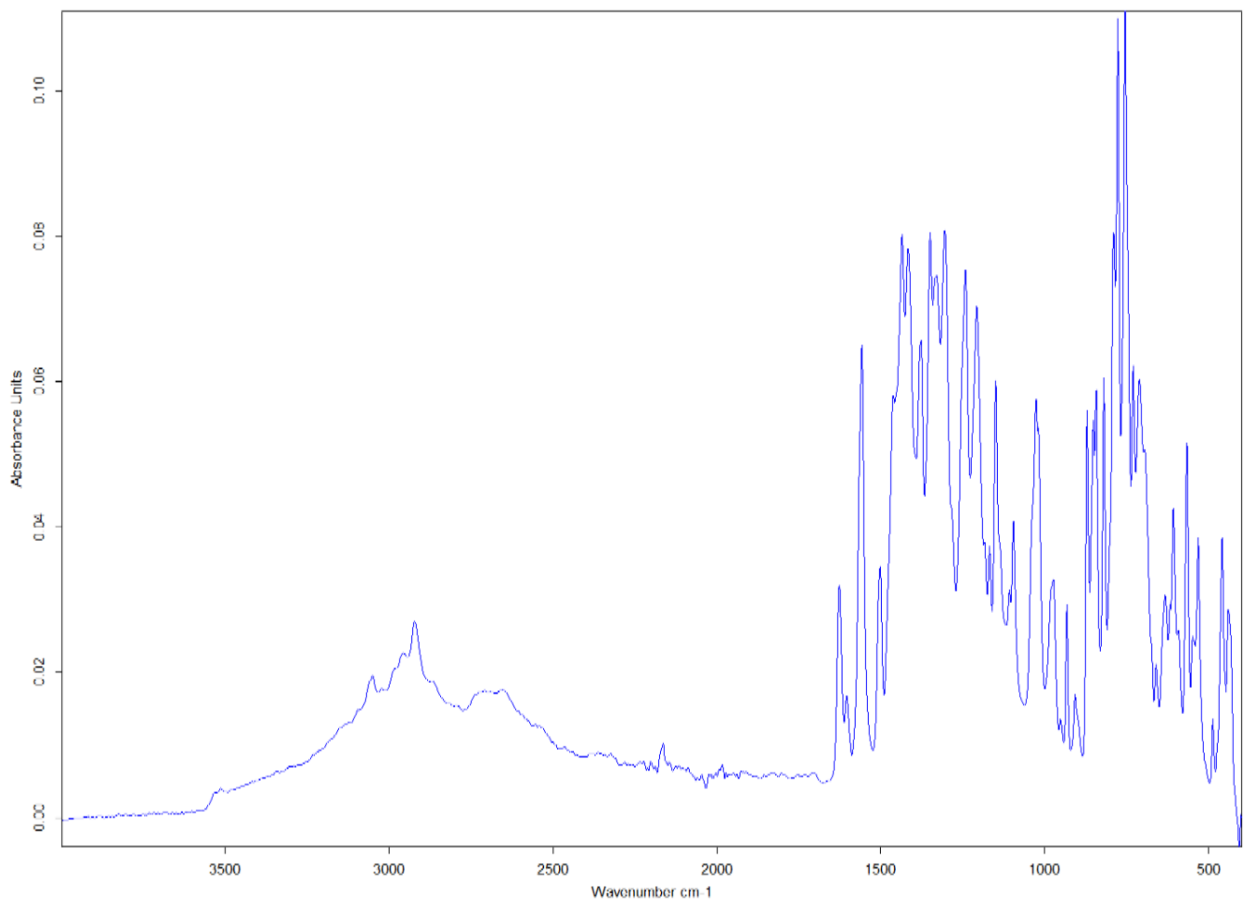

Figure S3.12. Infrared spectrum of **1**-Me_2, diamond ATR.

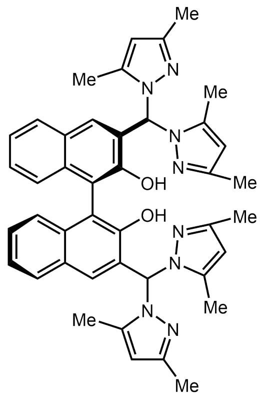

(*R*)-**1**-Me$_2$

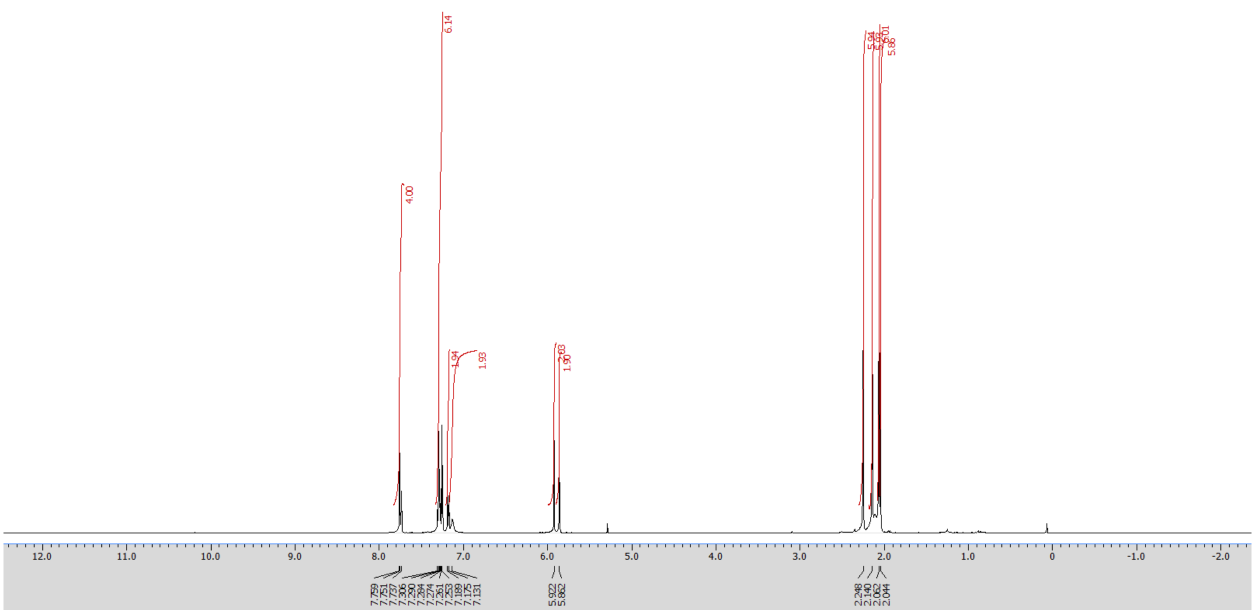

Figure S3.13. ^{1}H-NMR of (*R*)-**1**-Me$_2$, $CDCl_3$, 400 MHz.

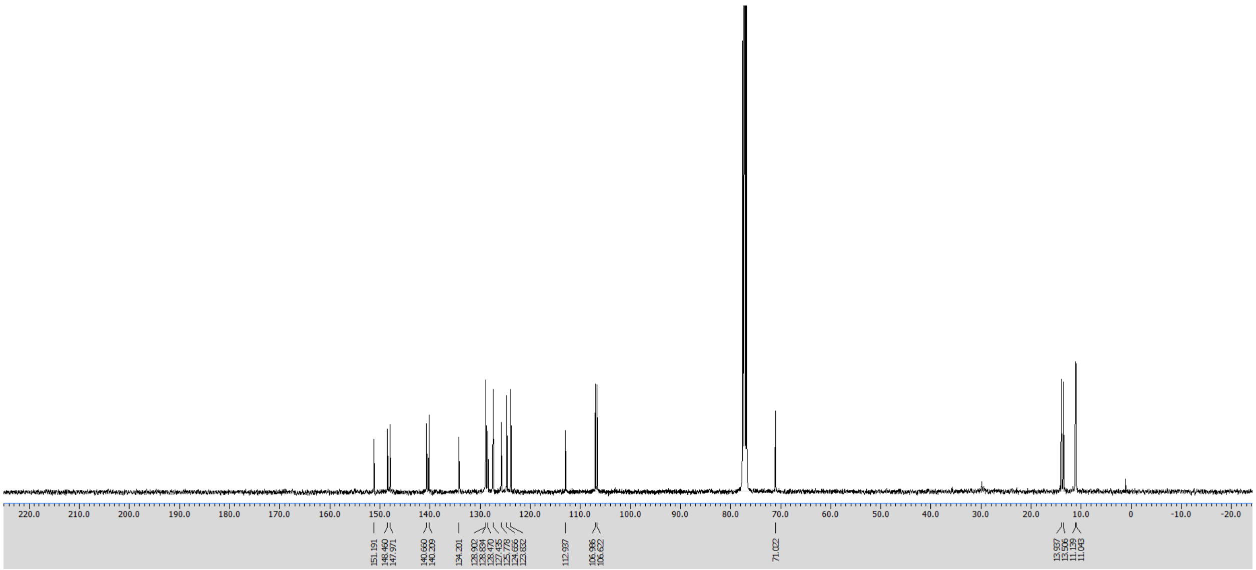

Figure S3.14. ^{13}C-NMR of (*R*)-**1**-Me_2, $CDCl_3$, 100 MHz.

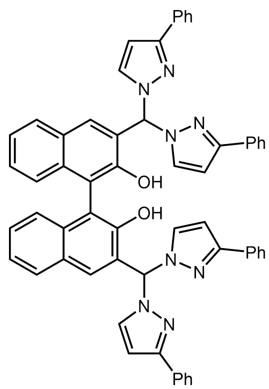

1-Ph.

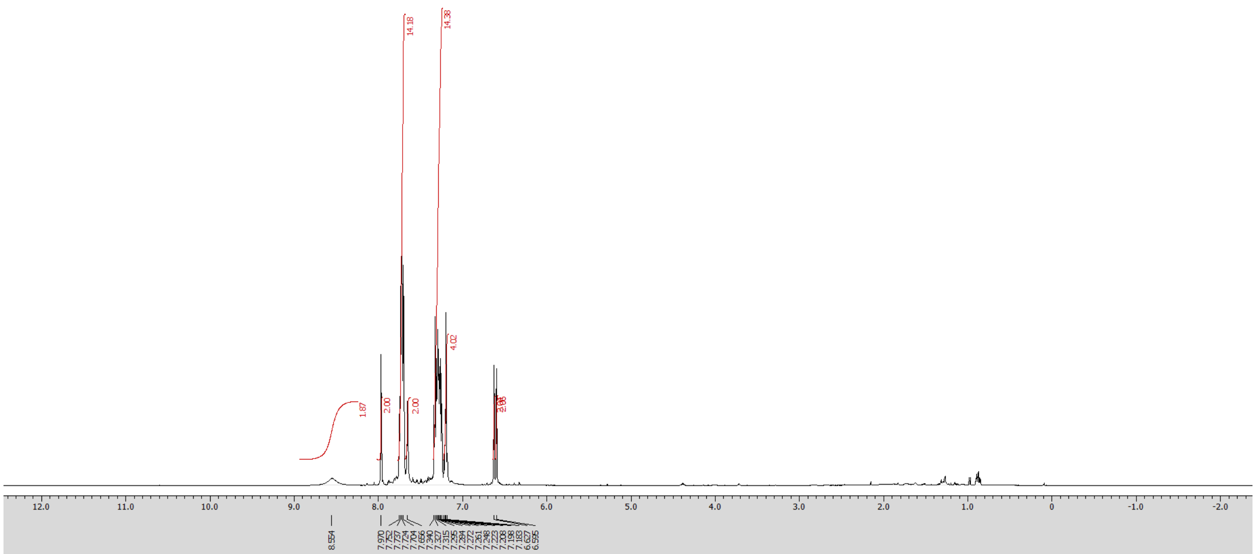

Figure S3.15. ^{1}H-NMR of **1**-Ph, $CDCl_3$, 400 MHz.

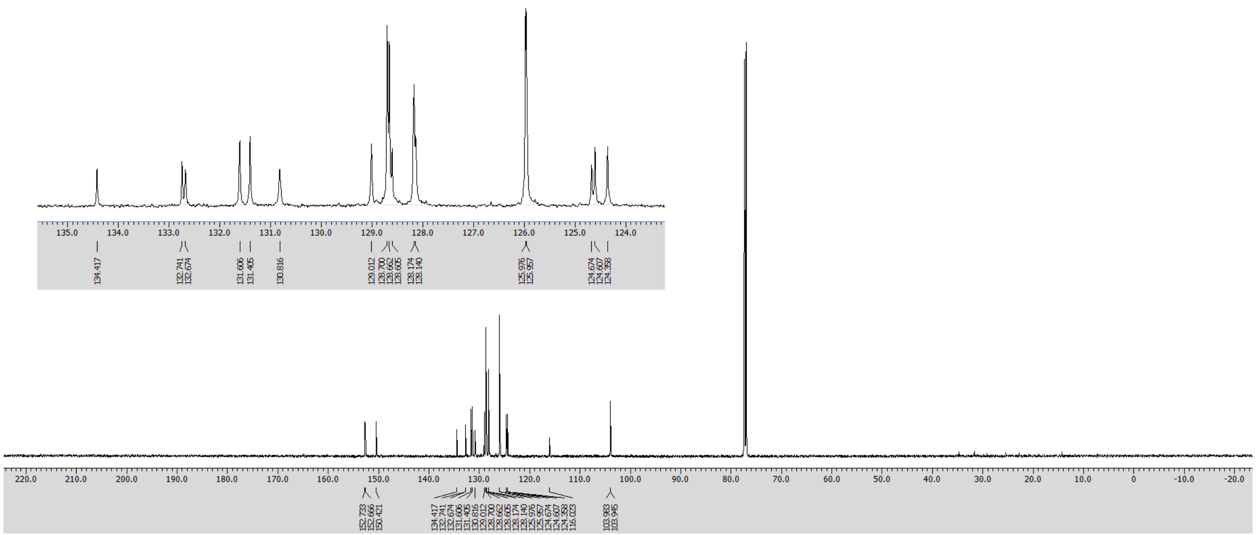

Figure S3.16. ^{13}C-NMR of **1**-Ph, $CDCl_3$, 100 MHz.

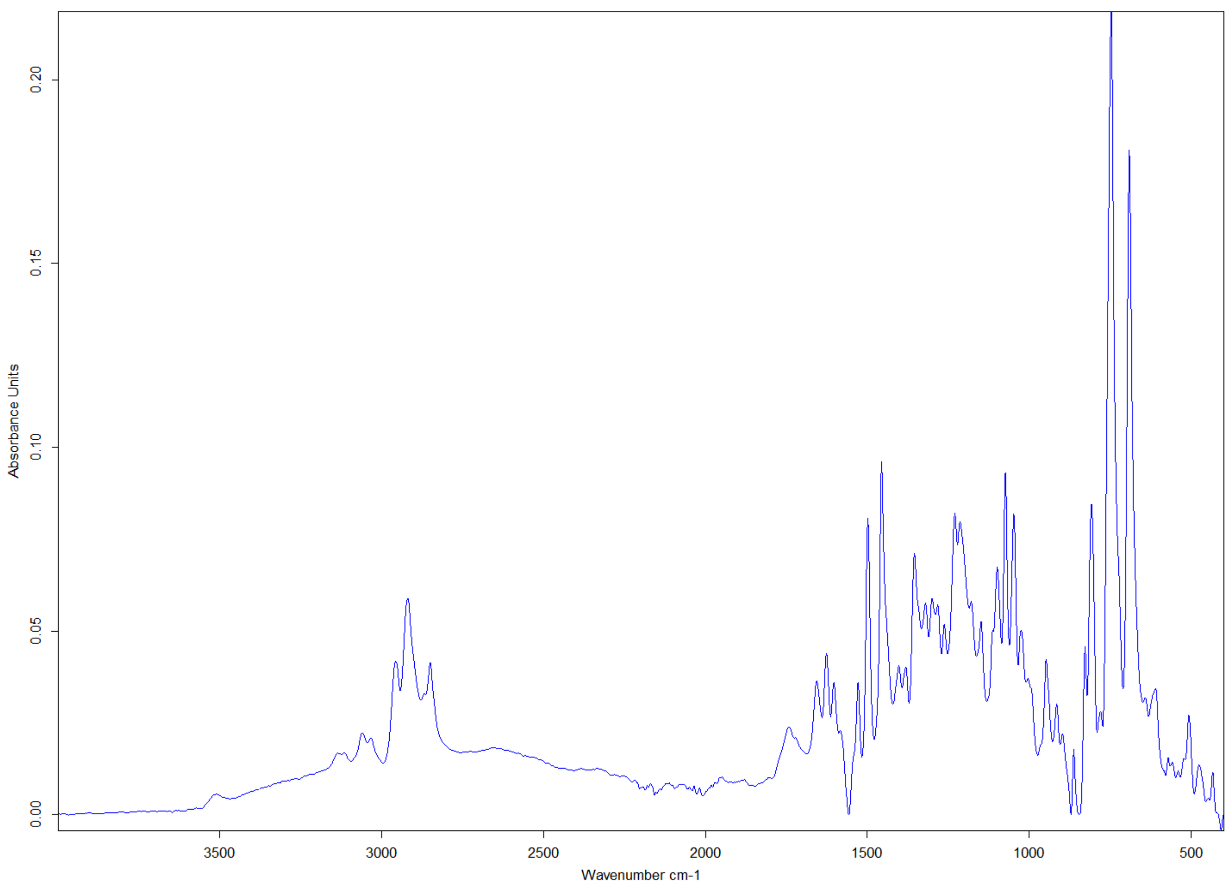

Figure S3.17. Infrared spectrum of **1**-Ph, diamond ATR.

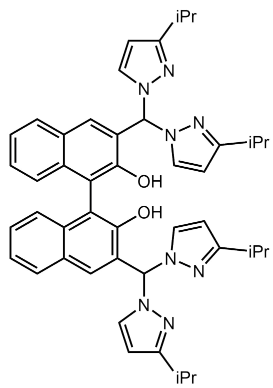

1-iPr.

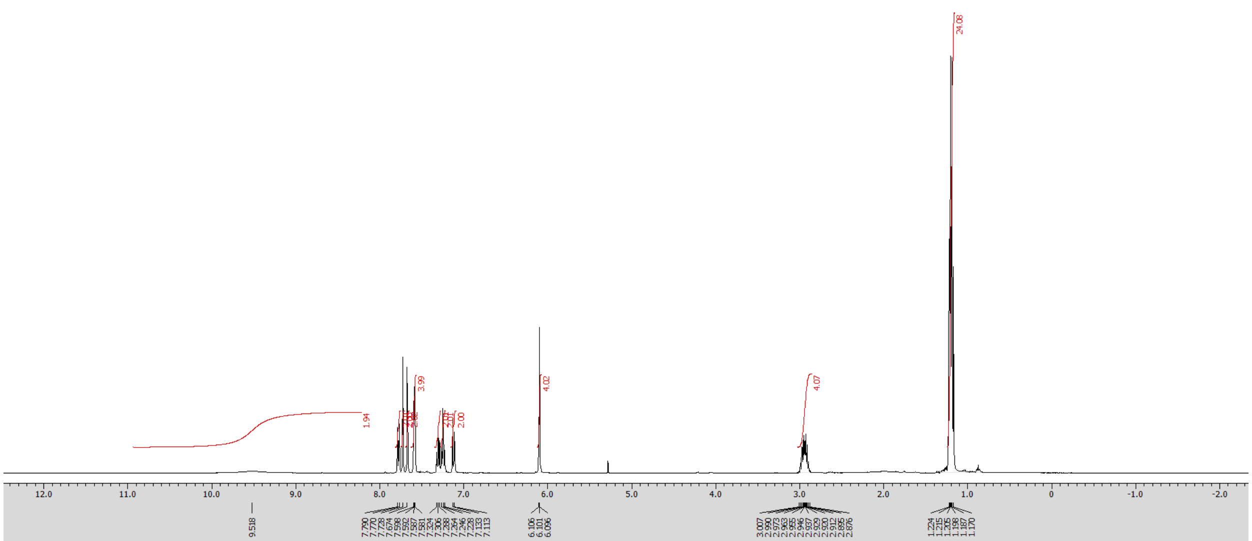

Figure S3.18. ^{1}H-NMR of **1**-iPr, $CDCl_3$, 400 MHz.

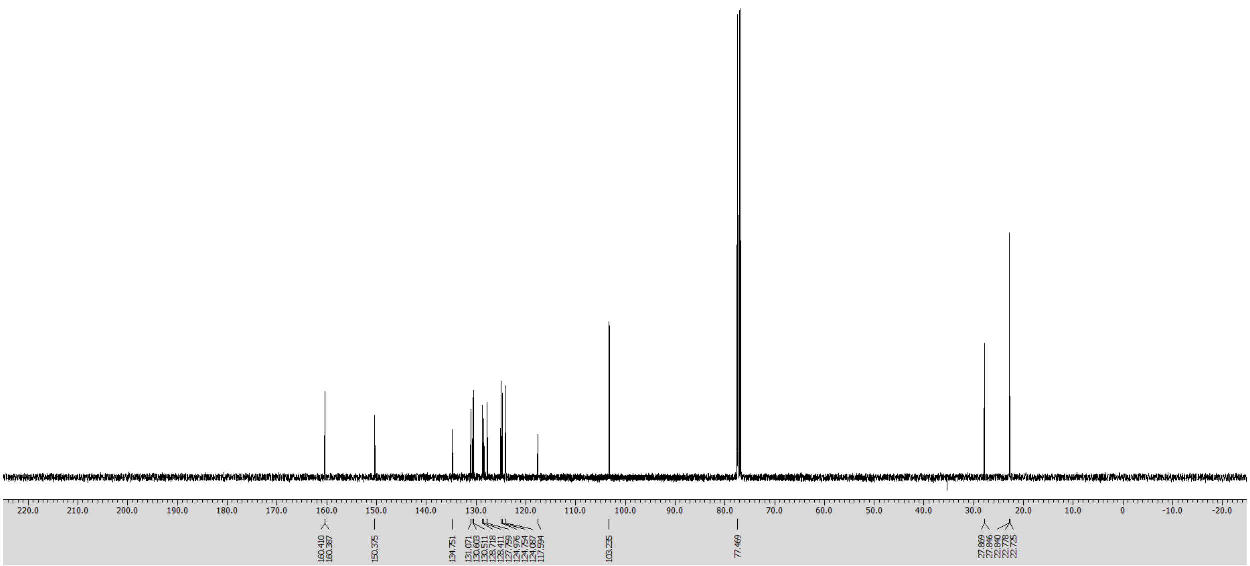

Figure S3.19. ^{13}C-NMR of **1**-iPr, $CDCl_3$, 100 MHz.

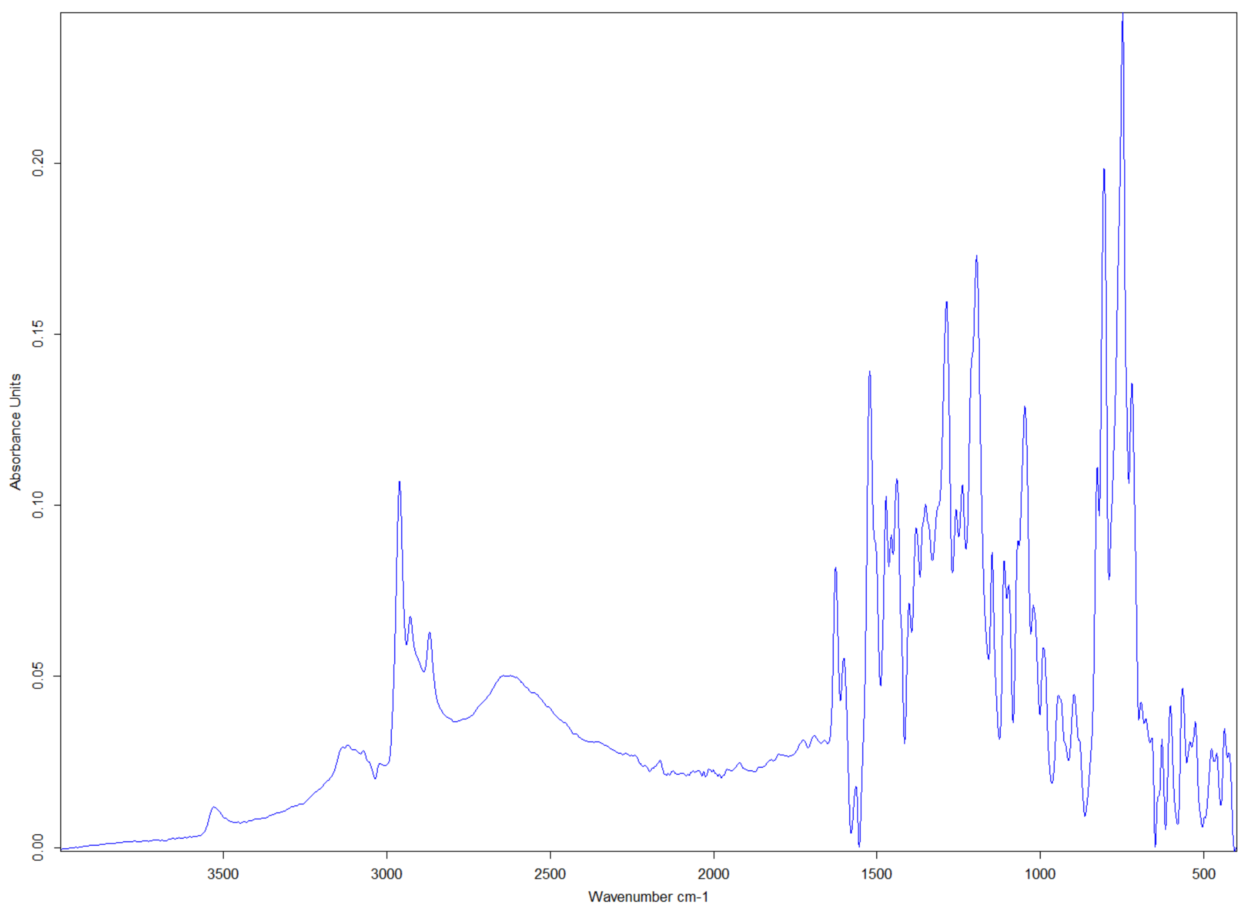

Figure S3.20. Infrared spectrum of **1**-iPr, diamond ATR.

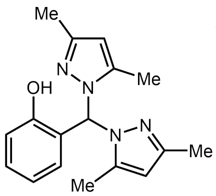

2-*bis*(3,5-dimethylpyrazol-1-ly)methyphenol (4)

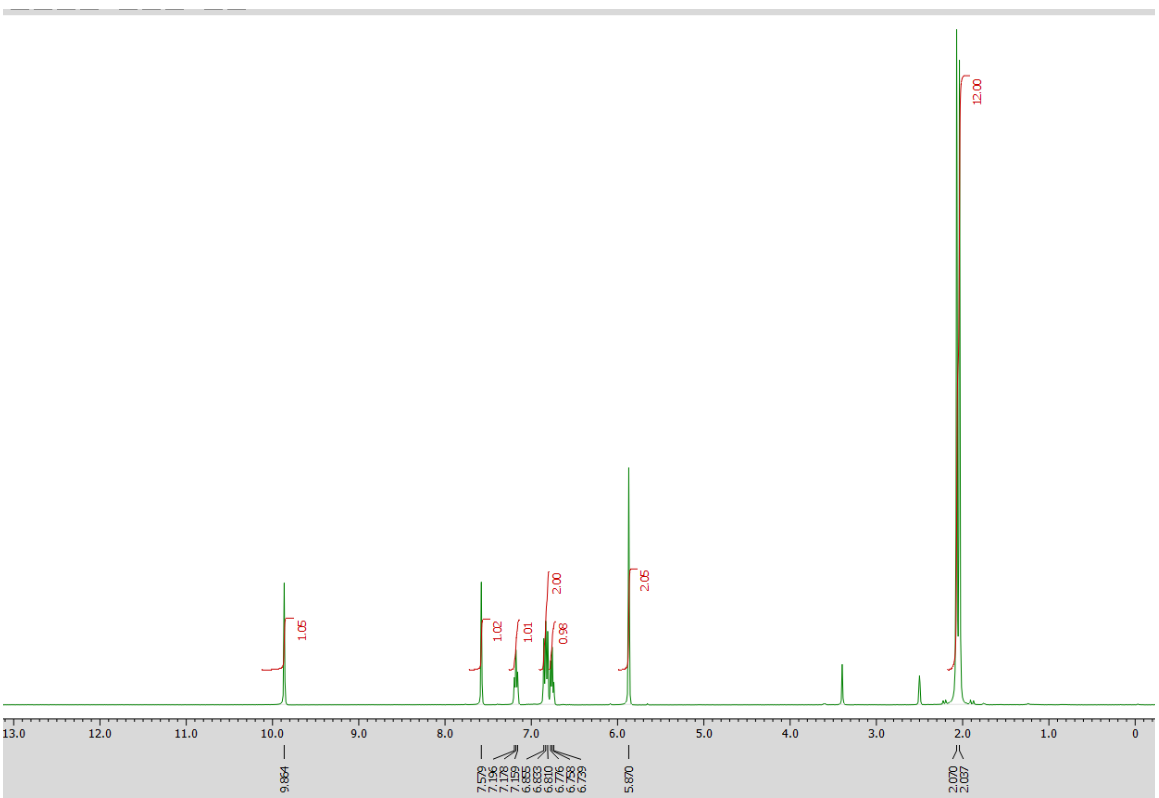

Figure S3.21. ^{1}H-NMR of **4**, DMSO-d6, 400 MHz.

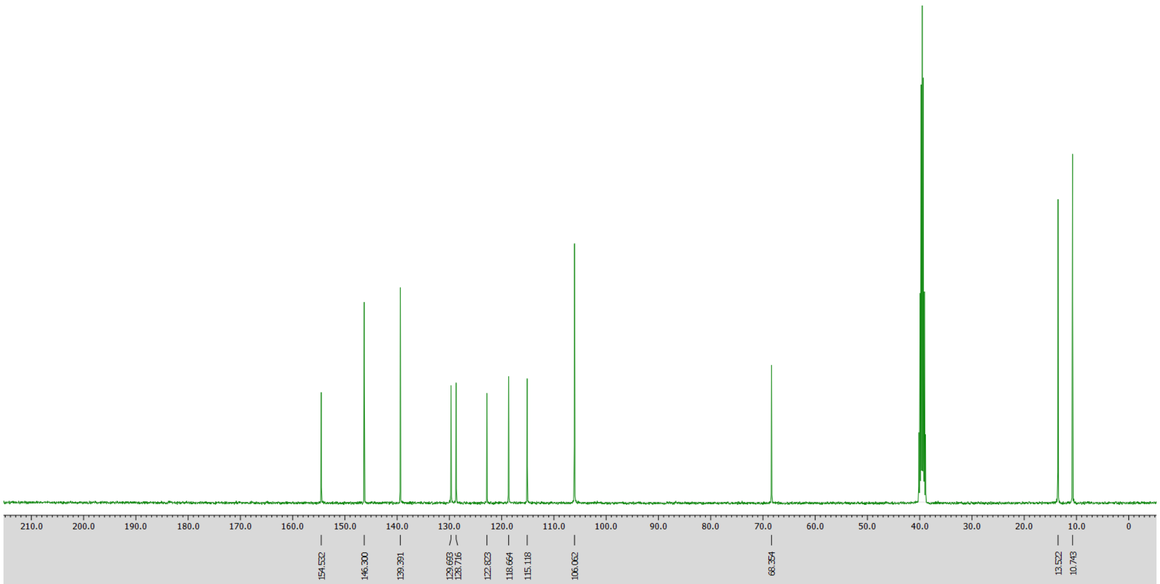

Figure S3.22. ^{13}C-NMR of **4**, DMSO-d6, 100 MHz.

S4. Synthesis of metal complex 5.

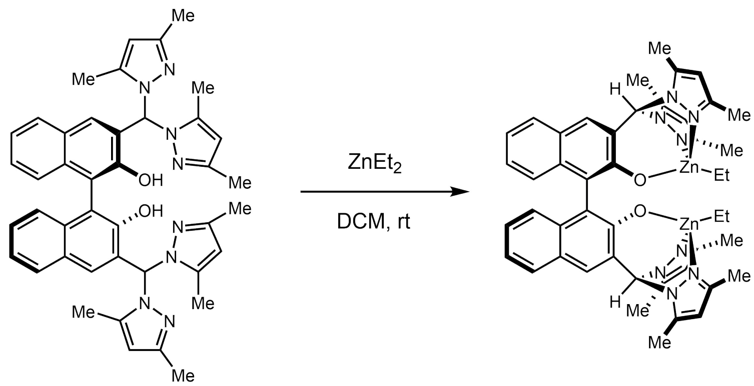

Diethyl dizinc complex with (*R*)-1-Me$_2$ (5). In a nitrogen glovebox, a vial was charged with (*R*)-**1**-Me$_2$ (100 mg, 0.145 mmol, 1 equivalent), diethylzinc (30 μL, 0.29 mmol, 2 equivalents), and dichloromethane (5 mL). After 18 hours all volatiles were removed in vacuo giving a yellow microcrystalline solid. This material was resuspended in 1:1 toluene/hexanes and filtered, rinsing with hexanes (2 x 2 mL) and drying, giving the desired material as a yellow solid (103 mg, 0.117 mmol, 81% yield). Crystals of sufficient quality for X-ray diffraction analysis were grown by dissolving the solid in a minimal amount of dichloromethane followed by storage at –37 ºC for a few days giving yellow blocks. ^{1}H-NMR (400 MHz, CD_2Cl_2) δ 7.57-7.60 (m, 4H), 7.15 (s, 2H), 6.94-6.99 (m, 6H), 5.98 (s, 2H), 5.90 (s, 2H), 2.54 (s, 6H), 2.53 (s, 6H), 2.37 (s, 6H), 2.15 (s, 6H), 0.79 (t, J = 8.1 Hz, 6H), -0.06 (q, J = 8.2 Hz, 4H). ^{13}C-NMR (101 MHz, CD_2Cl_2) δ 161.0, 151.1, 149.0, 141.0, 140.7, 135.9, 129.2, 127.6, 126.2, 125.4, 125.4, 124.5, 123.9, 119.5, 106.6, 106.0, 73.3, 12.9, 12.9, 12.1, 11.6, 11.5, –2.6. IR (Diamond ATR) 3133, 3050, 2983, 2920, 2884, 2846, 2810, 1616, 1584, 1557, 1485, 1454, 1419, 1357, 1318, 1244, 1181, 1166, 1145, 1108, 1042, 1020, 981, 943, 917, 851, 835, 780, 762, 735, 711, 695, 629, 606, 557, 528, 515, 459 cm^{-1}. Elemental analysis (based on formula $C_{46}H_{50}N_8O_2$): C (61.57% found, 62.95% expected, -1.4% difference), H (5.54% found, 5.74% expected, -0.2% difference), N (12.78% found, 12.77% expected, 0.01% difference). Note that although we could isolate a complex from racemic **1**-Me$_2$, we could not obtain diffraction-quality crystals from racemic **5**.

S5. Spectral data of metal complex 5.

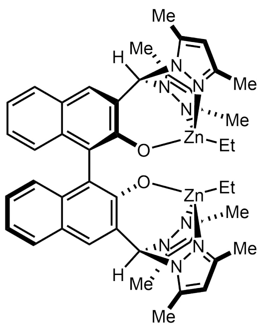

(**5**)

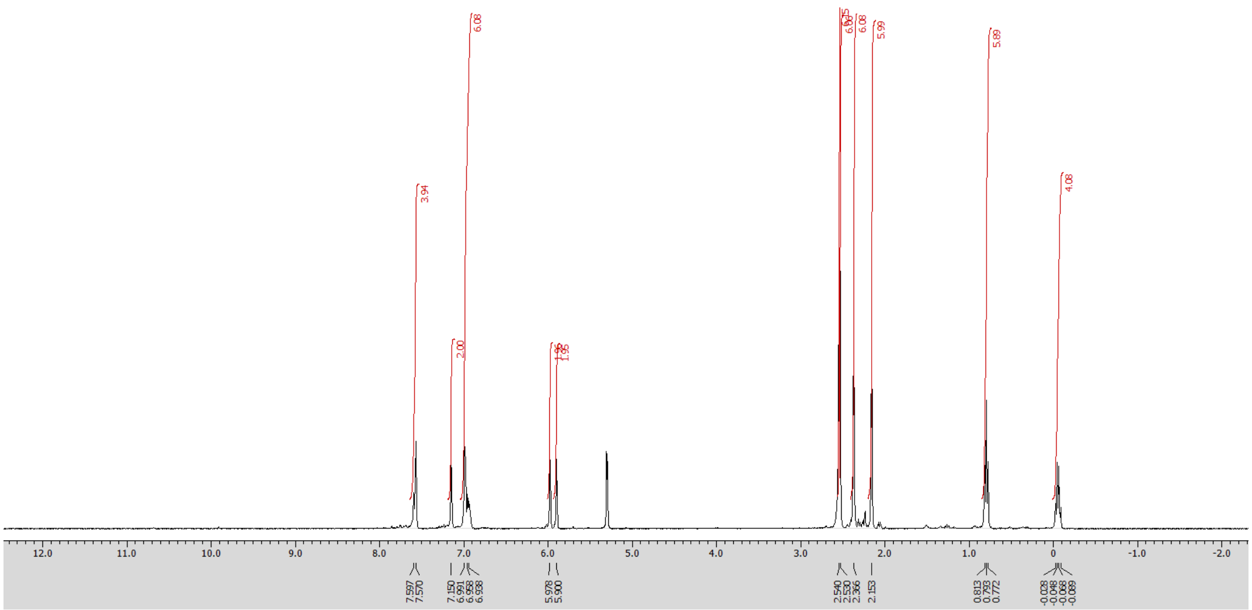

Figure S5.1. ^{1}H-NMR of **5**, CD_2Cl_2, 400 MHz.

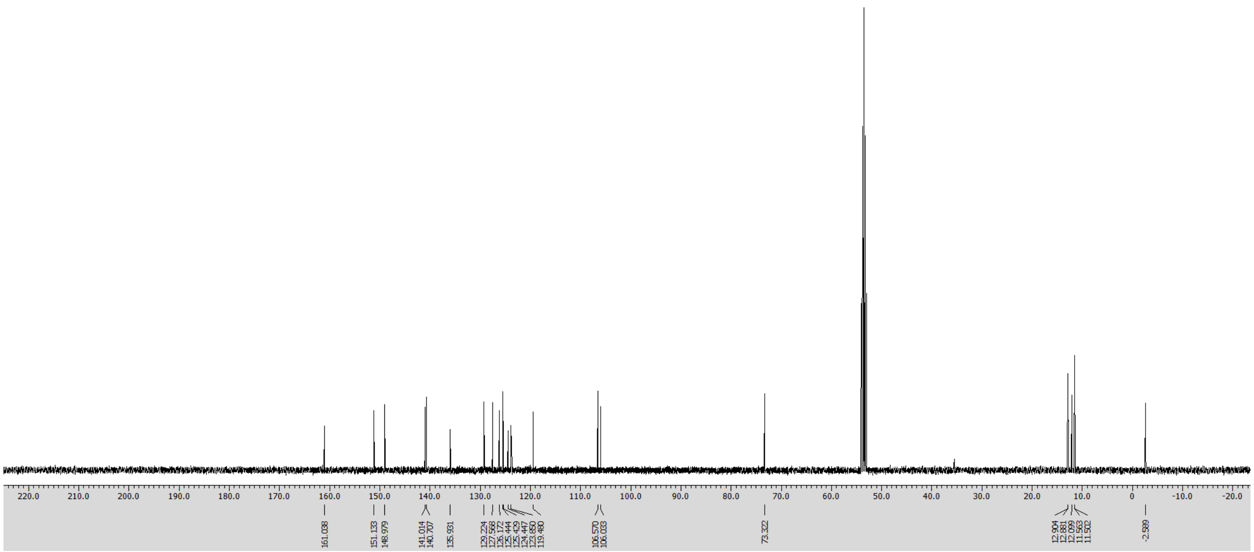

Figure S5.2. ^{13}C-NMR of **5**, CD_2Cl_2, 100 MHz.

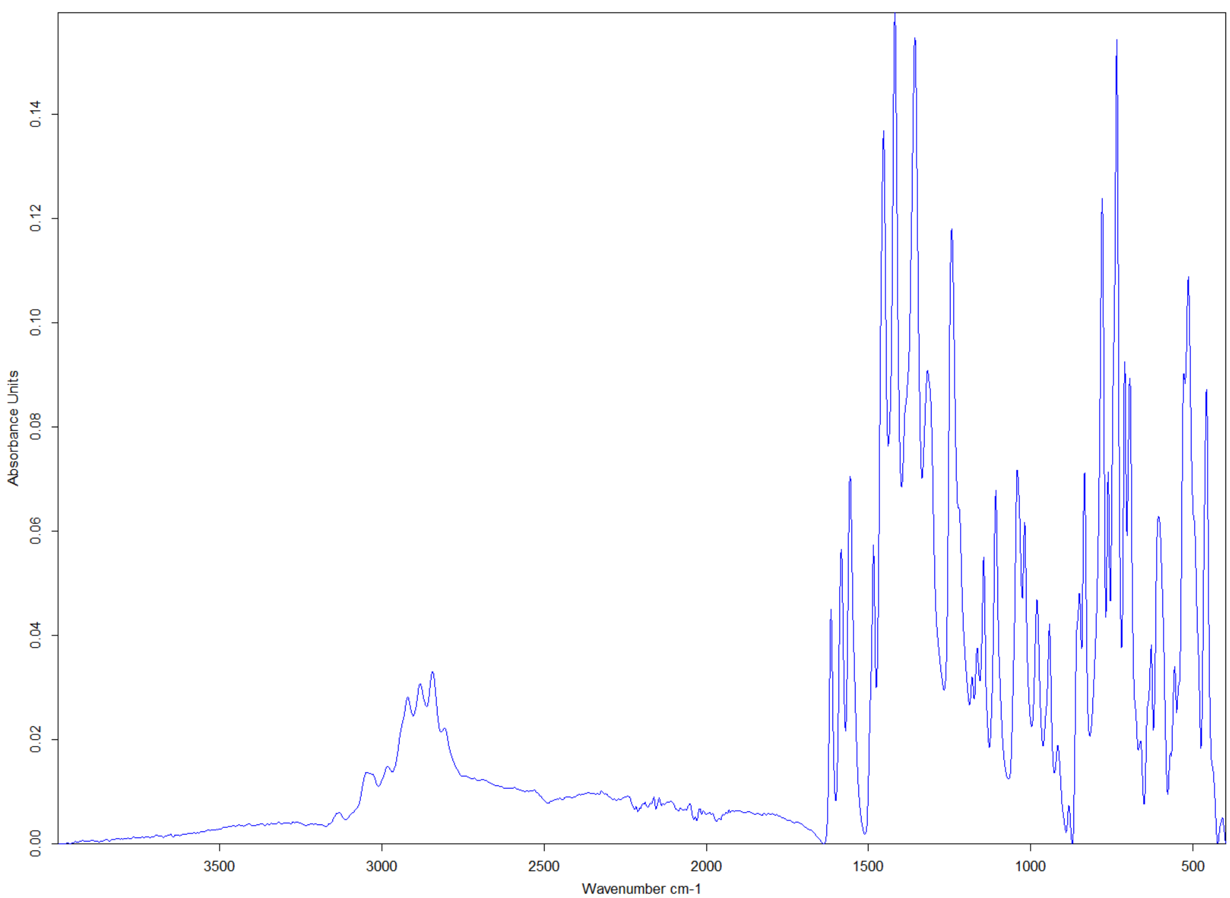

Figure S5.3. Infrared spectrum of **5**, diamond ATR.

S6. X-ray crystallography data for 5.

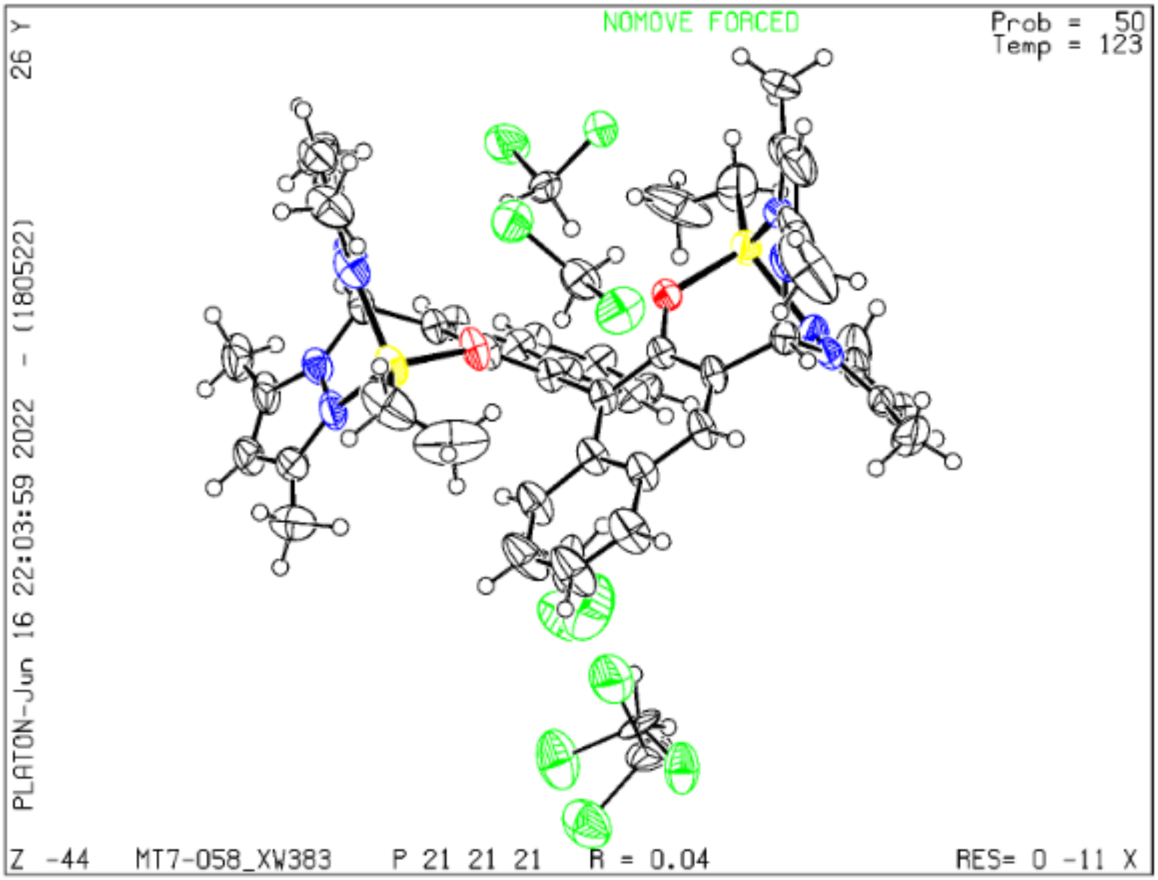

Table S6.1 Crystal data and structure refinement for complex 5.

Identification code	MT7-058_XW383
Empirical formula	$C_{50}Cl_8N_8O_2Zn_2H_{58}$
Formula weight	1217.38
Temperature/K	123(2)
Crystal system	orthorhombic
Space group	$P2_12_12_1$
a/Å	11.8551(4)
b/Å	11.8538(4)
c/Å	38.9071(11)
α/°	90
β/°	90
γ/°	90
Volume/Å^3	5467.5(3)
Z	4
ρ_{calc}g/cm^3	1.479

μ/mm^{-1}	5.050
F(000)	2504.0
Crystal size/mm^3	0.28 × 0.24 × 0.04
Radiation	CuKα (λ = 1.54178)
2Θ range for data collection/°	2.27 to 132.22
Index ranges	$-13 \le h \le 14$, $-13 \le k \le 14$, $-45 \le l \le 45$
Reflections collected	55221
Independent reflections	9444 [R_{int} = 0.0431, R_{sigma} = 0.0339]
Data/restraints/parameters	9444/624/671
Goodness-of-fit on F^2	1.076
Final R indexes [I>=2σ (I)]	R_1 = 0.0400, wR_2 = 0.1118
Final R indexes [all data]	R_1 = 0.0401, wR_2 = 0.1119
Largest diff. peak/hole / e Å^{-3}	0.62/-0.41

S7. In situ NMR analysis of 1-Me$_2$ and Mg(HMDS)$_2$ and Zn(HMDS)$_2$.

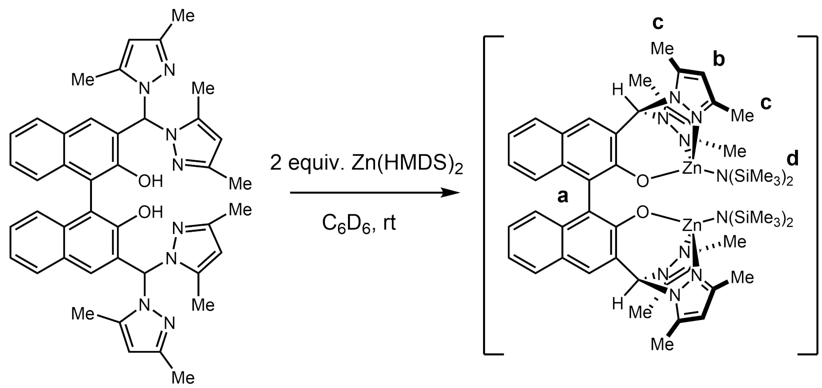

S7.1. Reaction between 1-Me$_2$ and Zn(HMDS)$_2$. In a nitrogen glovebox, **1**-Me$_2$ (25 mg, 0.036 mmol, 1 equivalent), Zn(HMDS)$_2$ (28 mg, 0.072 mmol, 2 equivalents) and benzene-d6 (2 mL) were stirred in a sealed vial for 12 hours. The resulting solution was transferred to an NMR tube and analyzed by ^{1}H-NMR. The resulting spectrum shows the clean formation of a single complex as evidenced by peaks corresponding to the proposed structure with proper peak integration. However, the expected sharp singlet for the –N(Si(C***H***$_3$)$_3$)$_2$ moiety bonded to zinc is overlapped with the signal for free HN(Si(C***H***$_3$)$_3$)$_2$ generated as a byproduct of proton exchange with **1**-Me$_2$. No significant peak corresponding to unreacted Zn(HMDS)$_2$ is observed at 0.2 ppm, indicating complete consumption of starting material and suggesting the binding of two Zn per **1-Me$_2$**.

Figure S7.1. ^{1}H-NMR of a mixture of **1-Me$_2$**, Zn(HMDS)$_2$, and C_6D_6, 400 MHz.

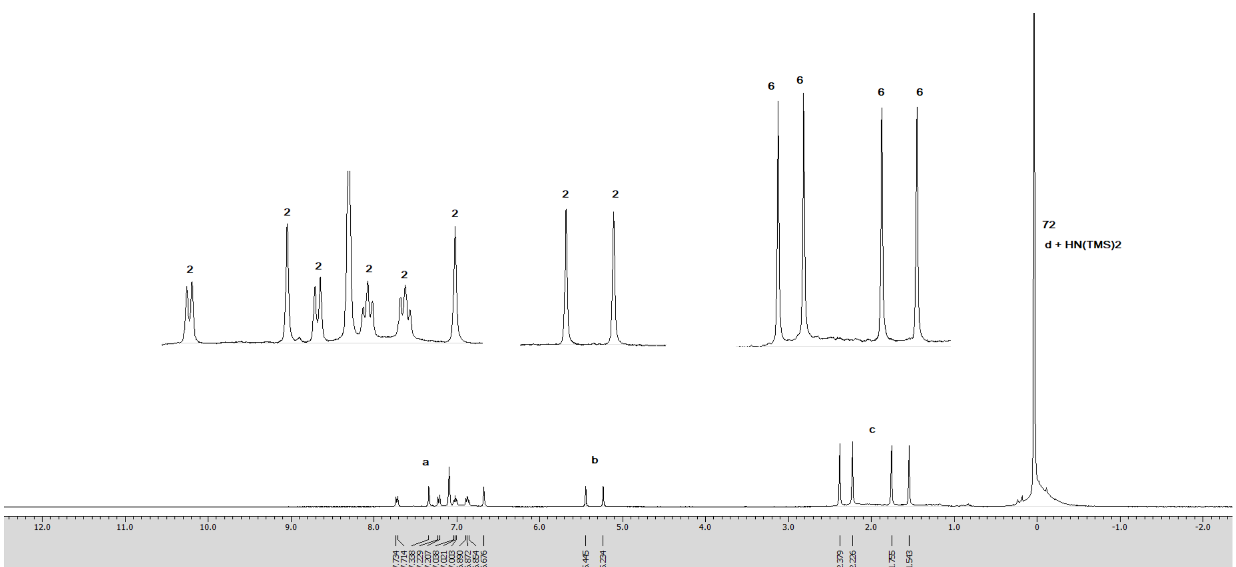

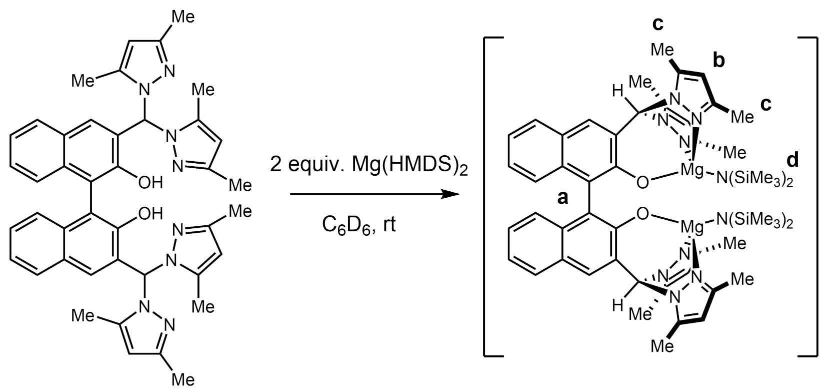

S7.2. **Reaction between 1-Me₂ and Mg(HMDS)₂**. In a nitrogen glovebox, **1**-Me_2 (25 mg, 0.036 mmol, 1 equivalent), $Mg(HMDS)_2$ (25 mg, 0.072 mmol, 2 equivalents) and benzene-d6 (2 mL) were stirred in a sealed vial for 12 hours. Then the resulting solution was transferred to an NMR tube and analyzed by ^{1}H-NMR. The resulting spectrum shows the formation of the major desired complex as evidenced by peaks corresponding to the proposed structure with correct integration. Additionally, peaks corresponding to the $–N(Si(C\boldsymbol{H}_3)_3)_2$ moiety bonded to Mg are resolved from the peaks for the $HN(Si(C\boldsymbol{H}_3)_3)_2$ byproduct. However, unlike the analogous dizinc complex (Figure S7.1), small peaks corresponding to a minor product with lower symmetry are also observed. This is in agreement with the increased tendency of Mg complexes to partake in Schlenk-type rearrangements.

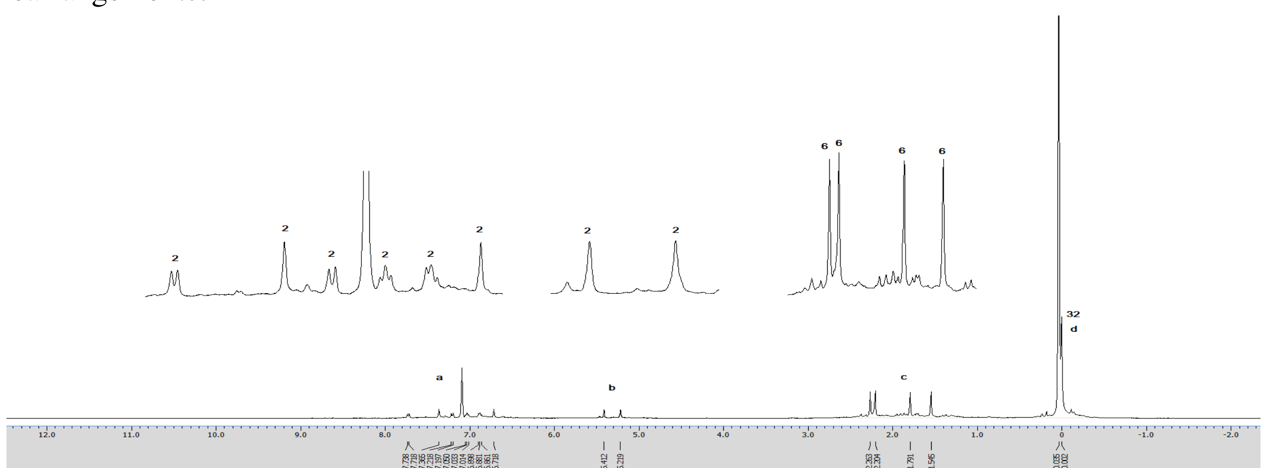

Figure S7.2. in situ ^{1}H-NMR of **1-Me₂** and $Mg(HMDS)_2$, C_6D_6, 400 MHz.

S8. Polymerization.

S8.1 Catalyst Optimization.

General procedure. In the glovebox, ligand was dissolved in a vial in anhydrous degassed CH_2Cl_2 (1 mL) and treated with $M(HMDS)_2$ ($M^{2+} = Zn^{2+}$, Mg^{2+}, Ca^{2+}). This solution was sealed and stirred vigorously for 30 minutes and then treated with alcohol as a freshly prepared stock solution in CH_2Cl_2 (1 equivalent per metal, 1% v/v). This solution was sealed again and stirred another 30 minutes. This solution was then taken by syringe or pipette and injected all at once into a rapidly stirring solution of *rac*-lactide (144 mg, 1.00 mmol, 100 equivalents per metal) in CH_2Cl_2 (2 mL) in a vial. 0.2 mL aliquots were taken at 10 minutes and 30 minutes by syringe and quenched by injecting into 0.1 M solution of benzoic acid in CH_2Cl_2. Particularly slow reactions were also run out to 24 hours and quenched by injecting into 0.1 M solution of benzoic acid in CH_2Cl_2. For particularly fast polymerizations, the first aliquot was collected after five minutes. The quenched aliquots were dried in vacuo and the resulting residue redissolved in $CDCl_3$. Assay conversions were determined by comparing the integrations for the polymer signal with remaining monomer signal in the ^{1}H-NMR spectrum. Polymer material for GPC analysis was obtained by precipitation of the quenched reaction solution from methanol at –20 ºC, filtration, and vacuum drying.

Table S8.1. Catalyst Optimization.

Entry	catalyst	alcohol	Conversion (10 min)[a]	Conversion (30 min)[a]	Conversion (24 hr)[a]	M_N[b]	M_W/M_N[b]	DP[b]
1	**1**-Me_2 + 2 $Zn(HMDS)_2$	none	0%	0%	99%	44248	1.87	307
2	**1**-Me_2 + 2 $Zn(HMDS)_2$	*p*-cresol	<1%	<1%	--	--	--	--
3	**1**-Me_2 + 2 $Zn(HMDS)_2$	TFE*	56%	90%	--	11426	1.09	79
4	**1**-Me_2 + 2 $Zn(HMDS)_2$	HFIP*	<1%	<1%	--	--	--	--
5	**1**-Me_2 + 2 $Zn(HMDS)_2$	benzyl alcohol	64%	93%	--	11340	1.08	79
6	**1**-Me_2 + 2 $Zn(HMDS)_2$	2-methoxy-ethanol	37%	77%	--	11092	1.10	77
7	**1**-Me_2 + 2 $Zn(HMDS)_2$	MeOH	28%	76%	--	13680	1.12	95
8	**1**-Me_2 + 2 $Zn(HMDS)_2$	iPrOH	45%	86%	--	11260	1.04	78
9	**1**-Me_2 + 2 $Zn(HMDS)_2$	nPrOH	72%	95%	--	13512	1.08	94
10	**1**-H + 2 $Zn(HMDS)_2$	nPrOH	47%	89%	--	12209	1.14	85
11	**1**-Ph + 2 $Zn(HMDS)_2$	nPrOH	7%	21%	99%	17460	1.84	121

12	**1**-iPr + 2 $Zn(HMDS)_2$	nPrOH	20%	67%	99%	17880	1.08	124
13	**4** + $Zn(HMDS)_2$	nPrOH	29%	69%	--	8945	1.05	62
14	$Zn(HMDS)_2$ only	nPrOH	0%	2%	58%	4308	1.33	30
15	**5** (ethylzinc complex)	none	0%	0%	3%	--	--	--
16	**5** (ethylzinc complex)	n-propanol	0%	<1%	34%	4162	1.03	29
17	**1**-Me_2 + 2 $Mg(HMDS)_2$	none	7%	42%	97%	12271	1.71	85
18	**1**-Me_2 + 2 $Mg(HMDS)_2$	nPrOH	60%[d]	98%	--	17333	1.45	120
19	**4** + $Mg(HMDS)_2$	nPrOH	8%[d]	29%	--	4518	1.05	31
20	$Mg(HMDS)_2$ only	nPrOH	20%	96%	99%	12955	2.06	90
21	**1**-Me_2 + 2 $Ca(HMDS)_2(THF)_2$	none	21%	25%	25%	2147	1.99	15
22	**1**-Me_2 + 2 $Ca(HMDS)_2(THF)_2$	nPrOH	16%	37%	--	4221	1.06	29
23	**4** + $Ca(HMDS)_2(THF)_2$	nPrOH	19%	44%	--	5682	1.11	39
24	$Ca(HMDS)_2(THF)_2$ only	nPrOH	43%	54%	--	3356	1.47	23

Conditions as in section S8.1. [a]Conversions obtained by ^{1}H-NMR assay by integrating the polymer methine region relative to the signal for unreacted monomer. [b]Number-average molecular weight (M_N), polydispersity index (M_M/M_N), and degree of polymerization by gel permeation chromatography using the Mark-Houwink correction factor 0.58 for M_N. [d]Conversion measured at 5 minutes reaction time instead of 10 minutes.

4 = 2-*bis*(3,5-dimethylpyrazol-1-yl)methylphenol
*HFIP = hexafluoroisopropanol, TFE = trifluoroethanol

S8.2 Stereoselectivity.
General procedure. Polymer was prepared by the same method as in **S8.1**.
Assignment of P_r values was done by the comparison of integrated methine signals in the homodecoupled ^{1}H-NMR spectrum by the equation $P_r = 2I_1/(I_1 + I_2)$, where I_1 is the integration interval from 5.20-5.25 ppm and I_2 is the integration interval from 5.13-5.20 ppm, and represents the probability that an incoming monomer unit forms an *r* linkage upon propagation[7].

[7] Chamberlain, B. M.; Cheng, M.; Moore, D. R.; Ovitt, T. M.; Lobkovsky, E. B.; Coates, G. W. *J. Am. Chem. Soc.* **2001**, *123*, 3229.

Polymerization of *l*-lactide gave clearly isotactic poly(lactide) with no signs of racemization in all cases which is represented by $P_m > 0.99$.

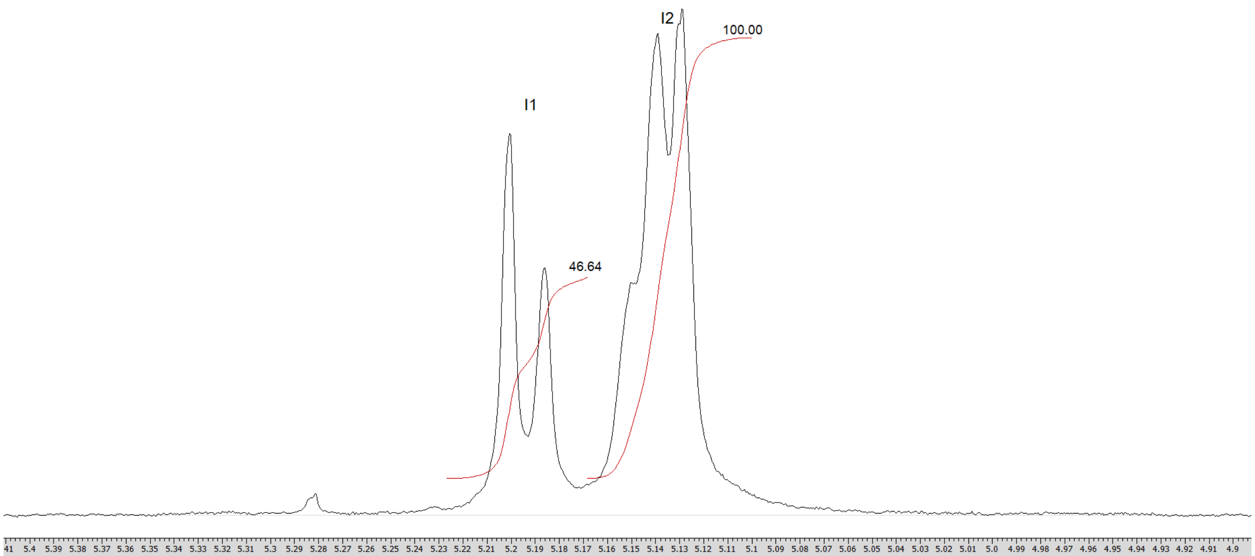

Figure S8.1. Sample homodecoupled ^{1}H NMR spectrum (400 MHz) of poly(*rac*-lactide).

Table S8.2. Polymerization of various lactides.

Entry	Catalyst	Monomer	Conversion (24 h)[a]	Tacticity[b]	M_N[c]	M_M/M_N[c]	DP[c]
1	**1**-Me$_2$ + 2 Zn(HMDS)$_2$ + 2 nPrOH	*rac*-lactide	95%	P_r = 0.63	13510	1.08	94
2	**1**-Me$_2$ + 2 Mg(HMDS)$_2$ + 2 nPrOH	*rac*-lactide	98%	P_r = 0.58	17330	1.45	120
3	**4** + Zn(HMDS)$_2$ + nPrOH	*rac*-lactide	69%	P_r = 0.55	4308	1.33	30
4	**4** + Mg(HMDS)$_2$ + nPrOH	*rac*-lactide	99%	P_r = 0.51	12955	2.06	90
5	(*R*)-**1**-Me$_2$ + 2 Zn(HMDS)$_2$ + 2 nPrOH	*l*-lactide	99%	P_m > 0.99	13425	1.52	93
6	(*R*)-**1**-Me$_2$ + 2 Mg(HMDS)$_2$ + 2 nPrOH	*l*-lactide	99%	P_m > 0.99	12813	1.96	89
7	(*S*)-**1**-Me$_2$ + 2 Zn(HMDS)$_2$ + 2 nPrOH	*l*-lactide	99%	P_m > 0.99	14236	1.30	99
8	(*S*)-**1**-Me$_2$ + 2 Mg(HMDS)$_2$ + 2 nPrOH	*l*-lactide	99%	P_m > 0.99	16705	2.19	116
9	(*R*)-**1**-Me$_2$ + 2 Zn(HMDS)$_2$ + 2 nPrOH	*meso*-lactide	100%	P_r = 0.52	3862	1.50	27
10	(*R*)-**1**-Me$_2$ + 2 Mg(HMDS)$_2$ + 2 nPrOH	*meso*-lactide	100%	P_r = 0.62	6191	1.47	43
11	**4** + Zn(HMDS)$_2$ + nPrOH	*meso*-lactide	99%	P_r = 0.52	9928	3.76	69
12	**4** + Mg(HMDS)$_2$ + nPrOH	*meso*-lactide	99%	P_r = 0.51	14189	1.24	98

Conditions as in Section S8.2. [a]Conversions obtained by ^{1}H-NMR assay by integrating the polymer methine region relative to the signal for unreacted monomer. [b]Isolated tacticity obtained by ^{1}H-NMR as described in section S8.2. [c]Number-average molecular weight (M_N), polydispersity index (M_M/M_N), and degree of polymerization by gel permeation chromatography using the Mark-Houwink correction factor 0.58 for M_N.

S8.3. Block Copolymerization.

ε-caprolactone homopolymerization general procedure. In the glovebox, **1**-Me_2 (3.5 mg, 0.005 mmol, 1 equivalent) was dissolved in a vial in anhydrous de-gassed CH_2Cl_2 (1 mL) and treated with $M(HMDS)_2$ ($M^{2+} = Zn^{2+}$, Mg^{2+}). This solution was sealed and stirred vigorously for 30 minutes and then treated with alcohol as a freshly prepared stock solution in CH_2Cl_2 (1 equiv. per metal, 1% v/v). This solution was sealed again and stirred another 30 minutes. This solution was then taken by syringe or pipette and injected all at once into a rapidly stirring solution of ε-caprolactone (111 μL, 1.00 mmol, 100 equivalents per metal) in CH_2Cl_2 (2 mL) in a vial. The reaction was stirred for 24 hours and then an aliquot for NMR analysis was withdrawn and quenched using 0.1 M benzoic acid in CH_2Cl_2 solution. The reaction mixture was then similarly quenched. The quenched aliquot was dried in vacuo and the resulting residue redissolved in $CDCl_3$. Assay conversions in ε-caprolactone were determined by comparing the polymer signal to the residual monomer signal in the ^1H NMR spectrum. Polymer material for GPC analysis was obtained by precipitation of the quenched reaction solution from methanol at -20 ºC, filtration, and drying in vacuo.

Copolymerization general procedure. In a nitrogen glovebox, a solution of **1**-Me_2 (3.5 mg, 0.005 mmol, 1 equivalent) and CH_2Cl_2 (1 mL) was treated with $M(HMDS)_2$ ($M^{2+} = Zn^{2+}$ or Mg^{2+}). This solution was sealed and stirred vigorously for 30 minutes and then treated with alcohol as a freshly prepared stock solution in CH_2Cl_2 (1 equivalent per metal, 1% v/v). This solution was sealed again and stirred for another 30 minutes, and then injected all at once into a rapidly stirring solution of monomer 1 (1.00 mmol, 100 equivalents per metal) in CH_2Cl_2 (2 mL) in a vial. This solution was then stirred for 3 hours and then monomer 2 (1.00 mmol, 100 equivalents per metal) was added either neat (ε-caprolactone) or as a solution in CH_2Cl_2 (1 mL) (*l*-lactide). This solution was stirred for an additional 3 hours and then quenched by injecting several drops of 0.1 M benzoic acid solution in CH_2Cl_2. An aliquot for NMR analysis was withdrawn and dried in vacuo and the resulting residue redissolved in $CDCl_3$. Assay conversions were determined by comparing the integrations for the polymer signals with remaining respective monomer signals in the ^1H NMR spectrum. Polymer material for GPC analysis was obtained by precipitation of the quenched reaction solution from methanol at -20 ºC, filtration, and drying in vacuo.

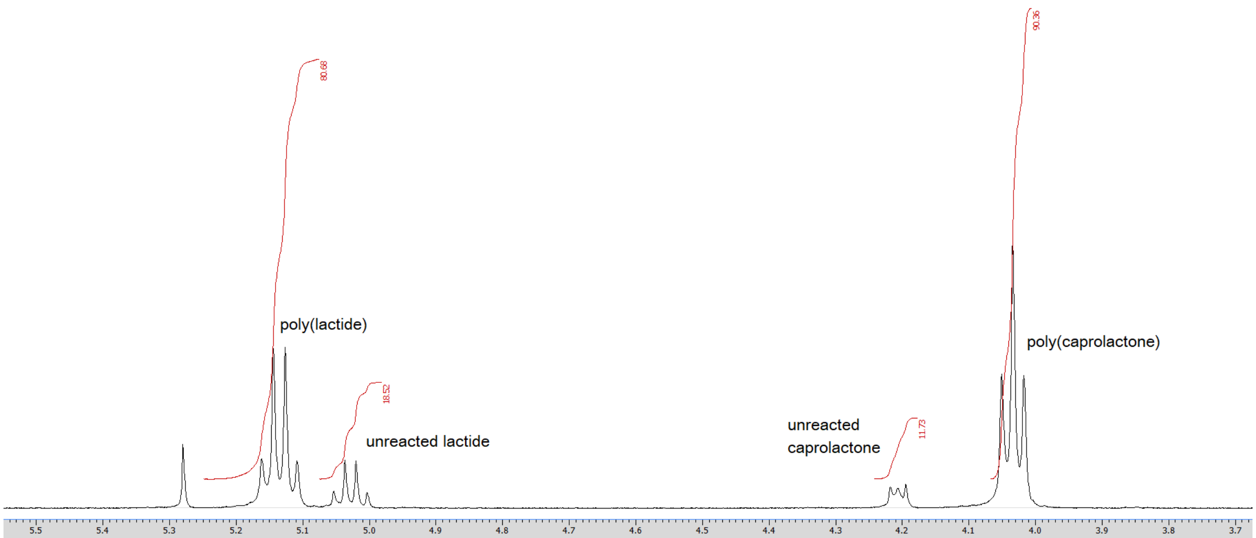

Figure S8.3. Sample [1]H-NMR spectrum of poly(ε-caprolactone-*co*-lactide) showing diagnostic signals.

Table S8.3. Block copolymerization.

Entry	Catalyst	First monomer	% conversion of first monomer[a]	Second monomer	% conversion of second monomer[a]	M_N[b]	M_M/M_N[b]
1	**1**-Me_2 + 2 $Zn(HMDS)_2$ + 2 nPrOH	ε-caprolactone	85%	none	--	6800	1.09
2	**1**-Me_2 + 2 $Zn(HMDS)_2$ + 2 nPrOH	ε-caprolactone	83%	*l*-lactide	72%	19900	1.08
3	**1**-Me_2 + 2 $Zn(HMDS)_2$ + 2 nPrOH	*l*-lactide	95%	ε-caprolactone	0%	16200	1.22
4	**1**-Me_2 + 2 $Mg(HMDS)_2$ + 2 nPrOH	ε-caprolactone	91%	none	--	8900	1.06
5	**1**-Me_2 + 2 $Mg(HMDS)_2$ + 2 nPrOH	ε-caprolactone	90%	*l*-lactide	80%	28800	1.12
6	**1**-Me_2 + 2 $Mg(HMDS)_2$ + 2 nPrOH	*l*-lactide	96%	ε-caprolactone	0%	16100	1.74

[a]Assay conversion. [b]Number-average molecular weight (M_N), polydispersity index (M_M/M_N), and degree of polymerization by gel-permeation chromatography using the correction factors 0.58 for poly(lactide) and 0.56 for poly(ε-caprolactone).

S8.4. In situ ^{1}H-NMR analysis of 1-Me$_2$/Zn(HMDS)$_2$/nPrOH and 1-Me$_2$/Zn(HMDS)$_2$/nPrOH/lactide.

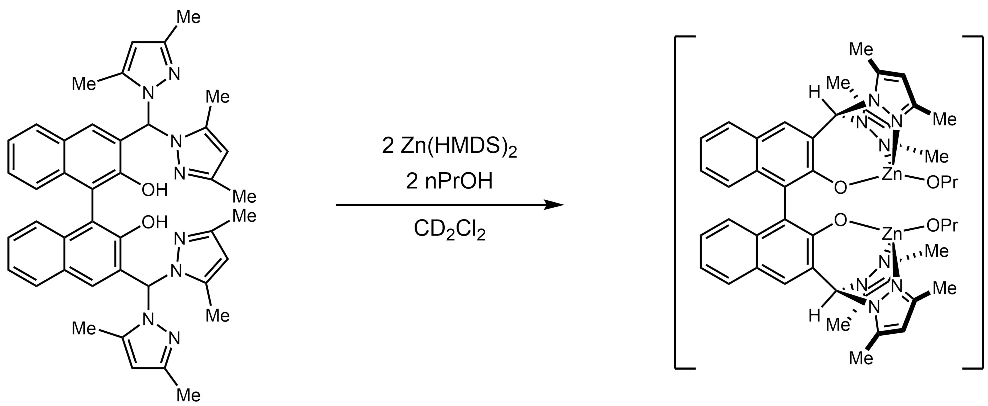

1-Me$_2$/Zn(HMDS)$_2$/nPrOH. In a nitrogen glovebox, **1**-Me$_2$ (10 mg, 0.014 mmol, 1 equivalent), Zn(HMDS)$_2$ (11.3 uL, 0.028 mmol, 2 equivalents) and methylene chloride-*d*2 (0.75 mL) were combined in a vial. After stirring for 30 minutes, nPrOH was added as a freshly prepared stock solution in methylene chloride-*d*2 (3% v/v; 933 uL, 2 equivalents) by micropipette, and then stirred another 30 minutes. The resulting solution was transferred into an airtight NMR tube and immediately analyzed. The ^{1}H-NMR spectrum is shown below:

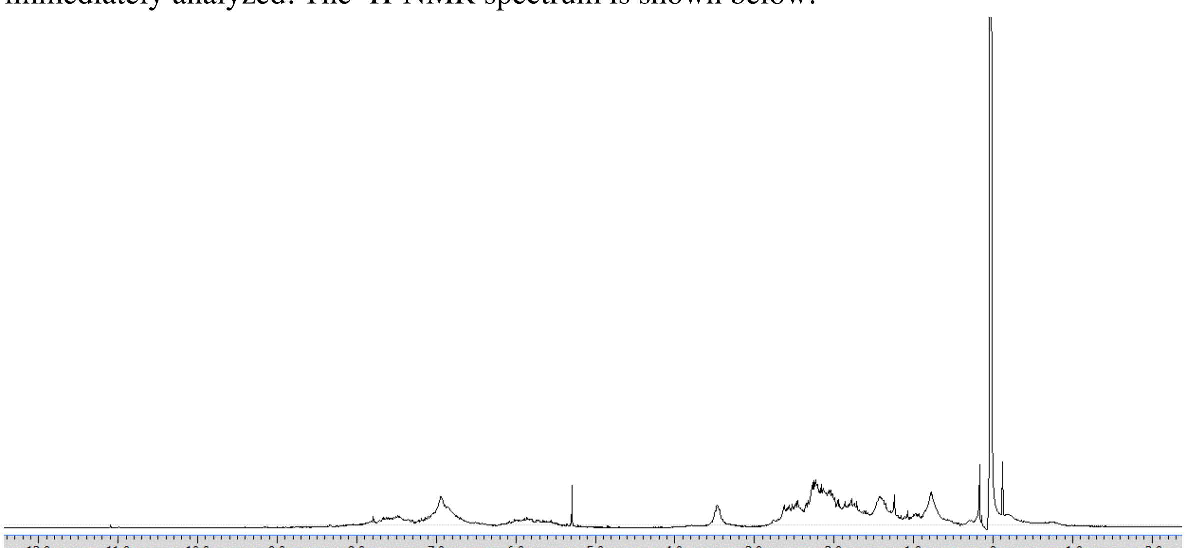

Figure S8.4. ^{1}H-NMR spectrum of in situ-prepared **1**-Me$_2$/Zn(HMDS)$_2$/nPrOH in methylene chloride-*d*2.

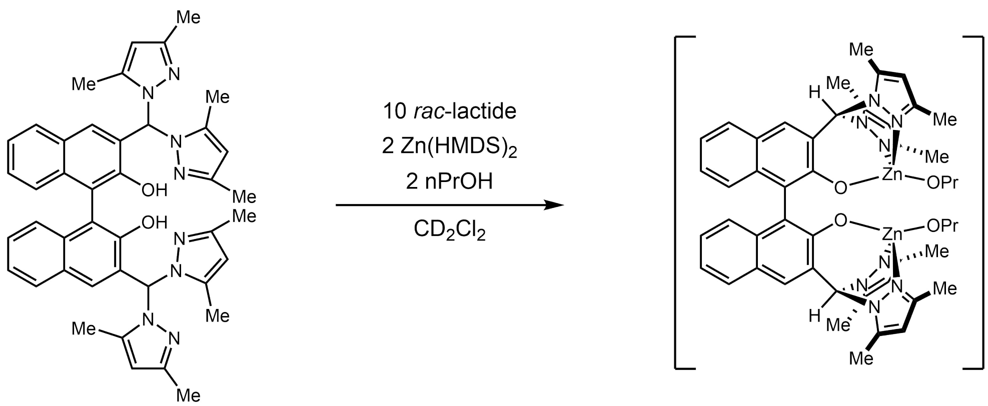

1-Me$_2$/Zn(HMDS)$_2$/nPrOH/DL-lactide. In a nitrogen glovebox, **1**-Me$_2$ (10 mg, 0.014 mmol, 1 equivalent), Zn(HMDS)$_2$ (11.3 uL, 0.028 mmol, 2 equivalents) and methylene chloride-*d*2 (0.75 mL) were combined in a vial. After stirring for 30 minutes, nPrOH was added as a freshly prepared stock solution in methylene chloride-*d*2 (3% v/v; 933 uL, 2 equivalents) by micropipette, and then stirred another 30 minutes. Then, DL-lactide (20 mg, 0.14 mmol, 10 equivalents) was added to the solution as a solid. This solution was transferred into an NMR tube and immediately analyzed. The ^{1}H-NMR spectrum is shown below:

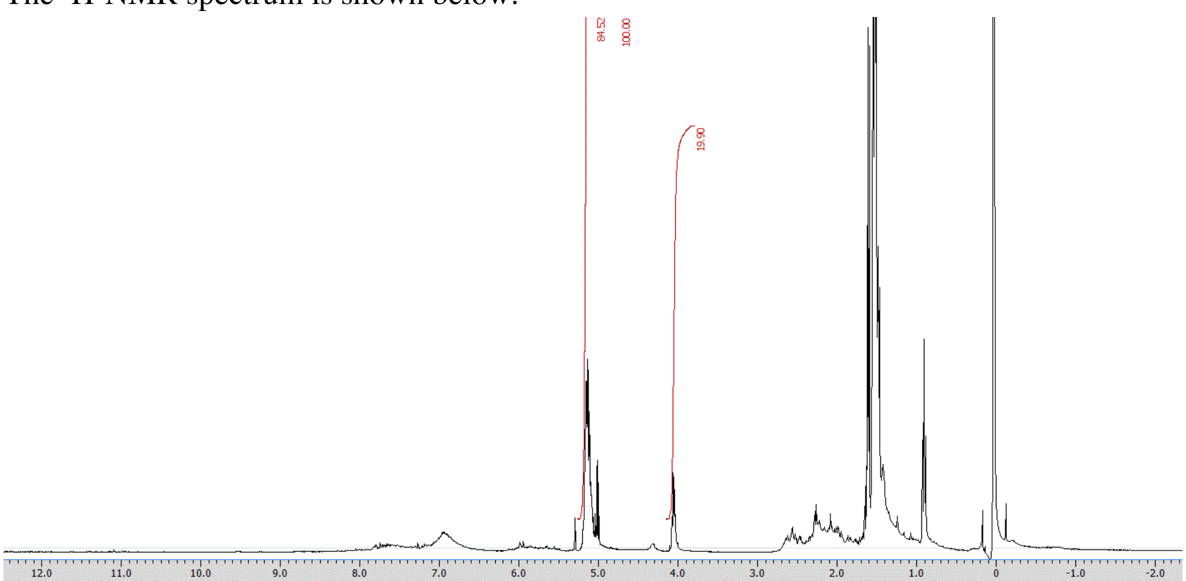

Figure S8.5. ^{1}H-NMR spectrum of in situ-prepared **1**-Me$_2$/Zn(HMDS)$_2$/nPrOH/DL-lactide in methylene chloride-*d*2.

S9. Chromatograms and physical characterization data for polymers.

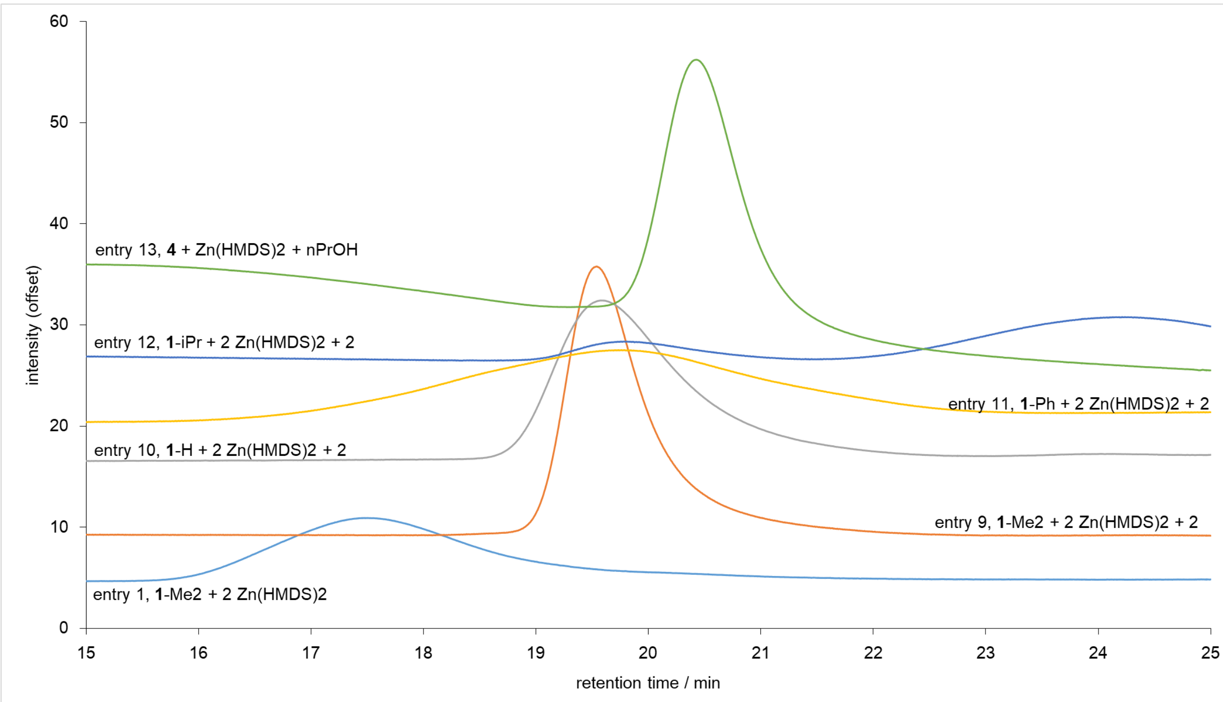

Figure S9.1. GPC Analyses from zinc-catalyst optimization (From Section S8.1).

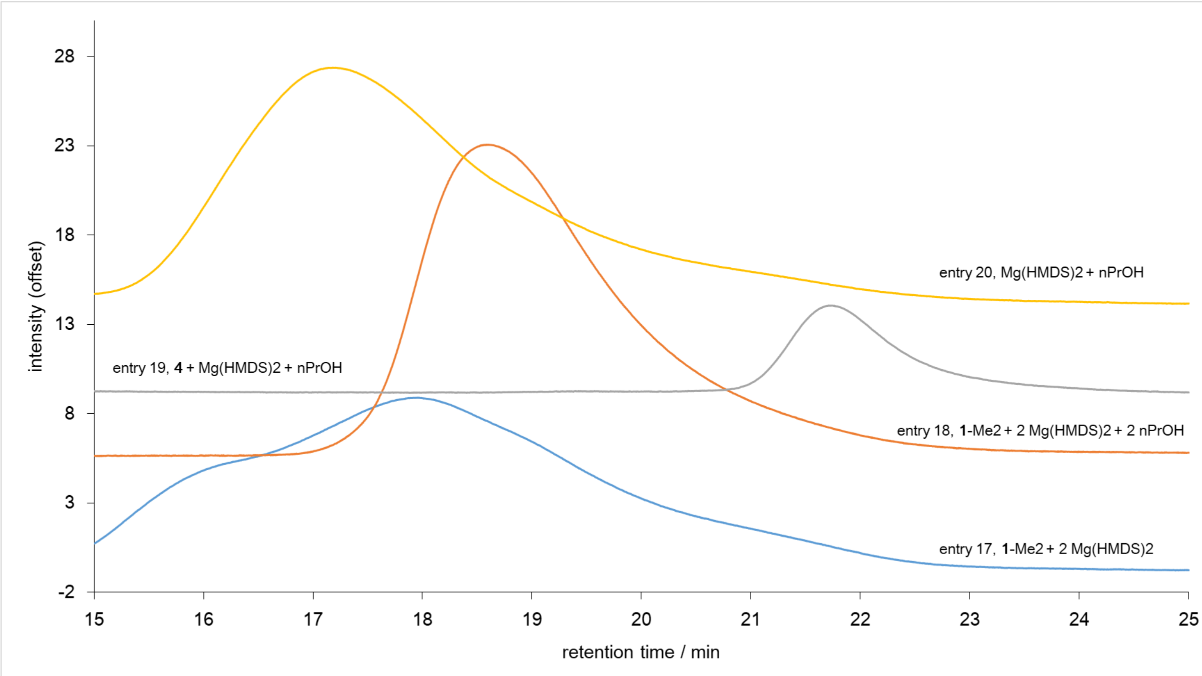

Figure S9.2. GPC Analyses from magnesium-catalyst optimization (From Section S8.1).

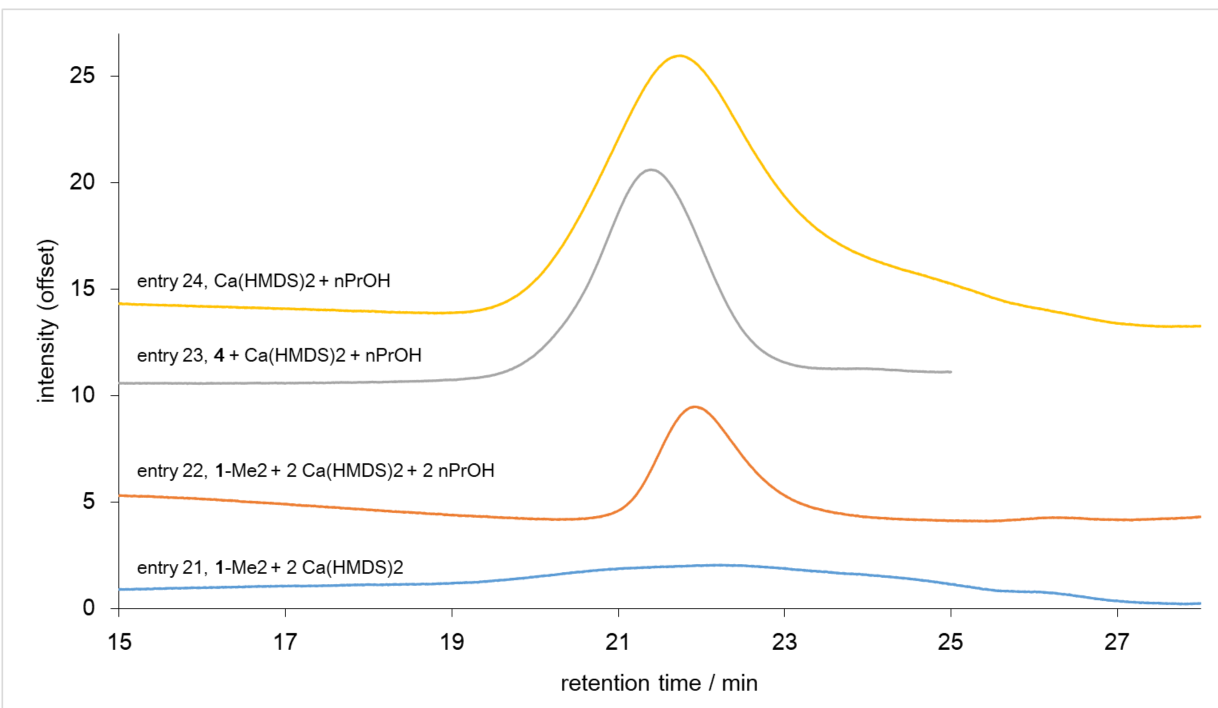

Figure S9.3. GPC Analyses from calcium-catalyst optimization (From Section S8.1).

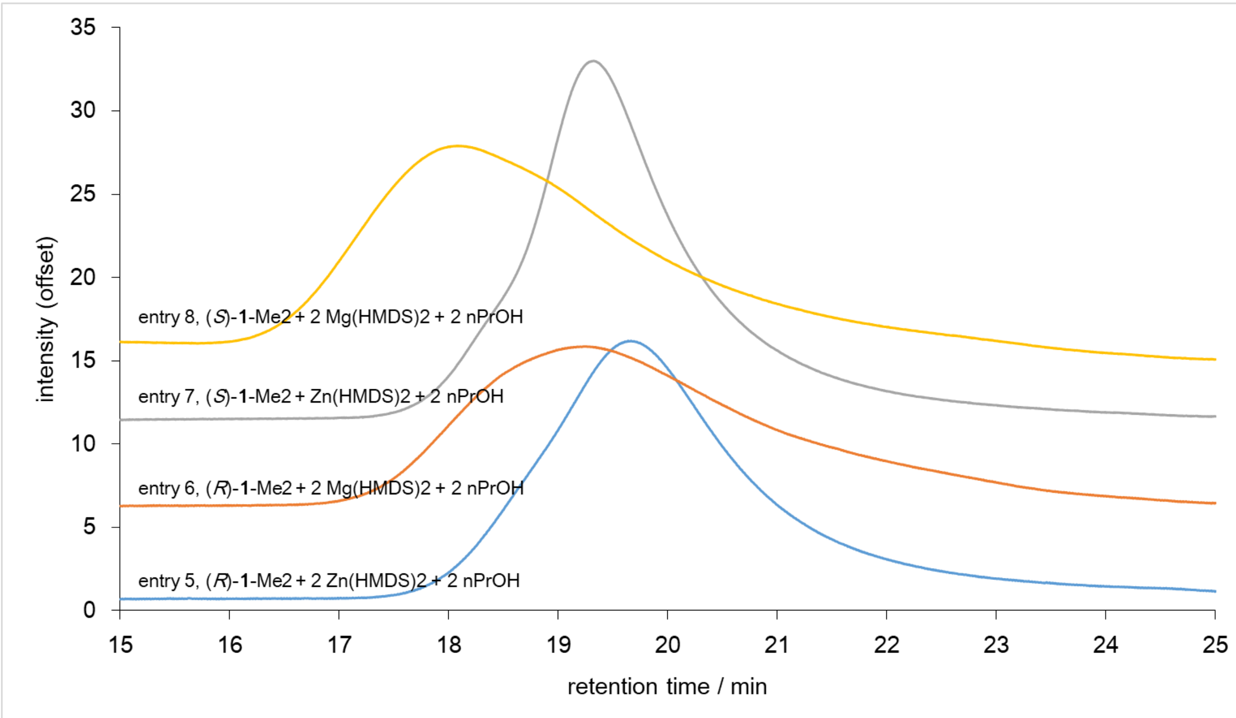

Figure S9.4. GPC Analyses from *l*-lactide polymerization (From Section S8.2).

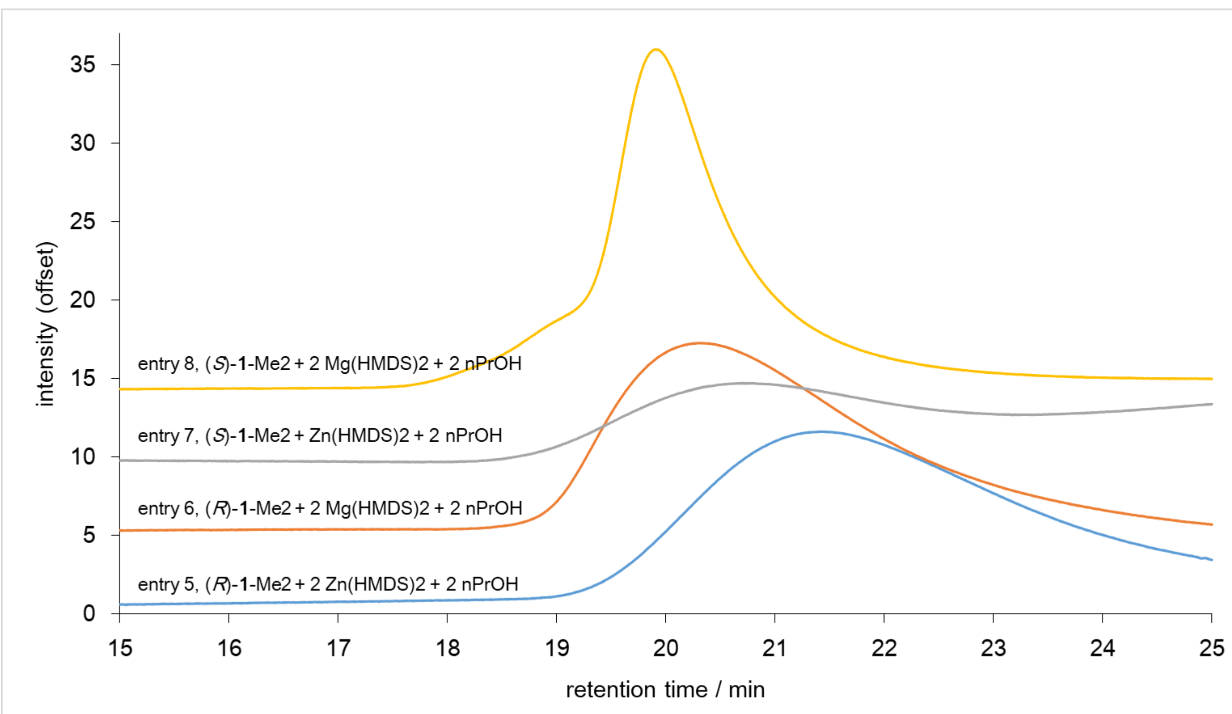

Figure S9.5. GPC Analyses from *meso*-lactide polymerization (From Section S8.2).

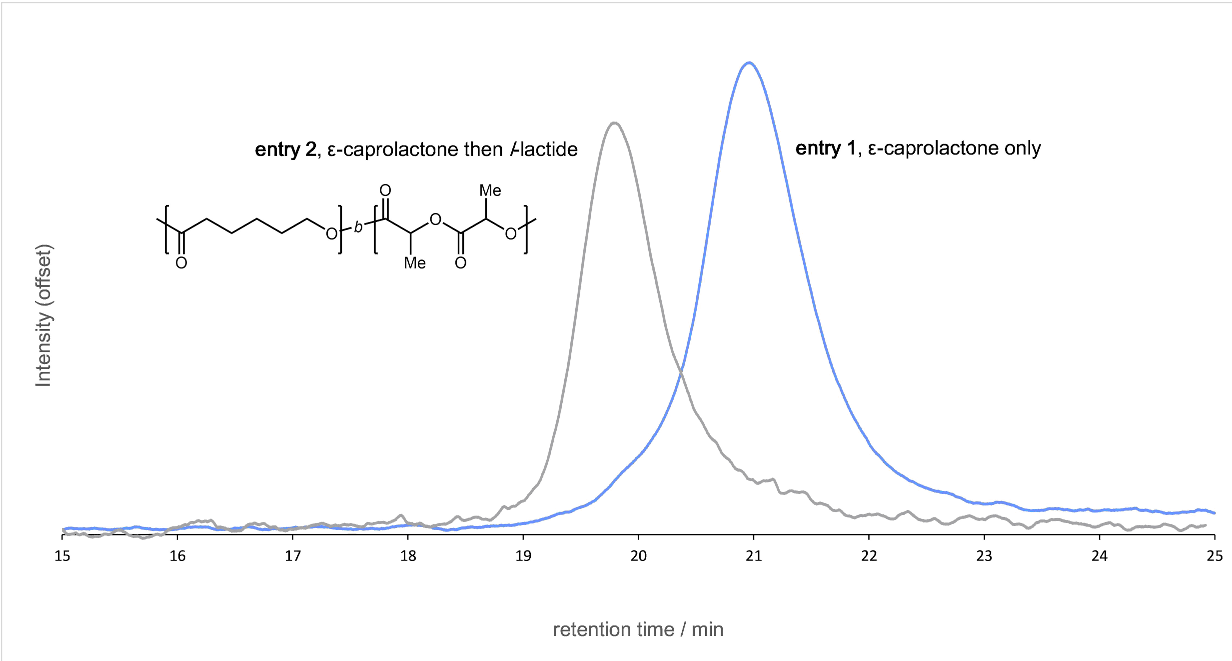

Figure S9.6. GPC Analyses from block copolymerization of ε-caprolactone and then *l*-lactide with zinc (From Section S8.3).

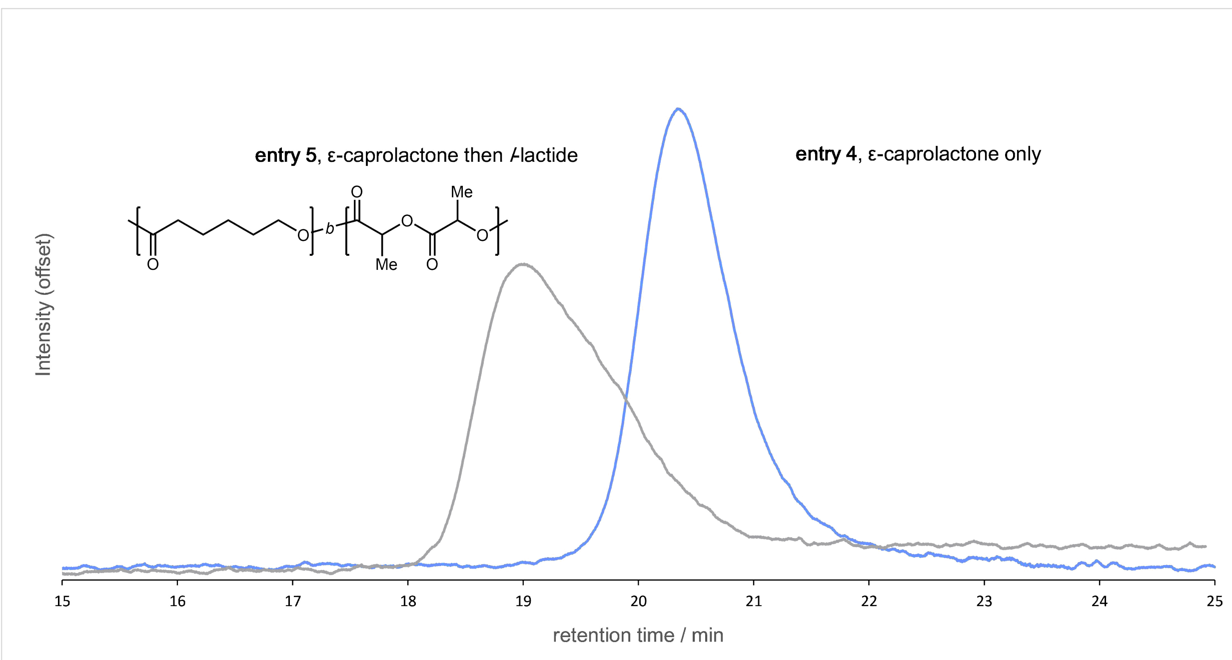

Figure S9.7. GPC Analyses from block copolymerization of ε-caprolactone and then *l*-lactide with magnesium (From Section S8.3).

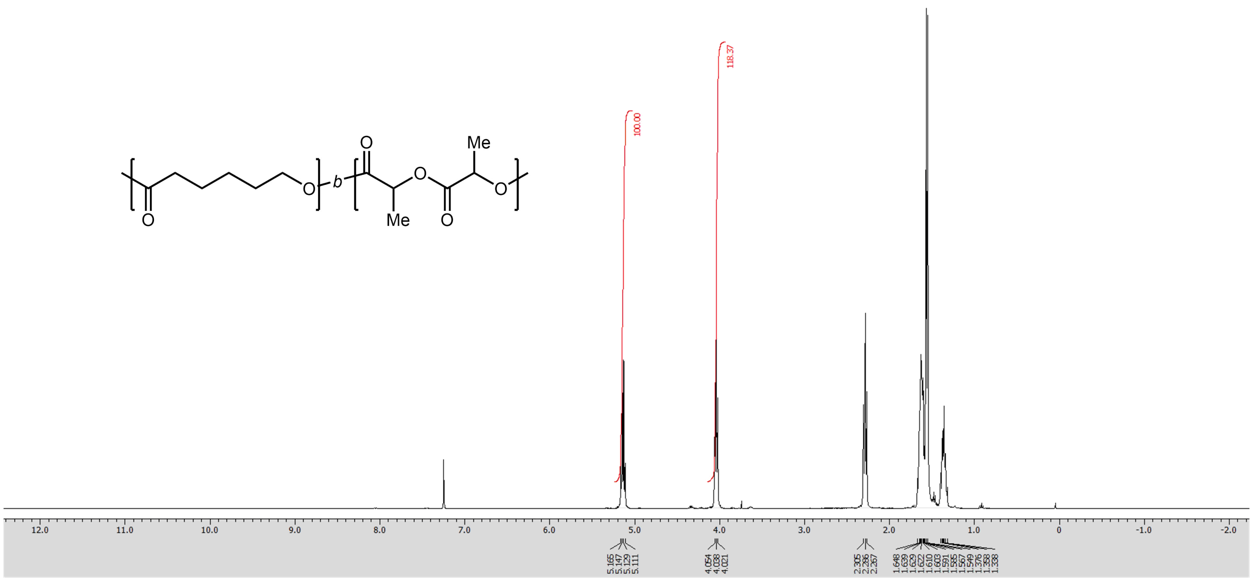

Figure S9.8. ^{1}H-NMR analysis of block copolymer prepared by **1**-Me_2, 2 $Zn(HMDS)_2$, and 2 nPrOH, $CDCl_3$, 400 MHz

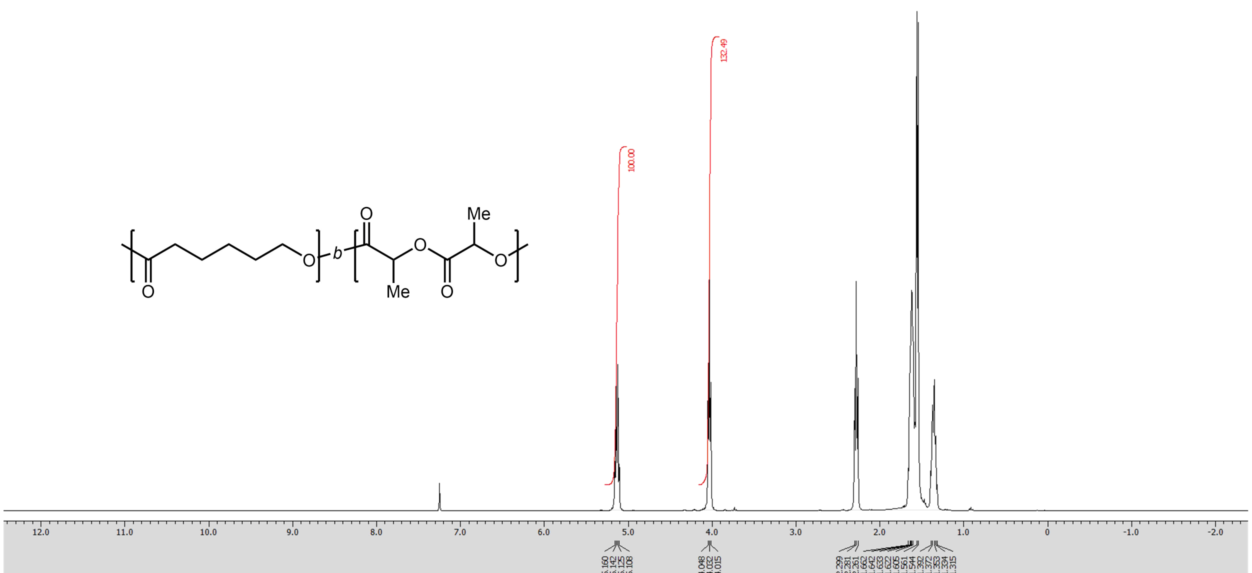

Figure S9.9. ^{1}H-NMR analysis of block copolymer prepared by **1**-Me_2, 2 $Mg(HMDS)_2$, and 2 nPrOH, $CDCl_3$, 400 MHz

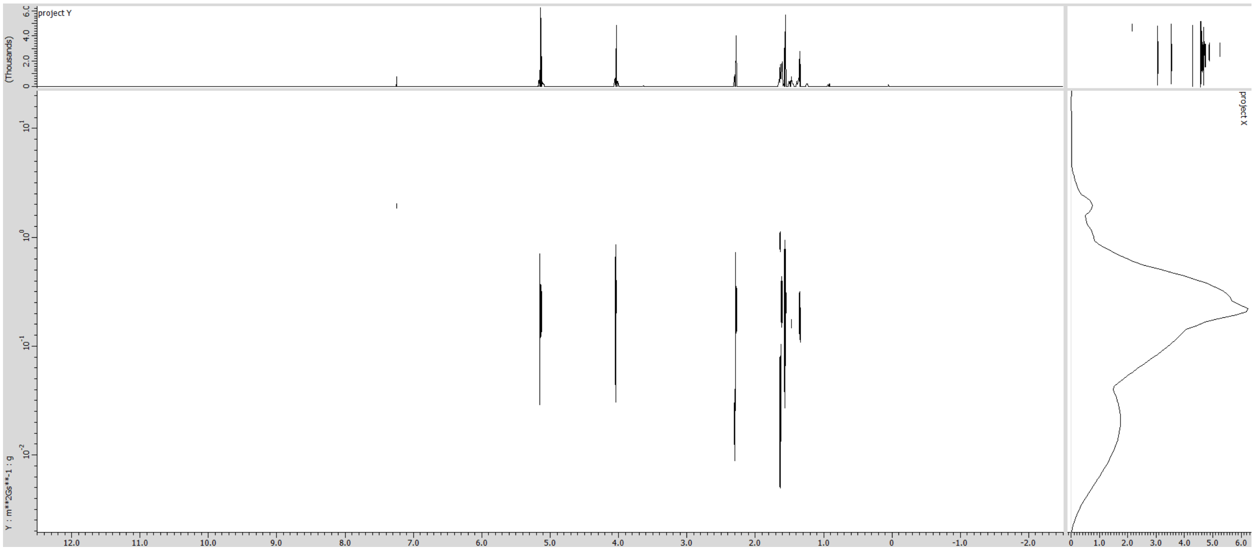

Figure S9.10. ^{1}H-DOSY NMR analysis of block copolymer prepared by **1**-Me_2, 2 $Zn(HMDS)_2$, and 2 nPrOH, $CDCl_3$, 400 MHz

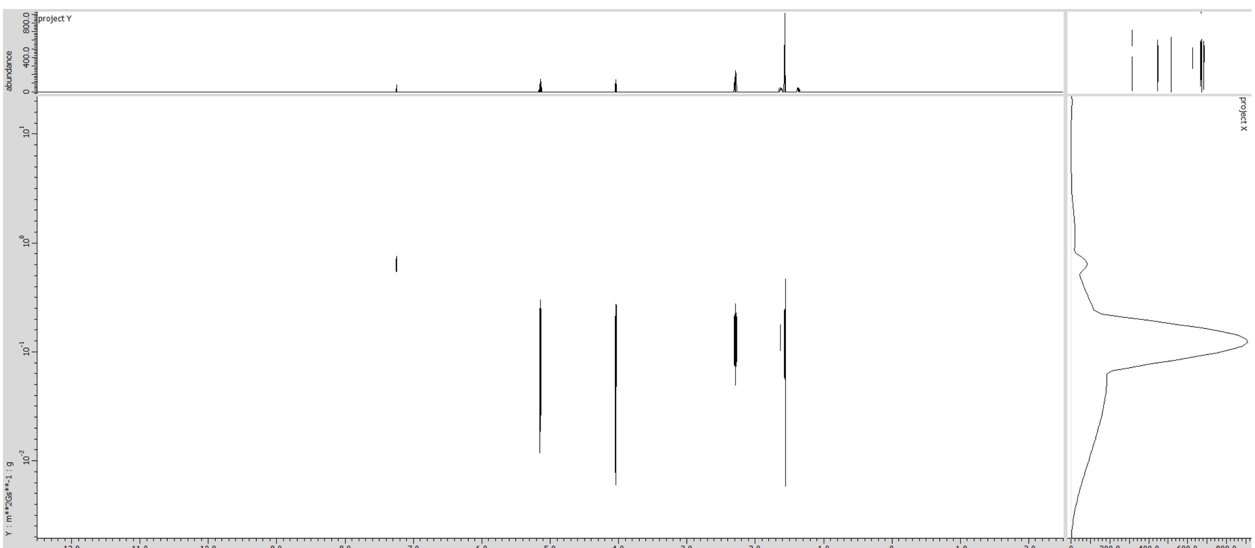

Figure S9.11. ^{1}H-DOSY NMR analysis of block copolymer prepared by **1**-Me_2, 2 $Mg(HMDS)_2$, and 2 nPrOH, $CDCl_3$, 400 MHz

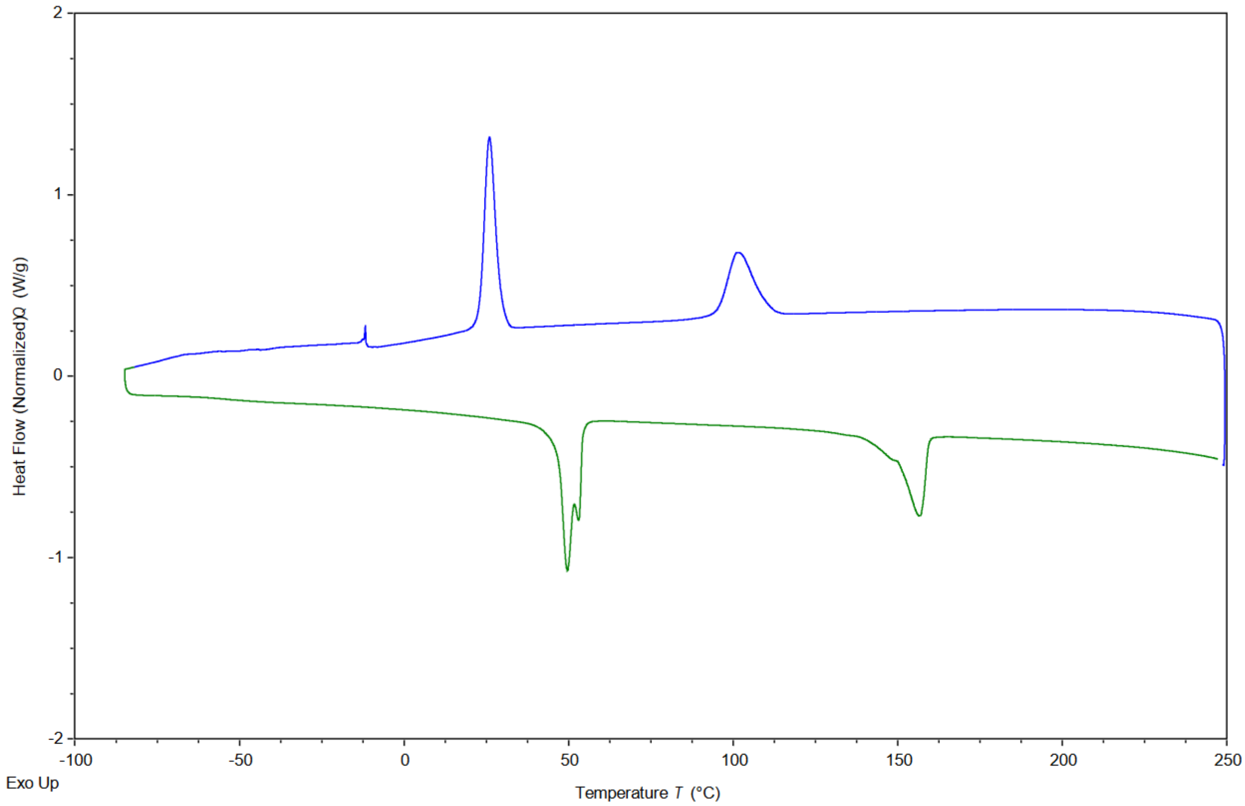

Figure S9.12. DSC heat-cool-heat trace (first heat cycle not shown) of block copolymer prepared by **1**-Me_2, 2 $Zn(HMDS)_2$, and 2 nPrOH,

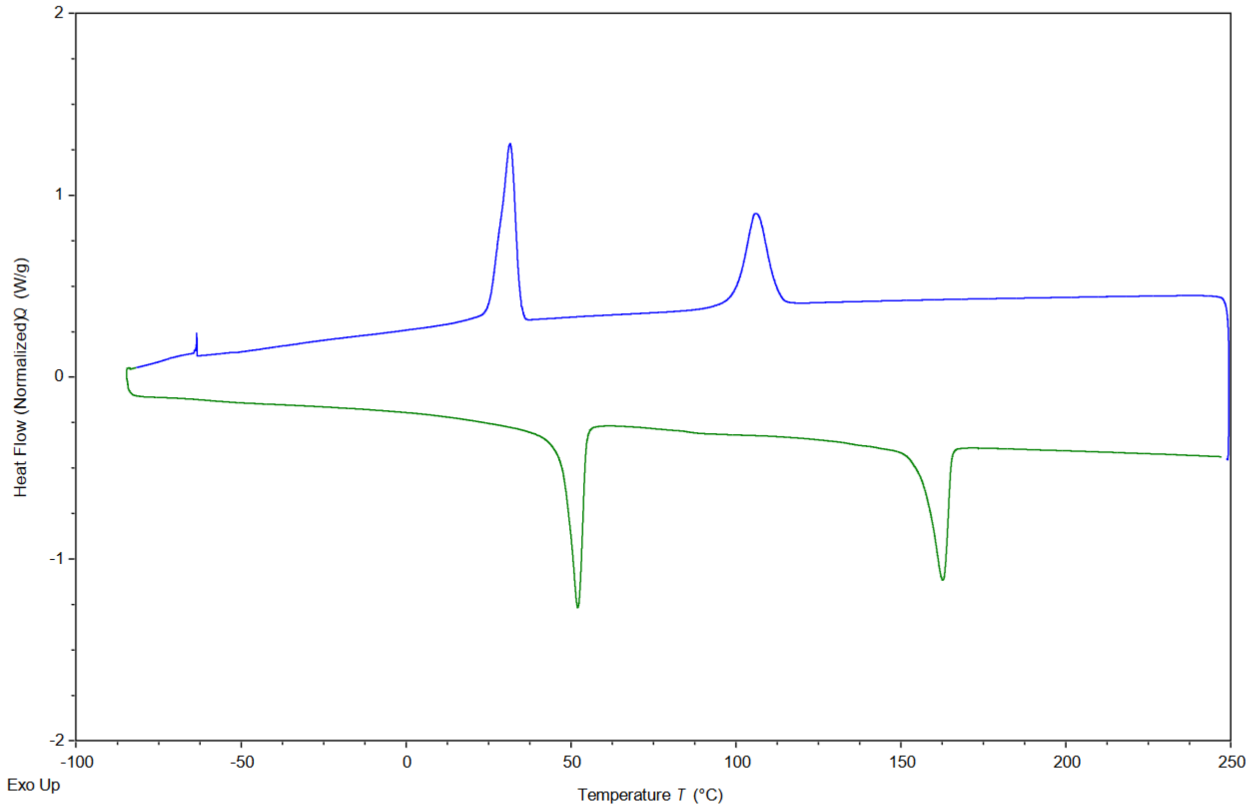

Figure S9.13. DSC heat-cool-heat trace (first heat cycle not shown) of block copolymer prepared by **1**-Me_2, 2 $Mg(HMDS)_2$, and 2 nPrOH,

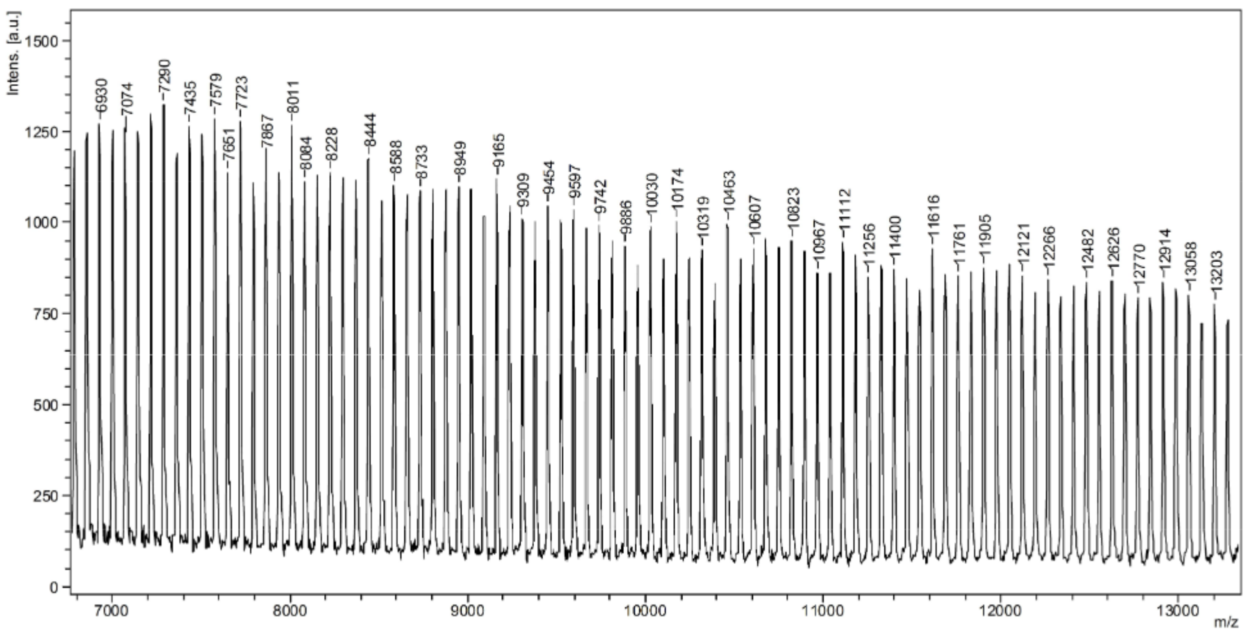

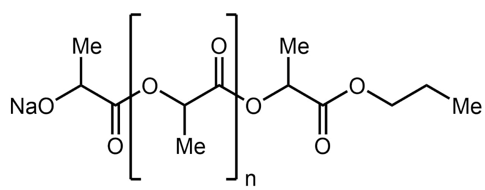

m/z = 72.1n + 203 + 23

n = 100; m/z = 7436
n = 101; m/z = 7508
n = 102; m/z = 7580
n = ...

Figure S9.14. MALDI-ToF MS spectrum of polymer prepared by **1**-Me_2, 2 $Zn(HMDS)_2$, and 2 nPrOH. Example m/z calculation provided.

S10. Kinetics

S10.1. General procedure for kinetics experiments. In the glovebox, a solution of precatalyst and CH_2Cl_2 (1 mL, varying concentration) was treated with a solution of $M(HMDS)_2$ ($M^{2+} = Zn^{2+}$, Mg^{2+}, or Ca^{2+}) in CH_2Cl_2. This solution was sealed and stirred vigorously for 30 minutes and then treated with alcohol as a freshly prepared stock solution in CH_2Cl_2 (1 equivalent per metal, 1% v/v). This solution was sealed again and stirred another 30 minutes, and then injected all at once into a rapidly stirring solution of *rac*-lactide in CH_2Cl_2 (2 mL) in a vial. 0.2 mL aliquots were taken at various time points by syringe and quenched by injecting into 0.1 M solution of benzoic acid in CH_2Cl_2. The quenched aliquots were dried in vacuo and the resulting residue redissolved in $CDCl_3$. Assay conversions were determined by comparing the integrations for the polymer signal with remaining monomer signal in the ^1H-NMR spectrum. Initial rates were calculated by linear regression of a polymer yield versus time plot as slope. Deviation from linear behavior was generally observed above 50% conversion, and thus those points were removed from the linear fit. In all cases, we obtained positive x-intercepts indicating a lack of extrapolation to 0% conversion at 0 seconds, consistent with a short induction time.

S10.2. Conversion vs time plots for monometallic complex 4 + Zn(HMDS)$_2$ + nPrOH. Each line represents an initial concentration of **4** for which individual time points were taken. For each concentration, the experiment was performed at least twice with aliquots taken at the same intervals. Individual data points therefore represents the average of at least two experiments at the same initial concentration of **4**. All experiments were performed with an initial concentration of 0.33 M of rac-Lactide.

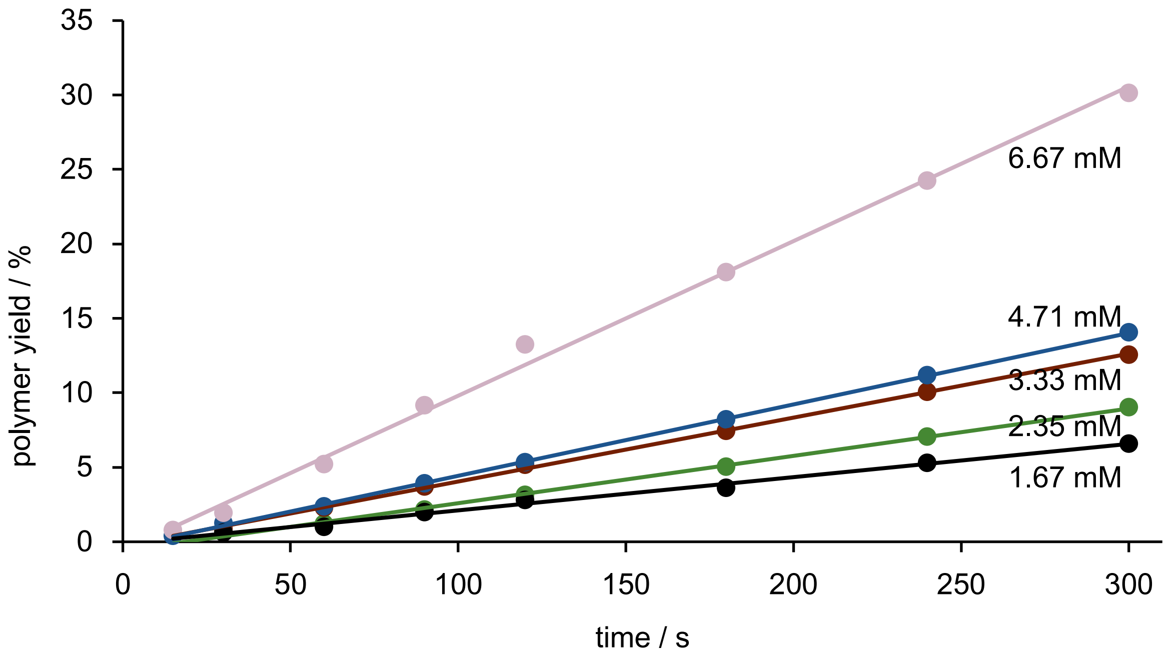

Figure S10.1. Polymer yield (%) vs reaction time for the polymerization of *rac*-lactide by in-situ formed complex **4** + Zn(HMDS)$_2$ + nPrOH. Initial concentrations of **4** are indicated.

Table S10.1. Steady state rates obtained for **4** + Zn(HMDS)$_2$ + nPrOH.

Initial concentration of 4	1.67mM	2.35 mM	3.33 mM	4.71 mM	6.67 mM
Rate (d[polymer]/dt) from slope (M/h)	0.267	0.378	0.514	0.574	1.24

S10.3. Conversion vs time plots for bimetallic complex 1-Me$_2$ + 2 Zn(HMDS)$_2$ + 2 nPrOH. Each line represents an initial concentration of **1**-Me$_2$ for which individual time points were taken. For each concentration, the experiment was performed at least twice with aliquots taken at the same intervals. Individual data points therefore represents the average of at least two experiments at the same concentration of **1**-Me$_2$. All experiments were performed with an initial concentration of 0.33 M of *rac*-Lactide.

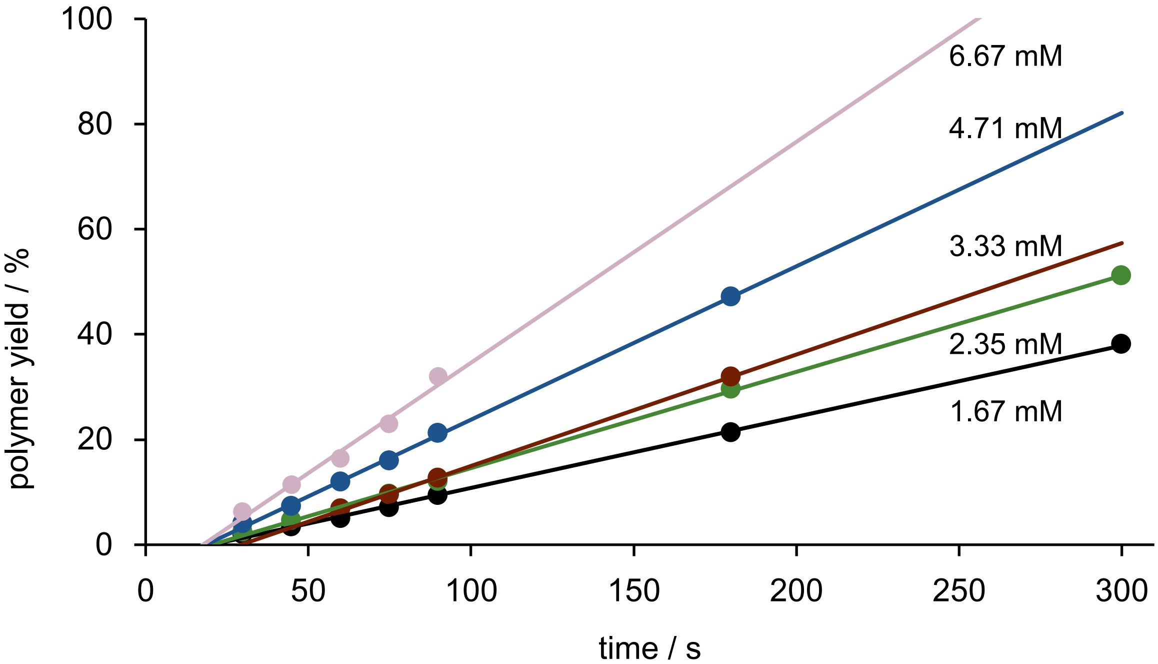

Figure S10.2. Polymer yield (%) vs reaction time plot for the polymerization of *rac*-lactide by in-situ formed complex **1**-Me$_2$ + Zn(HMDS)$_2$ + nPrOH. Initial concentrations of **1**-Me$_2$ are indicated.

Table S10.2. Steady state rates obtained for **1**-Me$_2$ + Zn(HMDS)$_2$ + nPrOH.

Initial concentration of 1-Me$_2$	1.67 mM	2.35 mM	3.33 mM	4.71 mM	6.67 mM
Rate (d[polymer]/dt) from slope (M/h)	1.26	2.21	2.54	3.54	5.47

S10.4. ln(d[P]/dt) vs ln[catalyst] plot for monometallic and bimetallic complexes. Steady-state rates from Sections 10.2 and 10.3 were plotted against catalyst concentration in a double logarithm plot. Assuming constant catalyst and lactide concentrations and a rate law of the form d[polymer]/dt = k[L][catalyst]^n, this double logarithm plot should be governed by the relationship ln{d[polymer]/dt} = ln{k[L]$_0$} + ^{n}[catalyst]$_0$, where [L]$_0$ is initial lactide concentration and [catalyst]$_0$ = initial catalyst concentration. Thus the kinetic rate order (n) in each catalyst would be the slope of its particular line. Furthermore, the relative rates for the two catalysts (k_1/k_2) should be obtained by comparing the intercepts of this plot (ln{k_1[L]$_0$} and ln{k_2[L]$_0$}) by the following equation: k_1/k_2 = e^(ln{k$_1$[L]$_0$} – ln{k$_2$[L]$_0$}) since the same [L]$_0$ was used in both cases. In this way, we obtained kinetic orders of 1.01 for **4**/Zn(HMDS)$_2$ and 0.98 for **1**-Me$_2$/Zn(HMDS)$_2$, and a k_1/k_2 = 5.34.

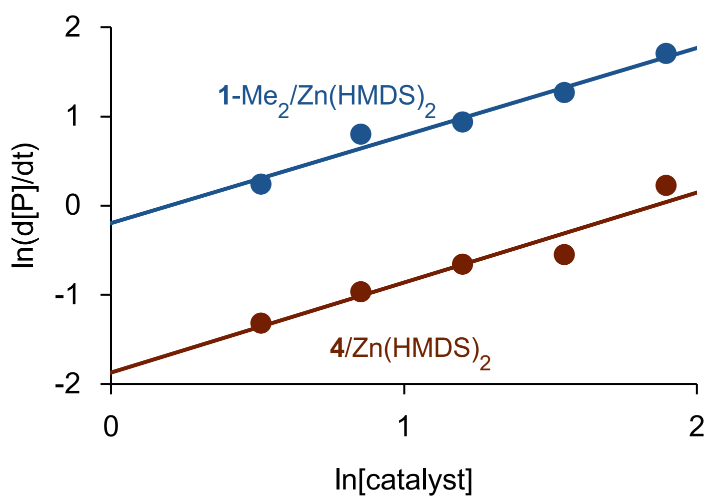

Figure S10.3. ln(d[P]/dt) vs ln[catalyst] plot for the polymerization of *rac*-lactide by in-situ formed complexes **1**-Me$_2$ + Zn(HMDS)$_2$ + nPrOH (top, blue) and 4 + Zn(HMDS)$_2$ + nPrOH (bottom, red).

S10.5. ln(d[P]/dt) vs ln[Zn] plot for monometallic and bimetallic complexes. The data from Table S10.1 and S10.2 were replotted as a double logarithm plot of steady state rate versus zinc concentration to allow a comparison at constant metal concentration. By the method described in Section S10.4 we obtained a $k_1/k_2 = 2.71$.

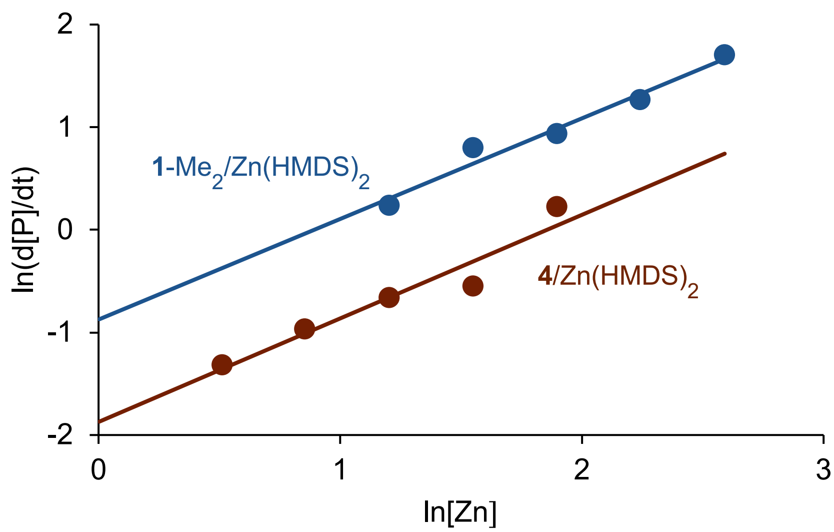

Figure S10.4. ln(d[P]/dt) vs ln[Zn] plot for the polymerization of rac-lactide by in-situ formed complexes **1**-Me_2 + $Zn(HMDS)_2$ + nPrOH (top, blue) and 4 + $Zn(HMDS)_2$ + nPrOH (bottom, red).

S10.6. Conversion vs time plots for bimetallic complex 1-Me$_2$/(*S*)-1-Me$_2$/(*R*)-1-Me$_2$ + 2 Zn(HMDS)$_2$ + 2 nPrOH with L or DL lactide. Each line represents a different precatalyst (*rac*-**1**-Me$_2$, (*S*)-**1**-Me$_2$, (*R*)-**1**-Me$_2$), for which individual time points were taken at a constant initial precatalyst concentration of 3.33 mM and an initial lactide (L or DL) concentration of 0.33 M. For each precatalyst, the experiment was performed at least twice with aliquots taken at the same intervals. Individual data points therefore represents the average of at least two experiments.

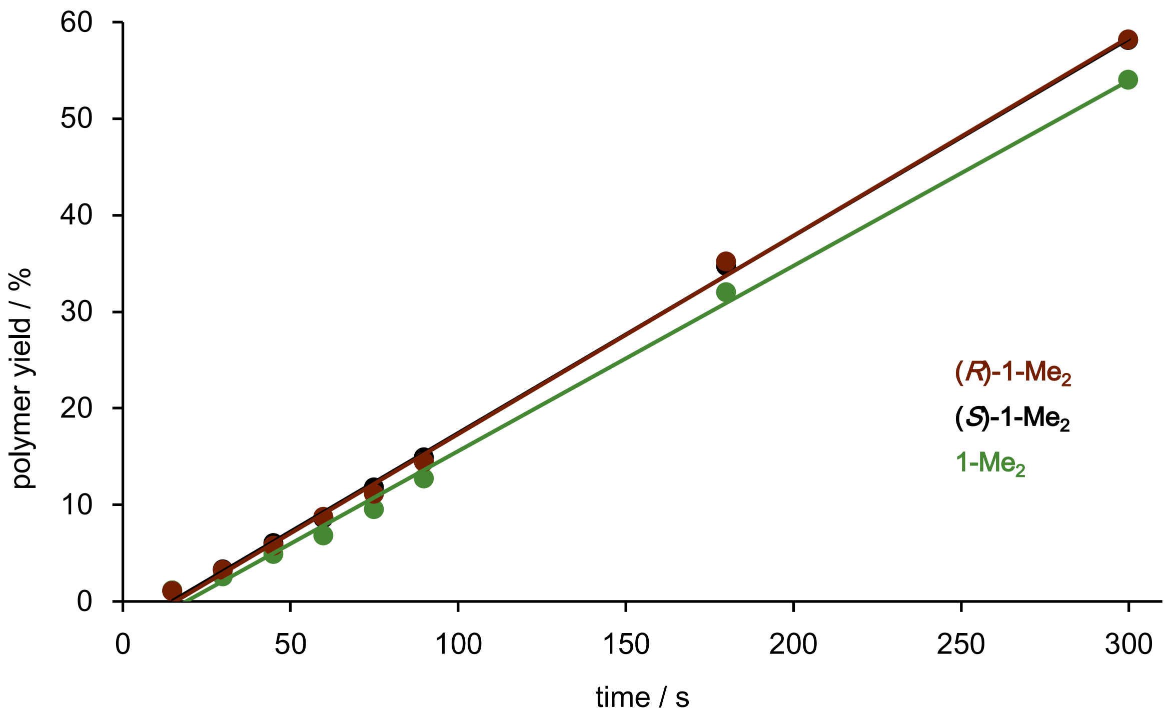

Figure S10.5. Polymer yield (%) vs reaction time for the polymerization of *rac*-lactide by precatalyst (*rac*-**1**-Me$_2$, (*S*)-**1**-Me$_2$, or (*R*)-**1**-Me$_2$), 2 Zn(HMDS)$_2$, and 2 nPrOH at [catalyst]$_0$ = 3.33 mM.

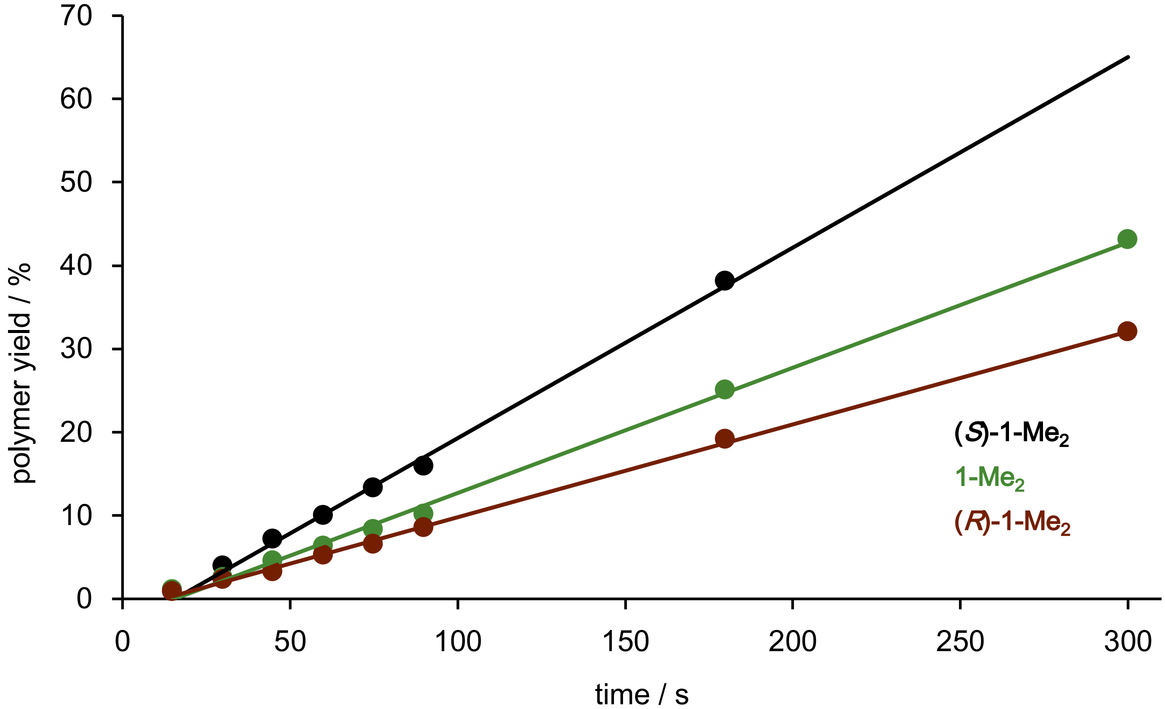

Figure S10.6. Polymer yield (%) vs reaction time plot for the polymerization of L-lactide by precatalyst (*rac*-**1**-Me_2, (*S*)-**1**-Me_2, or (*R*)-**1**-Me_2), 2 $Zn(HMDS)_2$, and 2 nPrOH at $[\text{catalyst}]_0 = 3.33$ mM.

Table S10.4. Observed steady-state rates of lactide polymerization by chiral ligands *rac*-**1**-Me_2, (*R*)-**1**-Me_2, and (*S*)-**1**-Me_2.

Entry[a]	Catalyst	Monomer	k_{obs} (turnovers per hour)
1	(*R*)-**1**-Me_2 + 2 $Zn(HMDS)_2$	*l*-lactide	406
2	*rac*-**1**-Me_2 + 2 $Zn(HMDS)_2$	*l*-lactide	558
3	(*S*)-**1**-Me_2 + 2 $Zn(HMDS)_2$	*l*-lactide	851
4	(*R*)-**1**-Me_2 + 2 $Zn(HMDS)_2$	*rac*-lactide	754
5	*rac*-**1**-Me_2 + 2 $Zn(HMDS)_2$	*rac*-lactide	763
6	(*S*)-**1**-Me_2 + 2 $Zn(HMDS)_2$	*rac*-lactide	746

[a]Conditions: $[l\text{-lactide}]_0$ = 0.33 M in CH_2Cl_2 at room temperature, $[l\text{-lactide}]_0/[\text{Zn or Mg}]_0/[\text{n-propanol}]_0$ = 100/1/1.

S11. Computational models.

S11.1. General. All computations were performed using the Gaussian 16 Software package[8].

S11.2. Structural analysis for the formation of bimetallic Zn, Mg, and Ca hexamethyldisilazide complexes with 1-Me$_2$ (Scheme S11.1). All calculations were performed in the gas phase, using temperature = 298.15 K, pressure = 1 atm. A multiplicity of 0 and charge of 0 was assigned for all structures in this section. Geometries for the zinc, magnesium, and calcium complexes (**S11-1**, **S11-2**, and **S11-3**) were all optimized at the level of B3LYP/6-31G(d, p). Free energies of formation were then obtained by a single frequency calculation at this same level and are reported below, but were not the basis of our discussion and conclusions. The geometry optimization and frequency steps were performed together in a single calculation using the Gaussian keyword combination "Opt Freq." For all of the analyzed structures, the Opt Freq calculations resulted in no negative harmonic frequencies, confirming that the optimized structures were stable local minima on the energy surface.

[8] Gaussian 16, ES64L-G16RevC.01, Frisch, M. J.; Trucks, G. W.; Schlegel, H. B.; Scuseria, G. E.; Robb, M. A.; Cheeseman, J. R.; Scalmani, G.; Barone, V.; Petersson, G. A.; Nakatsuji, H.; Li, X.; Caricato, M.; Marenich, A. V.; Bloino, J.; Janesko, B. G.; Gomperts, R.; Mennucci, B.; Hratchian, H. P.; Ortiz, J. V.; Izmaylov, A. F.; Sonnenberg, J. L.; Williams-Young, D.; Ding, F.; Lipparini, F.; Egidi, F.; Goings, J.; Peng, B.; Petrone, A.; Henderson, T.; Ranasinghe, D.; Zakrzewski, V. G.; Gao, J.; Rega, N.; Zheng, G.; Liang, W.; Hada, M.; Ehara, M.; Toyota, K.; Fukuda, R.; Hasegawa, J.; Ishida, M.; Nakajima, T.; Honda, Y.; Kitao, O.; Nakai, H.; Vreven, T.; Throssell, K.; Montgomery, J. A., Jr.; Peralta, J. E.; Ogliaro, F.; Bearpark, M. J.; Heyd, J. J.; Brothers, E. N.; Kudin, K. N.; Staroverov, V. N.; Keith, T. A.; Kobayashi, R.; Normand, J.; Raghavachari, K.; Rendell, A. P.; Burant, J. C.; Iyengar, S. S.; Tomasi, J.; Cossi, M.; Millam, J. M.; Klene, M.; Adamo, C.; Cammi, R.; Ochterski, J. W.; Martin, R. L.; Morokuma, K.; Farkas, O.; Foresman, J. B.; Fox, D. J. Gaussian, Inc., Wallingford CT, 2016.

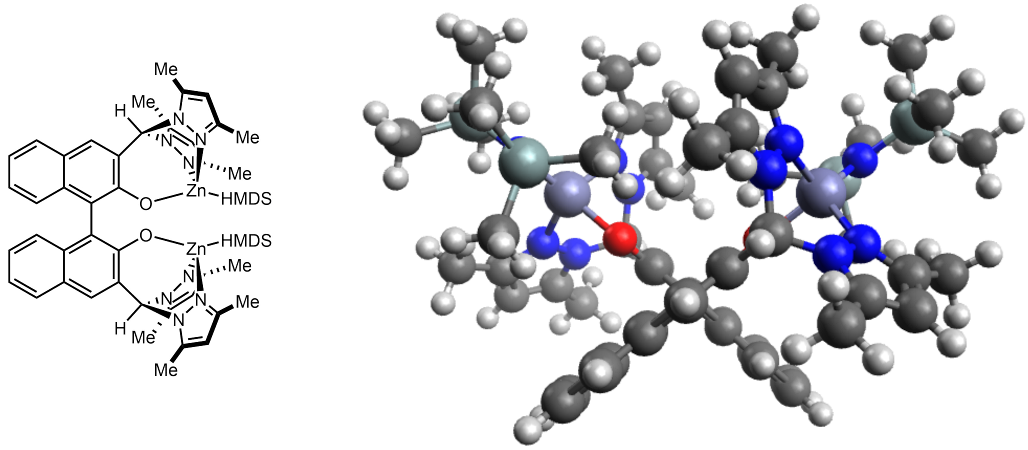

Figure S11.1. Optimized geometry for S**11-1**

XYZ coordinates for optimized structure **S11-1.**

C	0.263719	0.699633	2.14171
C	-0.368196	1.697181	2.932506
C	1.399301	0.991551	1.350731
C	1.89426	2.355075	1.369998
C	1.264285	3.319827	2.136756
C	0.135604	3.039484	2.933414
N	2.985517	2.831416	-0.867955
N	3.026074	1.671358	-1.579287
N	4.395195	2.28288	1.027453
N	4.741847	0.99575	0.747781
C	2.604155	3.878521	-1.659856
C	2.415759	3.360069	-2.926713
C	2.68277	1.979109	-2.832289
C	5.828058	0.726101	1.475958
C	6.182392	1.857591	2.239438
C	5.247603	2.831709	1.94472
C	3.108112	2.84891	0.595095
O	1.955703	0.035104	0.649239
Zn	3.463793	-0.085947	-0.530545
C	-0.263965	-0.699185	2.14169
C	-1.400778	-0.990797	1.352374
C	-1.894908	-2.354645	1.370892

C	-1.263504	-3.319801	2.135947
C	-0.133952	-3.039623	2.931435
C	0.369377	-1.697141	2.930841
O	-1.95935	-0.033763	0.653438
C	-3.109294	-2.848395	0.596782
N	-4.396128	-2.281813	1.02919
N	-4.744471	-0.995981	0.745738
N	-2.986956	-2.831592	-0.8663
N	-3.023972	-1.671459	-1.577635
C	-5.830335	-0.725312	1.474133
C	-6.1825	-1.854698	2.241675
C	-5.24684	-2.828662	1.949176
C	-2.681203	-1.980061	-2.830567
C	-2.418375	-3.361833	-2.925003
C	-2.608527	-3.879784	-1.658194
Zn	-3.464249	0.085812	-0.530613
H	1.645254	4.341033	2.138353
H	-1.64397	-4.341195	2.137088
C	-0.492239	4.036648	3.727462
C	-1.583184	3.735185	4.50681
C	-2.08622	2.408951	4.517446
C	-1.501437	1.42335	3.757333
C	1.503606	-1.423535	3.754388
C	2.089655	-2.409466	4.513114
C	1.58702	-3.735843	4.502222
C	0.495206	-4.037118	3.72401
H	1.893152	-0.41207	3.777776
H	2.950124	-2.170284	5.132442
H	2.063351	-4.50284	5.105583
H	0.093168	-5.048027	3.704183
H	-0.089872	5.04743	3.707846
H	-2.058537	4.501917	5.111281
H	-2.946016	2.169643	5.137657
H	-1.891312	0.412009	3.780472
H	3.199867	3.906641	0.831774
H	-3.201297	-3.906011	0.833898
N	4.061614	-1.645456	-1.466712
Zn	5.489876	-1.604815	-2.446722
Zn	3.123895	-3.071178	-1.100307
C	6.246511	0.141707	-2.476907
C	5.186193	-2.068618	-4.268941
C	6.872335	-2.767805	-1.839558

C	1.271279	-2.709812	-1.261886
C	3.448741	-3.657666	0.674332
C	3.482089	-4.545456	-2.252274
H	4.413635	-1.440636	-4.72538
H	4.871037	-3.110449	-4.380794
H	6.104765	-1.939872	-4.854826
H	5.558531	0.88575	-2.891943
H	7.147187	0.144253	-3.102302
H	6.538644	0.489365	-1.480702
H	3.195045	-4.33464	-3.287821
H	2.891905	-5.408177	-1.919376
H	4.532212	-4.854499	-2.251932
H	0.968848	-1.891159	-0.601027
H	0.679391	-3.592689	-0.990965
H	1.00732	-2.437319	-2.290686
H	7.201198	-2.51682	-0.825709
H	7.748831	-2.702401	-2.49605
H	6.553133	-3.815207	-1.827504
H	3.197166	-2.876749	1.400267
H	4.502727	-3.924723	0.817162
H	2.847049	-4.537992	0.929705
N	-4.061607	1.645295	-1.467153
Zn	-3.12447	3.070887	-1.098923
Zn	-5.488162	1.604267	-2.449577
C	-6.243817	-0.142637	-2.481535
C	-5.181639	2.068743	-4.27115
C	-6.872186	2.766531	-1.844594
C	-3.449392	3.654706	0.67659
C	-3.482999	4.546639	-2.248876
C	-1.271653	2.710529	-1.260609
H	-4.503322	3.921729	0.81992
H	-2.847517	4.534499	0.933364
H	-3.19786	2.872552	1.401215
H	-0.968932	1.891572	-0.60026
H	-0.680352	3.593524	-0.988766
H	-1.007206	2.439005	-2.289529
H	-4.408932	1.440491	-4.726981
H	-4.865651	3.110433	-4.382016
H	-6.099544	1.940959	-4.858298
H	-7.202917	2.515182	-0.831448
H	-7.747382	2.701043	-2.502811
H	-6.553326	3.814024	-1.831651

H	-5.555317	-0.885877	-2.897149
H	-7.144347	-0.145146	-3.107139
H	-6.535917	-0.491396	-1.485705
H	-4.533246	4.855252	-2.248363
H	-3.195587	4.337486	-3.284658
H	-2.893264	5.409112	-1.914543
C	-6.493988	0.61316	1.416681
C	-2.604507	-0.933363	-3.895441
C	6.489376	-0.613684	1.422625
C	2.609964	0.932454	-3.89763
H	7.0142	1.951882	2.921524
C	5.106161	4.217834	2.487508
H	-7.013425	-1.947704	2.925013
C	-5.103381	-4.213014	2.495918
H	-2.117147	-3.912045	-3.803789
C	-2.433573	-5.278802	-1.160438
H	2.113109	3.909386	-3.805572
C	2.4248	5.276858	-1.161898
H	2.762269	-0.059469	-3.467962
H	3.371149	1.097504	-4.667627
H	1.632237	0.957953	-4.388967
H	3.341685	5.679899	-0.716451
H	1.625793	5.340309	-0.415454
H	2.152409	5.924192	-1.997367
H	5.935412	4.425623	3.166177
H	4.173836	4.339141	3.049584
H	5.128027	4.976523	1.696898
H	5.876553	-1.320634	0.861033
H	6.639049	-1.005828	2.433199
H	7.472017	-0.551153	0.942927
H	-6.653207	1.003727	2.42636
H	-7.47233	0.549113	0.928401
H	-5.878088	1.322058	0.860927
H	-5.127798	-4.974206	1.707771
H	-5.930343	-4.418753	3.177994
H	-4.169153	-4.332426	3.055215
H	-1.623322	-0.955716	-4.380074
H	-2.76255	0.058127	-3.466849
H	-3.359826	-1.100915	-4.670623
H	-2.162999	-5.926784	-1.996
H	-3.351822	-5.679094	-0.715341
H	-1.634947	-5.344949	-0.413821

From the Opt Freq calculation (B3LYP/6-31G(d)):
Sum of electronic and thermal Free Energies= -7517.177136 e.u.
Sum of electronic and thermal Enthalpies= -7516.964170 e.u.
E(RB3LYP) = -7516.965114 e.u.

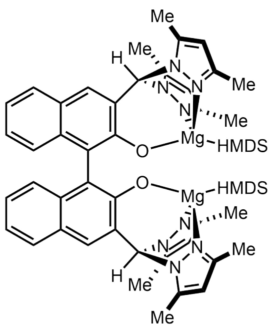

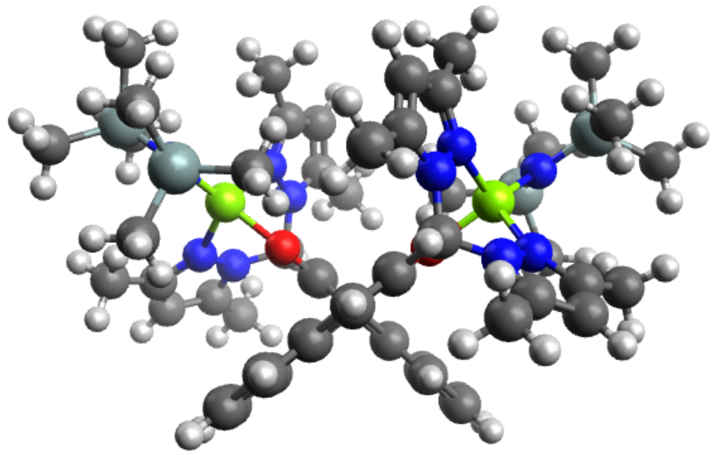

Figure S11.2. Optimized geometry for S**11-2**.
XYZ coordinates for optimized structure **S11-2**.

C	-0.222511	-0.713169	2.105843
C	0.466214	-1.681871	2.887215
C	-1.331776	-1.069982	1.308887
C	-1.747356	-2.457388	1.31258
C	-1.069145	-3.393173	2.07145
C	0.040568	-3.051658	2.87394
N	-2.798184	-2.919746	-0.953886
N	-2.982146	-1.767164	-1.661762
N	-4.250998	-2.525278	0.956368
N	-4.692364	-1.250015	0.745994
C	-2.320087	-3.91662	-1.757744
C	-2.213938	-3.380232	-3.026817
C	-2.633174	-2.039352	-2.922907
C	-5.809072	-1.112584	1.466085
C	-6.08767	-2.311162	2.153958
C	-5.076506	-3.191255	1.820165
C	-2.926487	-2.990688	0.511126
O	-1.958758	-0.171929	0.596677

Mg	-3.485331	0.00691	-0.542835
C	0.222636	0.713084	2.105908
C	1.33181	1.069965	1.308863
C	1.747529	2.457325	1.312784
C	1.06949	3.393023	2.071916
C	-0.040152	3.051447	2.874481
C	-0.465906	1.68169	2.887562
O	1.958591	0.171997	0.596371
C	2.926661	2.990648	0.511341
N	4.251149	2.525038	0.956448
N	4.692334	1.249734	0.745941
N	2.798292	2.919942	-0.953677
N	2.982203	1.767475	-1.661753
C	5.809039	1.112076	1.465993
C	6.087834	2.310558	2.153955
C	5.076782	3.190821	1.820276
C	2.633214	2.039891	-2.922844
C	2.214037	3.380809	-3.026519
C	2.320252	3.916983	-1.757361
Mg	3.48518	-0.006846	-0.543111
H	-1.388393	-4.435259	2.06058
H	1.388832	4.435081	2.061216
C	0.728628	-4.018174	3.655336
C	1.804189	-3.662492	4.433746
C	2.22954	-2.309842	4.45779
C	1.58386	-1.351334	3.711612
C	-1.583444	1.351083	3.712078
C	-2.228939	2.309502	4.45853
C	-1.803494	3.662124	4.434666
C	-0.728022	4.017869	3.656159
H	-1.912498	0.318454	3.746212
H	-3.075321	2.027121	5.079048
H	-2.325108	4.406753	5.028457
H	-0.385881	5.050296	3.626543
H	0.386564	-5.050622	3.625574
H	2.32595	-4.40719	5.02732
H	3.075998	-2.027513	5.078229
H	1.912845	-0.318688	3.745883
H	-2.955718	-4.059963	0.708804
H	2.956005	4.059889	0.709182
N	-4.275727	1.606999	-1.451759
Si	-5.715148	1.467264	-2.398984

Si	-3.501067	3.119167	-1.079598
C	-6.344651	-0.332744	-2.410886
C	-5.493455	1.9327	-4.233885
C	-7.162809	2.530299	-1.759311
C	-1.616974	2.89473	-1.018587
C	-4.052332	3.791948	0.612314
C	-3.821418	4.505674	-2.347768
H	-4.698345	1.346044	-4.707287
H	-5.240796	2.989496	-4.362438
H	-6.418363	1.745144	-4.793371
H	-5.605805	-1.029278	-2.822609
H	-7.243107	-0.407529	-3.035096
H	-6.611901	-0.694244	-1.412437
H	-3.439385	4.24306	-3.340179
H	-3.305589	5.419602	-2.028201
H	-4.882485	4.754706	-2.454879
H	-1.313496	2.094081	-0.335355
H	-1.135012	3.818086	-0.673789
H	-1.214391	2.661417	-2.01181
H	-7.44218	2.260577	-0.734838
H	-8.052342	2.403702	-2.388544
H	-6.914656	3.597354	-1.757087
H	-3.788992	3.10123	1.421855
H	-5.137544	3.945061	0.643292
H	-3.575261	4.752331	0.842221
N	4.27541	-1.606851	-1.452332
Si	3.500567	-3.119005	-1.080483
Si	5.714892	-1.467123	-2.399468
C	6.344628	0.332806	-2.411024
C	5.493218	-1.932175	-4.234469
C	7.162378	-2.530483	-1.759941
C	4.051845	-3.792291	0.611224
C	3.820647	-4.505241	-2.349018
C	1.616507	-2.894323	-1.019302
H	5.137039	-3.945556	0.642101
H	3.574662	-4.752671	0.840909
H	3.788643	-3.101748	1.420959
H	1.313171	-2.093777	-0.335886
H	1.13444	-3.817687	-0.674675
H	1.213897	-2.660746	-2.012453
H	4.698258	-1.345268	-4.707811
H	5.240354	-2.988896	-4.36324

H	6.418199	-1.744698	-4.79386
H	7.441701	-2.261048	-0.735379
H	8.051975	-2.403841	-2.389073
H	6.914093	-3.597509	-1.757999
H	5.605868	1.029506	-2.822624
H	7.243094	0.407593	-3.03522
H	6.61192	0.694094	-1.412511
H	4.881672	-4.754412	-2.456234
H	3.438616	-4.242313	-3.341347
H	3.304688	-5.41917	-2.029663
C	6.575571	-0.173174	1.479822
C	2.706694	0.997495	-3.994236
C	-6.575785	0.172557	1.480051
C	-2.706739	-0.996785	-3.994126
H	-6.920262	-2.510113	2.81212
C	-4.844863	-4.594582	2.2824
H	6.920477	2.509333	2.812105
C	4.845353	4.594139	2.282647
H	1.870148	3.893529	-3.912293
C	1.978028	5.288461	-1.270371
H	-1.870042	-3.892786	-3.912684
C	-1.977756	-5.288157	-1.270991
H	-2.944592	-0.018532	-3.570792
H	-3.475158	-1.2453	-4.734074
H	-1.751227	-0.925323	-4.523106
H	-2.83939	-5.79864	-0.824957
H	-1.17329	-5.262006	-0.528598
H	-1.636449	-5.893382	-2.112636
H	-5.667927	-4.899696	2.931179
H	-3.915546	-4.685321	2.855063
H	-4.801655	-5.304139	1.448254
H	-6.041915	0.951379	0.931925
H	-6.728603	0.514746	2.508405
H	-7.563401	0.047845	1.02353
H	6.728436	-0.515437	2.508144
H	7.563163	-0.048579	1.023215
H	6.041543	-0.951891	0.931701
H	4.802172	5.303772	1.448564
H	5.668506	4.899093	2.931389
H	3.916092	4.684949	2.855389
H	1.751115	0.926065	-4.523102
H	2.944647	0.019189	-3.571083

H	3.475002	1.246167	-4.734246
H	1.636695	5.893836	-2.111898
H	2.839719	5.798829	-0.824315
H	1.173612	5.262235	-0.527927

From the Opt Freq calculation (B3LYP/6-31G(d)):
Sum of electronic and thermal Free Energies= -4359.191720 e.u.
Sum of electronic and thermal Enthalpies= -4358.980723 e.u.
E(RB3LYP) = -4358.981667 e.u.

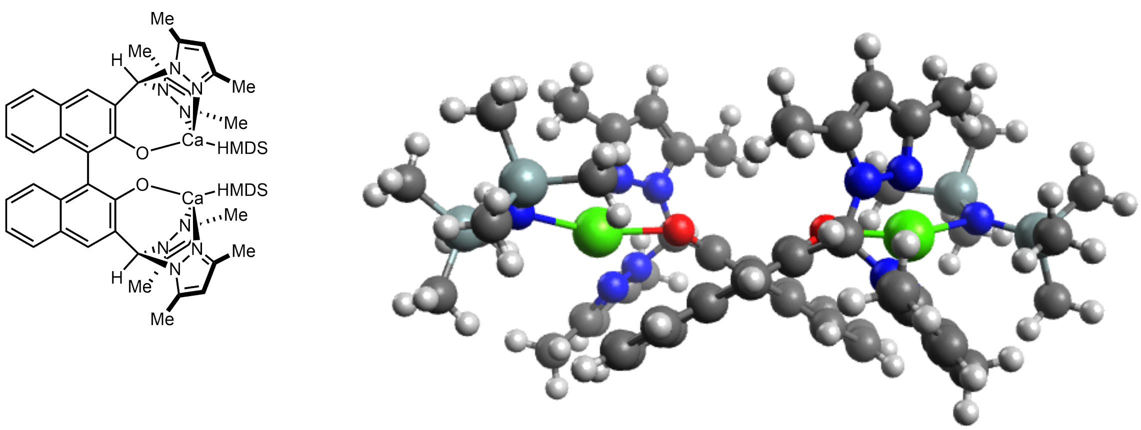

Figure S11.3. Optimized geometry for S**11-3**.

XYZ coordinates for optimized structure **S11-3**.

C	-0.101669	-0.735956	1.072766
C	0.842256	-1.617326	1.668931
C	-1.245694	-1.249066	0.414106
C	-1.474209	-2.677216	0.454396
C	-0.534652	-3.527872	0.99792
C	0.650116	-3.039635	1.598758
N	-3.215433	-2.925453	-1.406561
N	-4.19351	-2.007011	-1.647312
N	-3.880368	-3.212239	0.906422
N	-4.294185	-2.027728	1.453851
C	-2.730322	-3.45916	-2.564134
C	-3.435948	-2.862156	-3.594089
C	-4.337153	-1.970403	-2.978557

C	-5.163909	-2.355451	2.415531
C	-5.314104	-3.754727	2.490421
C	-4.482086	-4.27695	1.519348
C	-2.767577	-3.300176	-0.049149
O	-2.087156	-0.481815	-0.200671
Ca	-4.241202	0.020569	-0.093147
C	0.102263	0.737716	1.072598
C	1.24581	1.250488	0.41284
C	1.474946	2.678527	0.453234
C	0.536094	3.529477	0.997516
C	-0.648359	3.041605	1.599259
C	-0.840873	1.619352	1.669645
O	2.086331	0.483051	-0.203038
C	2.768398	3.300935	-0.050738
N	3.881212	3.212844	0.904786
N	4.294434	2.028336	1.45269
N	3.216103	2.925461	-1.407975
N	4.194017	2.006743	-1.64818
C	5.164569	2.356019	2.414033
C	5.316037	3.755203	2.487833
C	4.483609	4.277477	1.517125
C	4.337262	1.968964	-2.979439
C	3.43601	2.860325	-3.595486
C	2.730686	3.458224	-2.565838
Ca	4.240122	-0.020783	-0.09313
H	-0.700108	-4.605281	0.989184
H	0.701969	4.606823	0.988803
C	1.623285	-3.91693	2.147784
C	2.751423	-3.435157	2.770852
C	2.928371	-2.032202	2.889258
C	2.005956	-1.153436	2.361548
C	-2.004017	1.155837	2.363408
C	-2.925686	2.034885	2.891914
C	-2.748473	3.437775	2.773242
C	-1.620785	3.919209	2.149108
H	-2.128462	0.086757	2.502292

H	-3.784267	1.653054	3.440214
H	-3.483379	4.117653	3.192481
H	-1.453426	4.991349	2.071426
H	1.456164	-4.98912	2.070303
H	3.486888	-4.114805	3.189476
H	3.787265	-1.65011	3.436885
H	2.130133	-0.084308	2.500392
H	-2.573601	-4.370604	-0.11955
H	2.574804	4.371418	-0.121491
N	-6.071325	1.439277	-0.586686
Si	-7.693125	1.075014	-0.166756
Si	-5.481135	2.885929	-1.291451
C	-7.940871	-0.8194	-0.149296
C	-9.016131	1.760266	-1.354219
C	-8.17514	1.701865	1.569749
C	-3.572188	2.742495	-1.430853
C	-5.816011	4.469944	-0.290947
C	-6.084641	3.21645	-3.06776
H	-8.851341	1.419705	-2.382435
H	-9.020605	2.85634	-1.368233
H	-10.019549	1.43536	-1.053121
H	-7.829109	-1.238188	-1.156336
H	-8.942334	-1.087345	0.208449
H	-7.221453	-1.339041	0.496725
H	-5.845647	2.376079	-3.730088
H	-5.615748	4.114365	-3.488691
H	-7.169206	3.361721	-3.105844
H	-3.0552	2.679255	-0.463535
H	-3.175843	3.642382	-1.915902
H	-3.235401	1.902561	-2.057051
H	-7.514289	1.295004	2.344848
H	-9.204136	1.430593	1.836227
H	-8.095772	2.793707	1.623398
H	-5.380576	4.40029	0.712243
H	-6.891378	4.646862	-0.172001
H	-5.390281	5.355178	-0.779135

N	6.069748	-1.440539	-0.585881
Si	5.479171	-2.88663	-1.291457
Si	7.691561	-1.076849	-0.165507
C	7.940646	0.817405	-0.149918
C	9.015071	-1.764251	-1.351162
C	8.172013	-1.702304	1.571957
C	5.810177	-4.470635	-0.289631
C	6.085623	-3.218768	-3.066456
C	3.570665	-2.740908	-1.434631
H	6.885106	-4.648527	-0.168176
H	5.384691	-5.355671	-0.778395
H	5.372526	-4.40009	0.712529
H	3.051804	-2.676413	-0.468392
H	3.174113	-3.640591	-1.91988
H	3.236352	-1.900857	-2.061973
H	8.851283	-1.424976	-2.37996
H	9.019083	-2.860344	-1.363705
H	10.018379	-1.439377	-1.049665
H	7.510887	-1.294383	2.346251
H	9.200997	-1.431454	1.838917
H	8.091928	-2.794054	1.6265
H	7.830451	1.235076	-1.157593
H	8.941868	1.085026	0.208752
H	7.220797	1.338363	0.494557
H	7.169992	-3.365973	-3.102402
H	5.84936	-2.378295	-3.729631
H	5.615953	-4.11606	-3.487857
C	5.843804	1.307767	3.240721
C	5.352517	1.073323	-3.622678
C	-5.843616	-1.307158	3.241792
C	-5.352663	-1.075395	-3.622279
H	-5.945412	-4.313745	3.164978
C	-4.224984	-5.706576	1.161036
H	5.948118	4.314141	3.161732
C	4.227144	5.707091	1.158312
H	3.31335	3.048944	-4.65179

C	1.644382	4.484936	-2.607784
H	-3.313501	-3.051579	-4.650273
C	-1.643944	-4.485818	-2.6056
H	-5.799393	-0.392196	-2.894192
H	-6.15992	-1.662534	-4.074361
H	-4.897935	-0.478986	-4.419751
H	-1.948396	-5.428559	-2.133578
H	-0.740112	-4.135913	-2.097152
H	-1.390657	-4.706411	-3.644123
H	-4.89538	-6.346945	1.737316
H	-3.198059	-6.011941	1.392031
H	-4.40769	-5.90314	0.099312
H	-5.375601	-0.329341	3.1005
H	-5.781992	-1.556193	4.305425
H	-6.903348	-1.216051	2.982829
H	5.783365	1.557907	4.304162
H	6.903208	1.215244	2.980932
H	5.374596	0.330328	3.100768
H	4.409533	5.903077	0.096426
H	4.898132	6.34733	1.734044
H	3.200482	6.013136	1.389573
H	4.897505	0.476212	-4.419466
H	5.799417	0.390759	-2.894102
H	6.159674	1.659993	-4.075546
H	1.391119	4.705102	-3.646405
H	1.948889	5.427853	-2.136152
H	0.740523	4.135313	-2.099185

From the Opt Freq calculation (B3LYP/6-31G(d)):
Sum of electronic and thermal Free Energies= -5314.127528 e.u.
Sum of electronic and thermal Enthalpies= -5313.908839 e.u.
E(RB3LYP) = -5313.909783 e.u.